

TOPOLOGY FOR THE BASINS OF ATTRACTION OF
NEWTON'S METHOD IN TWO COMPLEX VARIABLES

A Dissertation

Presented to the Faculty of the Graduate School

of Cornell University

in Partial Fulfillment of the Requirements for the Degree of

Doctor of Philosophy

by

Roland K. Roeder

August 2005

© 2005 Roland K. Roeder

ALL RIGHTS RESERVED

TOPOLOGY FOR THE BASINS OF ATTRACTION OF NEWTON'S METHOD IN
TWO COMPLEX VARIABLES

Roland K. Roeder, Ph.D.

Cornell University 2005

In a recent paper, John H. Hubbard and Peter Papadopol study the dynamics of the Newton map, $N : \mathbb{C}^2 \rightarrow \mathbb{C}^2$, for finding the common zeros of two quadratic equations $P(x, y) = 0$ and $Q(x, y) = 0$. The map N has points of indeterminacy, critical curves, and invariant circles that are non-uniformly hyperbolic. Most of the work in their paper is spent resolving the points of indeterminacy of N , and creating a compactification of \mathbb{C}^2 in a way that is both compatible with the dynamics of N and that has “tame” topology. This part of their work requires two very technical tools called *Farey Blow-ups* and *Real-oriented blow-ups*. In a different direction, Hubbard and Papadopol show that the basin of attraction for each of the four common zeros of P and Q is path connected. However, most further questions about the topology of these basins of attraction remain a mystery.

The dynamics of N is much simpler if the common roots of P and Q lie on parallel lines, for instance when $P(x, y) = x(x - 1) = 0$ and $Q(x, y) = y^2 + Bxy - y = 0$. The first component of N depends only on x , while the second component depends on both x and y . Many of the complexities described by Hubbard and Papadopol disappear: one must still do an infinite sequence of blow-ups in order to make N a well defined dynamical system, but one can avoid the Farey Blow-ups and the Real-oriented blow-ups.

Let r_1 and r_2 be the roots in the line $x = 0$ and r_3 and r_4 be the roots in the line $x = 1$ and let $W(r_1), W(r_2), W(r_3)$ and $W(r_4)$ be the corresponding basins of attraction of under

iteration of N after this infinite sequence of blow-ups has been performed. There is a symmetry exchanging r_1 with r_2 and exchanging r_3 with r_4 , but for a given B the pair (r_1, r_2) behaves differently from the pair (r_3, r_4) . More specifically, one pair “attracts” the points of indeterminacy of N , and the other does not. We consistently make the restriction that $B \in \Omega = \{|1 - B| < 1\}$ which guarantees that the pair (r_1, r_2) attracts the points of indeterminacy.

We will prove that $H_1(\overline{W(r_1)})$ and $H_1(\overline{W(r_2)})$ are infinitely generated for every $B \in \Omega$. There is an invariant circle within the line $x = 1$ that is super-attracting in the x -direction and hyperbolically repelling in the line $x = 1$. Let W_1 be the super-stable “manifold” corresponding to this invariant circle. For the values of $B \in \Omega$ for which W_1 intersects the critical value parabola $C(x, y) = 0$, $H_1(\overline{W(r_3)})$ and $H_1(\overline{W(r_4)})$ are infinitely generated. For all other $B \in \Omega$, $H_1(W(r_3))$ and $H_1(W(r_4))$ are trivial.

In addition, for the parameter values B that are not in the bifurcation locus—which is exceptional in the sense of Baire’s Theorem—the statements above remain true if we replace the closures of the basins with the basins themselves.

BIOGRAPHICAL SKETCH

Roland K. W. Roeder was born on March 9th, 1978 to Stephen and Phoebe Roeder. In high school, he enjoyed mathematics and developed a love for surfing. Professors David Lesley, Joseph Mahaffy, James Ross, and Peter Salamon from San Diego State University provided wonderful guidance during these years.

Roland graduated summa cum laude from the University of California, San Diego in 2000. He enjoyed mathematics courses by J. P. Fillmore and Peter Teichner and physics courses by Daniel Arovas.

Roland began work on his Ph.D. at Cornell University in the fall of 2000, where he especially enjoyed the challenging “core courses” and a summer research project with Todd Evans from General Atomics in San Diego.

Roland’s first project working with his adviser John Hubbard was writing a computer program implementing Andreev’s Classification of hyperbolic polyhedra. While debugging his program, he found an error in Andreev’s original proof. Following Professor Hubbard to the Université de Provence, in Marseille, Roland wrote a correction of Andreev’s proof, which he defended for a French Doctorate in May 2004.

Returning to Cornell, Roland began work on a second Ph.D., this time in complex dynamics under the guidance of John Hubbard, Allen Hatcher, and John Smillie.

Roland will spend next year at the Fields Institute in Toronto as the Jerrold E. Marsden postdoctoral fellow.

Dedicated to John Hamal Hubbard and Barbara Burke Hubbard.

ACKNOWLEDGEMENTS

I thank the Department of Defense for three years of financial support by means of a National Defense Sciences and Engineering Graduate (NDSEG) fellowship and I thank the National Science Foundation for one year of financial support via an Interdisciplinary Graduate Education and Research Traineeship (IGERT) fellowship.

During my years at Cornell, John Hamal Hubbard has provided incredible support and enthusiasm. He has shown me broad vistas of mathematics and he has shown me the technical details that make these vistas beautiful. Professor Hubbard has served as an example of what it is like to be a successful research mathematician, and how to enjoy it! Both he and Mrs Hubbard have given me essential help, mathematical and otherwise.

John Smillie and Allen Hatcher listened carefully to many precursors of this proof and have made insightful comments. Professor Smillie has shared sound guidance and perspective and he has given generous support to the dynamics community at Cornell. Professor Hatcher has offered advice on the topological aspects of this proof and he has been very generous with his time and enthusiasm.

Eric Bedford from Indiana University has given many additional kind suggestions, pointing me to subtle issues in this proof that I might have otherwise missed. In addition, both Professor Bedford and Professor Smillie have shown me the utility of invariant currents, which have become the cornerstone of my proof.

I would like to thank Karl Papadantonakis for writing the computer program FractalAsm [44] which was used to produce all of the computer images in this dissertation. This program was very helpful for gaining an intuition about the topology of basins of attraction.

The recent students from Cornell in complex dynamics, David Brown, Susanne Hruska, and Sylvain Bonnot welcomed me to the subject and the current Hubbard students Joshua Bowman, Sarah Koch, Gregory Muller, and Matthew Noonan have created an encouraging

feeling of community. In particular, Sarah Koch has been a helpful collaborator and shared boundless enthusiasm.

My parents Stephen and Pheobe Roeder, my sister Adrienne Roeder, and my girlfriend Johanna Kaufman have provided endless emotional support.

The department of Mathematics at Cornell as provided a very friendly environment and the staff especially have gone out of their way to help, when needed.

TABLE OF CONTENTS

1	Introduction	1
2	Newton's Method in \mathbb{C}^2	4
2.1	Standard background about Newton's Method	4
2.2	The intersection of conics	5
2.3	Global properties of N_F	7
2.4	Making N a well-defined dynamical system	12
3	General facts about the topology of the basins.	14
3.1	Facts proved by Hubbard and Papadopol about $W(r_i)$	14
3.2	Why do we use blow-ups?	14
4	The degenerate case, $A = 0$.	18
4.1	Basic properties	18
4.2	Computer exploration of N	22
4.3	Parameter space Ω	31
4.4	Statement of The Main Theorem	31
5	Compactification and resolution of points of indeterminacy	32
5.1	Construction of X_l^∞ and $N_\infty : X_l^\infty \rightarrow X_l^\infty$	33
5.2	The mappings from E_z to V	37
5.3	Homology of X_r and of X_l^∞	37
6	Superstable separatrices W_0 and W_1.	40
6.1	Superattracting invariant circles	40
6.2	Mayer-Vietoris computations	47
6.3	Replacement of $\overline{W(r_i)}$ with $W(r_i)$	48
7	Morse Theory for W_1 and W_0	49
7.1	Morse Theory for W_1 and W_0	49
8	Many loops in W_0 and W_1.	54
8.1	The mapping on fibers	54
8.2	Intersection of W_0 and W_1 with vertical lines.	55
8.3	Sizes	58
8.4	Many loops in W_0 and W_1	59
9	Linking numbers	60
9.1	Linking in manifolds M with non-trivial intermediate homology.	61
9.2	Linking kernel for X_l^∞	62
9.3	Linking with currents	62
9.4	Finding an element of $\mathcal{LZ}_+^{1,1}(X_l^\infty)$	63

9.5	Nice properties of λ_2 and λ_1 :	69
9.6	Linking with currents in X_l^∞	71
9.7	$H_1(W_0)$ is infinitely generated.	72
9.8	$H_1(\overline{W(r_1)})$ and $H_1(\overline{W(r_2)})$ are infinitely generated.	73
9.9	Linking with currents in X_r	76
A	The extension of N_F to \mathbb{CP}^2	78
B	Proof of Theorem 5.1.1	79
C	Blow-ups of complex surfaces at a point.	82
C.1	Blowing up \mathbb{C}^2 at a point	82
C.2	Examples:	82
C.3	Effect of blow-ups on homology	85
C.4	Repeated blow-ups	85
	Bibliography	89

LIST OF FIGURES

2.1	Slices through \mathbb{C}^2 along the line $y = (1 + .1i)x$ with parameters $(\alpha, \beta) = (1.2 + 0.3i, 0.2 + 0.5i)$. Three successive zooms are made, with the location of each zoom indicated by the black box in the previous image.	6
2.2	Geometric computation of $N_F(c, d)$	7
2.3	Invariant lines and invariant circles	9
2.4	Newton's Method in \mathbb{R}^2 with the root $(\alpha, \beta) = (2, 3)$	10
2.5	Geometric computation of inverse images	12
3.1	Without blow-ups, one can easily create non-trivial loops around the points of indeterminacy.	16
3.2	Does a curve surrounding this bubble correspond to a non-trivial loop in the orange basin? We will not be able to answer this question, but we will address a simpler but related question later in this dissertation.	17
4.1	The degenerate case $A = 0$	19
4.2	Superstable separatrices in the degenerate case, $A = 0$	20
4.3	The symmetry τ	21
4.4	The critical value parabola C for $B = 0.769 - 0.625i$. The boundary between the green and red basins is $W_1 \cap C$ and the boundary between the blue and gray basins is $W_0 \cap C$	23
4.5	Zoomed in view from Figure 4.4.	24
4.6	Vertical line through point a from Figure 4.5 and three inverse images of this line. The boundary between the blue and gray basins is the intersection of W_0 with these vertical lines. Notice that there are many closed loops in W_0 within these vertical lines. The center of the symmetry τ is at the center of these images.	25
4.7	Vertical line through the point labeled b in Figure 4.5 and three consecutive inverse images of this line. The boundary between the green and red basins is the intersection of W_1 with these lines. Notice how there are an increasing number of closed loops in W_1 within the repeated inverse images of the vertical line through b	26
4.8	Critical value parabola C for $B = 0.8871 - 0.1371i$. The boundary between the blue and the gray basins is $W_0 \cap C$. We see no boundaries between the green and the red basins, indicating that W_1 might not intersect C	27
4.9	Zoomed in views of C . There is no evidence of any boundaries between the green and red basins, nor any points in the green basin at all, hence there is no evidence of intersections between W_1 and C	28
4.10	Vertical line through a point of intersection between W_0 and C , from Figure 4.8, and three inverse images of this line. As for the previous value of B , repeated inverse images of the vertical line through a point of intersection between W_0 and C lead to an increasing number of closed loops in W_0 in each of these lines.	29

4.11	A vertical line through a point in the red basin, $W(r_3)$, within C , from Figure 4.8, and three inverse images of the vertical line. The common boundary between green and the red basins is W_1 . Notice that there are no closed loops in W_1 within any of these lines.	30
5.1	Blowing up a point on an exceptional divisor.	37
6.1	The Newton map N maps $\partial^H(\Delta_{\epsilon,\delta})$ outside of $\Delta_{\epsilon,\delta}$ and N maps $\partial^V(\Delta_{\epsilon,\delta})$ inside of inside of $ z < \epsilon$	42
7.1	Level curves of the Morse function h within the critical value parabola C . The points labeled k_1, k_2, k_3 and k_4 are all in K , as well as any others. The critical point of $h _C$ is labeled S	50
7.2	Level curves of the Morse function h within the critical value parabola C . The points labeled k_1, k_2 , and k_3 are all in K , as well as any others.	51
8.1	Forming many closed loops in W_0 . A sequence of vertical complex lines $\mathbb{P}_x, \mathbb{P}_{x_1}, \mathbb{P}_{x_2}$, and \mathbb{P}_{x_3} , one mapped to the next by N . Because W_0 intersects C in the line \mathbb{P}_{x_3} , Proposition 8.2.1 states that these vertical lines are divided by W_0 into at least 10, 6, 4, and 2 simply connected domains.	56
8.2	Example of a curve γ_i surrounding a simply connected domain U_i in some vertical line. In the next chapter we will prove that curves of this form are non-trivial in $H_1(W_0)$ (or $H_1(W_1)$) by linking these curves with an object that is disjoint from W_0 (or from W_1 .)	59
9.1	Linking in a weird space.	61
9.2	Newton map in \mathbb{R}^2 , $B = -0.3$. Top: $N^{-1}(L_2)$ in black and $N^{-1}(L_1)$ in gray. Bottom: $N^{-2}(L_2)$ in black and $N^{-2}(L_1)$ in gray.	66
9.3	Showing that $\partial(\tau_*[E_z]) = -\tau_*(\partial([E_z]))$	75
9.4	Diagram illustrating the proof of Lemma 9.8.5.	76

Chapter 1

Introduction

We will consider the dynamics of the Newton map, $N : \mathbb{C}^2 \rightarrow \mathbb{C}^2$, for finding the common roots of two quadratic equations $P(x, y) = 0$ and $Q(x, y) = 0$. This map has points of indeterminacy, critical curves, and invariant circles that are non-uniformly hyperbolic.

In a paper to appear as a Memoir of the American Mathematical Society, John Hubbard and Peter Papadopol [35] analyze the dynamics of this system, especially how to create a compactification of \mathbb{C}^2 that is both compatible with the dynamics of N and that has “tame” topology. In a different direction, Hubbard and Papadopol use general principles to show that the basin of attraction for each of the four common roots of P and Q is both path connected and is a Stein manifold. However, most further questions about the topology and the detailed structure of these basins of attraction remain a mystery.

In this dissertation we will restrict our attention to the degenerate case in which the four roots of P and Q lie on a pair of parallel lines. In this case, the first component of $N(x, y)$ depends only on x , while the second component depends on both x and y , providing a dramatic simplification of the dynamics. Systems of this form are commonly referred to as *skew products* in the literature and they are often used as “test cases” when developing new techniques. We develop techniques that allow a much more detailed study of the topology of the basins of attraction for this degenerate system. While we rely upon the fact that N becomes a skew product, we hope that some of the techniques developed here can eventually be adapted to more general systems.

The reader who would like to skip forward to see a statement of our main results should turn to Section 4.4 on page 31.

To put our work in perspective, we present a brief account of previous work on Newton’s Method and relevant work on complex dynamics in many variables. There is much more work than we can present here, and we apologize for any important works that are unmentioned.

Classical theory

Given $F : \mathbb{C}^n \rightarrow \mathbb{C}^n$ of class C^2 and a point $a_0 \in \mathbb{C}^n$, Kantorovitch’s Theorem [39] provides sufficient conditions depending on $\|F(a_0)\|$, $\|[DF(a_0)]^{-1}\|$ and the Lipschitz constant of DF guaranteeing that the initial seed a_0 is superattracted to some root r of F under iteration of the Newton map

$$N(x) = x - [DF(x)]^{-1}F(x).$$

The reader who would like to see a precise statement and proof of Kantorovich’s Theorem is encouraged to read sections 2.6 and 2.7, as well as appendices A5 and A6 of [37] or the original source [39].

Newton’s method as a dynamical system in one complex variable

When $F(z)$ is a polynomial, the Newton map N is a rational function, and many properties of the dynamics of N follow from general work on complex dynamics in one variable. Those interested in a survey of one variable dynamics may wish to consult Milnor’s textbook [43].

Specific results about Newton's method in one complex variable include the work of Hubbard, Schleicher, and Sutherland [31], who show that if F is a polynomial of degree d , there is a finite set S_d , dependent only on d , with the property that given any root r_i of F there is at least one point in S_d converging under iteration of N to r_i . An extension of this result by Schleicher [46] studies the number of iterations necessary to obtain good approximations to the roots starting with these initial seeds.

In a different direction, works by McMullen [41, 42] show that for polynomials of degree $d > 3$ there is no purely iterative rational root-finding method that works for almost all complex polynomials of degree d and for almost all initial conditions.

A study of Newton's Method applied to transcendental function is provided by Haruta [27].

Newton's method in many complex variables, as a dynamical system

The topological degree $d_t(g)$ of a mapping $g : \mathbb{P}^n \rightsquigarrow \mathbb{P}^n$ is defined as the generic number of inverse images of a point. When F is a function of more than one variable, the Newton map N has

- topological degree $d_t(N) > 1$ (and correspondingly N has critical curves), and
- points of indeterminacy.

To this author's knowledge, the only paper specifically about Newton's method as a global dynamical system in many complex variables is [35]. The papers [45] and [26], which we will describe in more detail below, study ergodic properties of more general classes of mappings than N and their results are applicable to the global dynamics of N as well.

Dynamics in many complex variables

Although not nearly as complete as the theory of dynamics in one complex variable, there are many papers on the dynamics of mappings with one or the other of the two difficulties mentioned above.

Mappings $g : \mathbb{P}^n \rightsquigarrow \mathbb{P}^n$ with $d_t(g) > 1$, but without points of indeterminacy are maps given by polynomials of degree > 1 in each component. Such systems have been studied by Briend [10], Briend and Duval [11], Dinh and Sibony [16], Fornaess and Sibony [21, 23, 22], Hubbard and Papadopol [36], Jonsson [38], and Ueda [49].

Meanwhile, birational maps $g : \mathbb{P}^n \rightsquigarrow \mathbb{P}^n$ (rational maps with rational inverse) are examples of systems with points of indeterminacy, but with $d_t(g) = 1$. The famous Henon mappings from $H : \mathbb{P}^2 \rightsquigarrow \mathbb{P}^2$ fall under this class. Such systems have been studied extensively by Bedford and Smillie [2, 3, 4, 5, 6, 8, 7], Bedford, Lyubich and Smillie [1], Devaney and Nitecki [14], Diller [15], Dinh and Sibony [17], Dujardin [18], Favre and Jonsson [19], Fornaess [20], Guedj [25], and Hubbard and Oberste-Vorth [32, 33, 34].

Dynamics of mappings $g : \mathbb{P}^n \rightsquigarrow \mathbb{P}^n$ with $d_t(g) > 1$ and with points of indeterminacy

Not nearly as much is known about mappings $g : \mathbb{P}^n \rightsquigarrow \mathbb{P}^n$ with topological degree $d_t(g) > 1$ and with points of indeterminacy.

The work of Russakovskii and Shiffman [45] considers a measure that is obtained by choosing a "generic" point, taking the each of its inverse images under g^{on} and giving them

all equal weight in order to obtain a probability measure μ_n . Under appropriate conditions on g they show that the measures μ_n converge to a measure μ that is independent of the initial point.

In [35], the authors present a proof by A. Douady that μ does not charge points in the line at infinity, a result not obtained in [45].

A recent paper by Guedj [26] proves further properties of the Russakovskii-Shiffman measure μ . He shows that if the topological degree $d_t(g)$ is sufficiently large, then μ does not charge the points of indeterminacy of g and does not charge any pluripolar set. He then uses these facts to establish ergodic properties of μ .

Chapter 2

Newton's Method in \mathbb{C}^2

In this chapter we review the basic facts from the paper *Newton's method applied to two quadratic equations in \mathbb{C}^2 viewed as a dynamical system* by John H. Hubbard and Peter Papadopol [35]. Our notation and perspective on Newton's Method is virtually entirely based on this paper. We will outline the first chapter of [35] and fill in the proofs which we feel will be useful for later in this dissertation.

Certain readers may wish to skip this chapter, returning to it for reference as needed.

2.1 Standard background about Newton's Method

Given two vector spaces V and W of the same dimension and a mapping $F : V \rightarrow W$, the associated Newton map $N_F : V \rightarrow V$ is given by the formula

$$N_F(\mathbf{x}) = \mathbf{x} - [DF(\mathbf{x})]^{-1}(F(\mathbf{x})). \quad (2.1)$$

It is important to allow that F maps a space V to a different space W (of the same dimension.) For example, in the real world, $F(x)$ will commonly represent a measurement in terms of some units (say Newtons force) and x will be some quantity in different units (say meters).

Having mentioned the real world, ever so briefly, we might as well mention that Newton's method is of immense importance in the real world. It is the most common (and almost the only) method used to numerically determine the roots of a nonlinear equation.

The most used and important property of the Newton Map N_F is that so long as the roots of F are non-degenerate, i.e. $DF(r_i)$ is invertible for each root r_i of F , then roots of F corresponds to a super attracting fixed point of N_F . Conversely, every fixed point of N_F is a root of F .

Since each fixed point r_i of N_F is super-attracting, there is some neighborhood U_i of r_i for which each initial guess $\mathbf{x}_0 \in U_0$ will converge to r_i . Probably the most used theorem about Newton's Method is Kantorovich's Theorem [39], which gives a precise lower bound on the size of this neighborhood U_i .

One of the most useful general properties of the Newton Map is that it transforms nicely under linear and affine changes of variables:

Proposition 2.1.1. (Transformation rules) *If $A : V \rightarrow V$ is affine, and invertible, and if $L : W \rightarrow W$ is linear and invertible, then:*

$$N_{L \circ F \circ A} = A^{-1} \circ N_F \circ A. \quad (2.2)$$

The proof is an exercise in the careful use of the chain rule. Those who wish to see it should consult [35], Lemma 1.1.1. The fact that L is linear, while A is merely affine indicates that we only care about the origin in W , but not in V .

2.2 The intersection of conics

In the paper [35], the authors quickly specialize to considering only the dynamics of Newton's Method for finding the intersection of two quadratic curves. Using a dimension count, they prove the following:

Proposition 2.2.1. *Newton's Method to find the intersection of two conics depends only on the intersection points and not on the choice of curves.*

For the proof, see Corollary 1.5.2 [35].

Using the transformation properties proved in Proposition 2.1.1, one can normalize the system N in many different ways. The normalization that we will most commonly use is:

Normalization 1: We can normalize so that the roots are at $\begin{pmatrix} 0 \\ 0 \end{pmatrix}$, $\begin{pmatrix} 1 \\ 0 \end{pmatrix}$, $\begin{pmatrix} 0 \\ 1 \end{pmatrix}$, and $\begin{pmatrix} \alpha \\ \beta \end{pmatrix}$. In this normalization if we let $A = \frac{1-\alpha}{\beta}$ and $B = \frac{1-\beta}{\alpha}$, then

$$F \begin{pmatrix} x \\ y \end{pmatrix} = \begin{pmatrix} x^2 + Axy - x \\ y^2 + Bxy - y \end{pmatrix} = \begin{pmatrix} P(x,y) \\ Q(x,y) \end{pmatrix}. \quad (2.3)$$

The Newton Map is given by:

$$\begin{aligned} N_F \begin{pmatrix} x \\ y \end{pmatrix} &= \begin{pmatrix} x \\ y \end{pmatrix} - \begin{bmatrix} 2x + Ay - 1 & Ax \\ By & 2y + Bx - 1 \end{bmatrix}^{-1} \begin{pmatrix} x^2 + Axy - x \\ y^2 + Bxy - y \end{pmatrix} \\ &= \frac{1}{\Delta} \begin{pmatrix} x(Bx^2 + 2xy + Ay^2 - x - Ay) \\ y(Bx^2 + 2xy + Ay^2 - Bx - y) \end{pmatrix}, \end{aligned} \quad (2.4)$$

where

$$\Delta = 2Bx^2 + 4xy + 2Ay^2 - (2+B)x - (2+A)y + 1. \quad (2.5)$$

Figure 2.1 shows a slice through \mathbb{C}^2 along the line $y = (1 + .1i)x$ for the parameters $(\alpha, \beta) = (1.2 + 0.3i, 0.2 + 0.5i)$. Three successive zooms are made, with the location of each zoom indicated by the black box in the previous image. This figure, and all of the computer images to follow were computed in the computer program FractalAsm [44], written by Karl Papadantonakis.

Normalization 2:

Hubbard and Papadopol also use another normalization in order to prove many of the basic properties about Newton's Method:

One can normalize to have

$$F \begin{pmatrix} x \\ y \end{pmatrix} = \begin{pmatrix} x^2 - y + a \\ y^2 - x + b \end{pmatrix}, \quad (2.6)$$

and correspondingly

$$\begin{aligned} N_F \begin{pmatrix} x \\ y \end{pmatrix} &= \begin{pmatrix} x \\ y \end{pmatrix} - \frac{1}{4xy - 1} \begin{bmatrix} 2y & 1 \\ 1 & 2x \end{bmatrix} \begin{pmatrix} x^2 - y + a \\ y^2 - x + b \end{pmatrix} \\ &= \frac{1}{4xy - 1} \begin{pmatrix} 2x^2y + y^2 - 2ay - b \\ 2xy^2 + x^2 - 2xb - a \end{pmatrix}. \end{aligned} \quad (2.7)$$

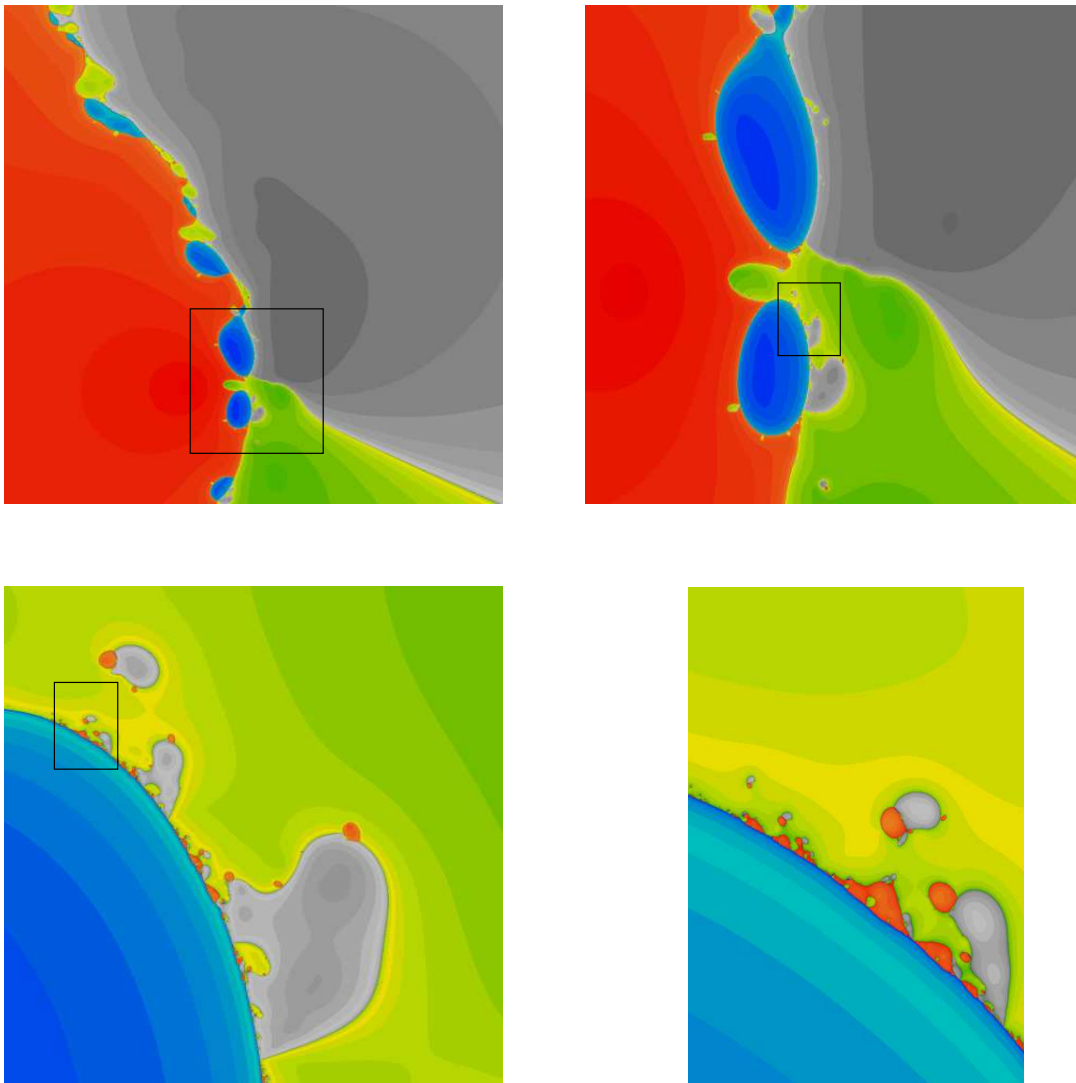


Figure 2.1: Slices through \mathbb{C}^2 along the line $y = (1 + .1i)x$ with parameters $(\alpha, \beta) = (1.2 + 0.3i, 0.2 + 0.5i)$. Three successive zooms are made, with the location of each zoom indicated by the black box in the previous image.

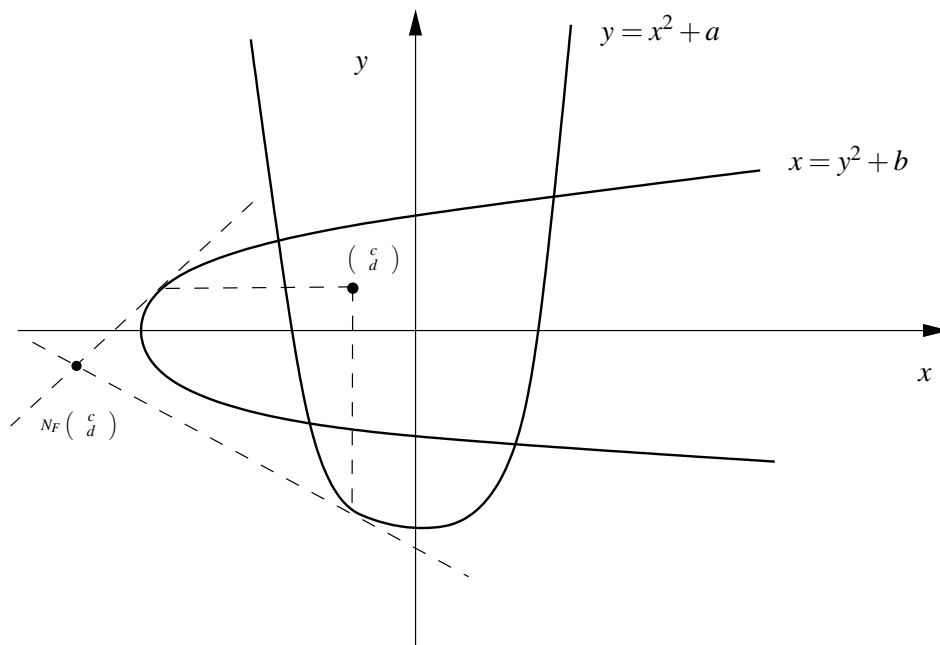


Figure 2.2: Geometric computation of $N_F(c, d)$

There is a nice geometric interpretation of N_F in this normalization. Given a point $(\frac{c}{d})$, to find $N_F(\frac{c}{d})$, one first finds the points $(\frac{c}{c^2+a})$ on the parabola $y = x^2 + a$ and the point $(\frac{d^2+b}{d})$ on the parabola $x = y^2 + d$. Then, $N_F(\frac{a}{d})$ is the intersection of the line tangent to the parabolas $y = x^2 + a$ at $(\frac{c}{c^2+a})$ with the line tangent to $x = y^2 + b$ at $(\frac{d^2+b}{d})$. Figure 2.2 illustrates this process.

One can easily check from Equation 2.7 that this geometric interpretation is accurate. Sometimes the two tangent lines are parallel, or even coincide. When they are parallel, one can define $N_F(\frac{a}{d})$ to be the point “at infinity” in \mathbb{P}^2 defined by the direction of the two parallel lines. When the two tangent lines coincide, this fails, and there is a point of indeterminacy of N_F at $(\frac{c}{d})$. Both of these issues will be discussed later.

2.3 Global properties of N_F

Many of the methods used in [35] and in this dissertation rely upon extending N_F to \mathbb{P}^2 , the complex projective plane.

Proposition 2.3.1. *N_F extends to a mapping $N_F : \mathbb{P}^2 \rightarrow \mathbb{P}^2$ with 5 points of indeterminacy, the three intersections of the invariant lines and the two points at infinity on the axes of the parabolas.*

We prove Proposition 2.3.1 in the appendix since it involves some lengthy, but elementary computations in homogeneous coordinates. The extension that we obtain is:

$$N_F([X : Y : Z]) =$$

$$[2YX^2 + Y^2Z - 2aYZ^2 - bZ^3 : 2XY^2 + X^2Z - 2XZ^2b - aZ^3 : 4XYZ - Z^3].$$

The points of indeterminacy are the points where $N_F([X : Y : Z]) = [0 : 0 : 0]$ for some triple $[X : Y : Z] \neq [0 : 0 : 0]$. They are easy to find using Equation 2.8 when $Z = 0$, this gives $[2YX^2 : 2XY^2 : 0]$, which is zero whenever $X = 0$ or $Y = 0$, corresponding to the point at infinity on the axes of the parabolas $y = x^2 + a$ and $x = y^2 + b$. It is more difficult to use Equation 2.8 to determine the points of indeterminacy in the finite plane ($Z \neq 0$). However, using the geometric interpretation of N_F in Normalization 2.4, we see that the points of indeterminacy in \mathbb{C}^2 are the points (c, d) that result in a common tangent to the two parabolas. There are three common tangents to the parabolas, so there are exactly three points of indeterminacy in \mathbb{C}^2 .

Note: if we were working in Normalization 2, these points of indeterminacy that are in \mathbb{C}^2 are the points of intersection of the lines joining the roots that are not the roots themselves.

One can do ‘‘Blow-ups’’ to extend N_F to a continuous mapping on a modification of \mathbb{P}^2 .

Proposition 2.3.2. *If the parabolas of equation $y = x^2 + a$ and $x = y^2 + b$ are not tangent, then the mapping N_F extends to the blow-up of \mathbb{P}^2 at the five points of indeterminacy, mapping each exceptional divisor to a line tangent to both parabolas.*

We will refer the reader to Proposition 1.5.4 from [35], since we will do plenty of blow-ups later in this paper.

In fact, performing the blow-ups at these points of indeterminacy is not sufficient to make N a well-defined *dynamical system*. We will say more about this in the following section.

It is a classical result (known to Cayley?) that the dynamics of the Newton map $N(z)$ to solve for the roots of a quadratic polynomial $p(z)$ is always conjugate to the map $z \mapsto z^2$. For the latter, the unit circle \mathbb{S}^1 forms the boundary between the basin of attraction of 0 and of ∞ . If ϕ is the map conjugating $N(z)$ to $z \mapsto z^2$, then $\phi^{-1}(\mathbb{S}^1)$ is the line in \mathbb{C} that is equidistant from the roots of p . This line forms the boundary between the the basin of the two roots of $p(z)$ and the dynamics on this line (once you add a point at infinity) are conjugate to angle doubling on the unit circle.

Proposition 2.3.3. (Invariant lines and invariant circles) *The lines joining the roots of F are invariant under Newton’s Method (N_F) and on these lines N_F induces the dynamics of the one dimensional Newton’s method to find the roots of a quadratic polynomial.*

Within each line is an invariant ‘‘circle,’’ corresponding to the points of equal distance from the two roots in the line.

(See Proposition 1.5.3 in [35])

Proof: This is easy to see in Normalization 2.4. Given any pair of roots of F , there is an affine mapping taking them to $\begin{pmatrix} 0 \\ 0 \end{pmatrix}$ and $\begin{pmatrix} 1 \\ 0 \end{pmatrix}$ and a third root to $\begin{pmatrix} 0 \\ 1 \end{pmatrix}$. The new system is also within the form of the normalization 2.4, but with the chosen pair of roots on the x -axis. Using Proposition 2.1.1, we see that if we can show that the x -axis is invariant under N_F , then we will have shown that the line connecting the chosen pair of roots is also invariant

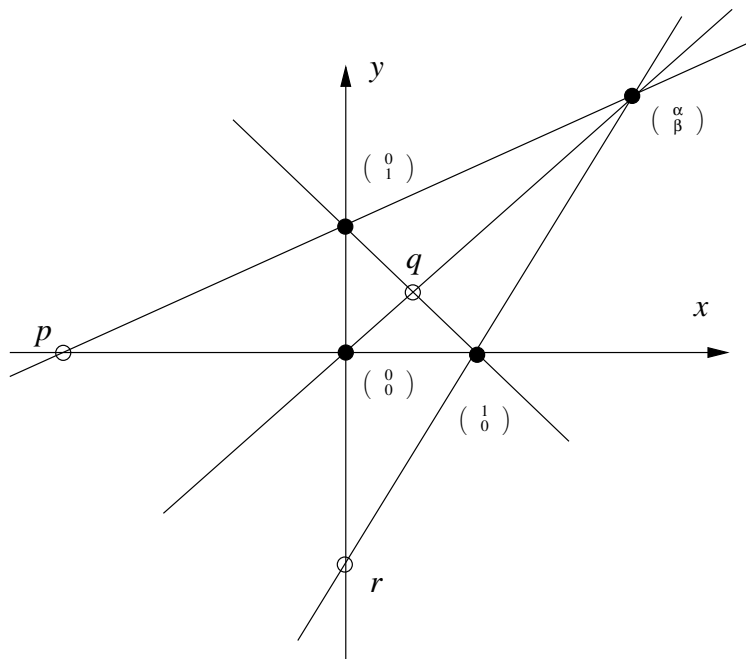


Figure 2.3: Invariant lines and invariant circles

under N_F . But this is easy to see because there is a factor of y in the second coordinate of equation 2.4 for N_F , giving that the x -axis is in fact invariant.

The dynamics on the x -axis correspond to taking the first coordinate of N_F in the normalization 2.4 with $y = 0$. One finds $x \mapsto \frac{x(Bx^2-x)}{2Bx^2-(2+B)x+1} = \frac{x^2}{2x-1}$. This is the Newton's Method to solve $x(1-x) = 0$. Using the transformation rules from Proposition 2.1.1, we see that the dynamics on each invariant line must be conjugate to this map via an affine map, hence it must be the dynamics of Newton's method for finding the roots of a quadratic polynomial. The "invariant circle" is the line of equal distance between the two roots, and the dynamics on this circle are conjugate to angle doubling on the circle. \square .

These invariant lines will be important throughout this paper. Figure 2.3 shows all six invariant lines for a certain choice of A and B . The roots of F are marked by filled dots, and the three points of indeterminacy of N_F are marked by open dots and labeled p , q , and r .

The fact that each invariant line intersects only two basins of attraction is visible in \mathbb{R}^2 . Figure 2.4 shows the basins of attraction in \mathbb{R}^2 in Normalization 1, when the fourth root is at $(\alpha, \beta) = (2, 3)$. Notice that each of the invariant lines appears to intersect only two basins.

Chapter 2 of [35] focuses on the stability of these invariant circles, which is quite a delicate issue, since they are not uniformly hyperbolic. For some parameter values Hubbard and Papadopol are able use holomorphic motions to prove that these circles have topological stable manifolds.

Given four points in \mathbb{C}^2 , so long as no three of these points lie on a line, they determine

exactly two parabolas.

Proposition 2.3.4. *The critical value locus of N_F is the union of the two parabolas that go through the four roots of F .*

In Normalization 2.7, the critical value locus is therefore the union of the two curves $y = x^2 + a$ and $x = y^2 + b$. The critical points locus is the union of the two cubics of equation $2xy^2 - x^2 + 2xb - y + a = 0$ and $2x^2y - y^2 + 2ay - x + b = 0$.

Proof: Denote the parabola $y = x^2 + a$ by Y and the parabola $x = y^2 + b$ by X . We first check that any point (u_0, v_0) that is not on the curves X or Y is a regular value. To do so, we'll show that given any inverse image (x_0, y_0) , there is a locally defined analytic inverse from a neighborhood U of (u_0, v_0) to a neighborhood of (x_0, y_0) . We denote this mapping by $\Phi = (\phi_1(u, v), \phi_2(u, v))$ for $(u, v) \in U$.

We choose U to be some small neighborhood of (u_0, v_0) which is disjoint from X and Y . We check that $\phi_1(u, v)$ is an analytic function in U . A tangent line from (u, v) to Y can be obtained by a slight change in the original tangent line from $(y_0^2 + b, y_0)$ to (u_0, v_0) . Using this new tangent line, define $\psi(u, v) = (x, y)$. Clearly $\phi_1(u, v)$ is the first coordinate of ψ , so checking that ψ is analytic will prove that ϕ_1 is analytic.

The mapping ψ is defined implicitly by the following equation:

$$\begin{aligned} G_1(x, y, u, v) &= 2x(u - x) - v + y = 0 \\ G_2(x, y, u, v) &= x^2 - y + b = 0 \end{aligned}$$

since the first equation states that (u, v) is on the tangent line to Y at (x, y) and the second states that (x, y) is a point on X . One can solve for (x, y) as an analytic function of (u, v) if the following Jacobian is non-singular:

$$\det \begin{bmatrix} 2(u-x) - 2x & 1 \\ 2x & -1 \end{bmatrix} = -2(u-x) + 2x - 2x = -2(u-x)$$

Hence, ψ is analytic for every (u, v) in the neighborhood U since $u = x$ for a solution of this equation implies that $v = y$, contrary to the fact that U is disjoint from the curves X and Y . Therefore, the first coordinate of Φ is analytic on U .

An entirely symmetric proof gives that the second coordinate of Φ is also analytic on U .

Looking carefully at the above proof, one can see that points on X and Y are actually critical values. At inverse images of these points DN_F only covers the line tangent to the curve. Hence, at inverse images of points on X or on Y , but not on both, DN_F has rank 1. At inverse images of points on both X and Y , i.e. the roots themselves, DN_F is identically zero.

In Normalization 2.7, one can check that N_F maps the cubics $2xy^2 - x^2 + 2xb - y + a = 0$ and $2x^2y - y^2 + 2ay - x + b = 0$ to X and Y with degree 2. \square

The reader should be aware that the critical value locus in Normalization 1 is not generally the union of the zero sets of P and Q . In this normalization the zero sets of P and Q are not parabolas.

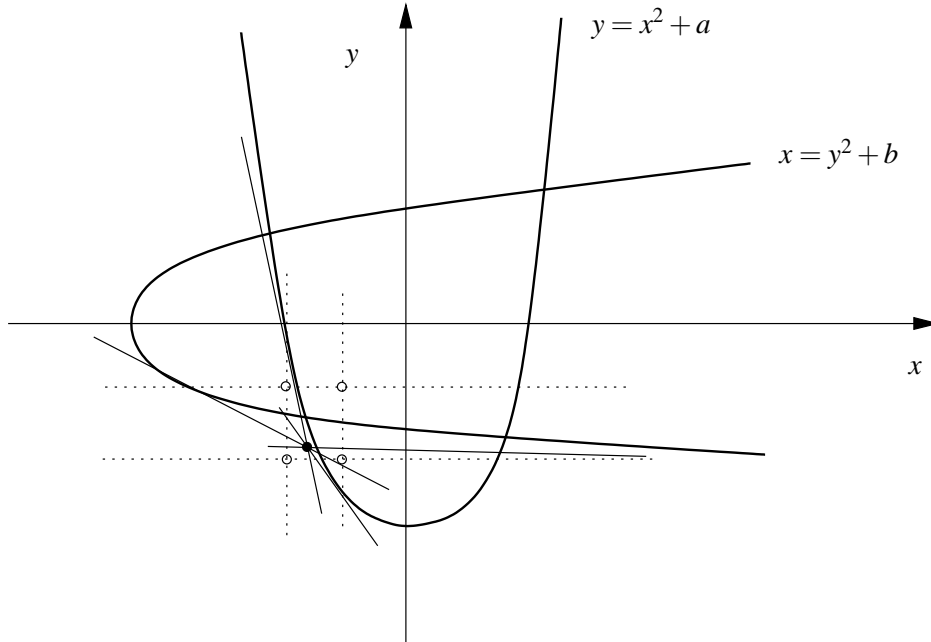


Figure 2.5: Geometric computation of inverse images

Proposition 2.3.5. *The Newton Map has topological degree 4.*

Proof: Recall the geometric interpretation of N_F in Normalization 2.7. Given a point $\begin{pmatrix} c \\ d \end{pmatrix}$ that is not in the critical value locus, hence not on either of the parabolas $y = x^2 + a$ or $x = y^2 + b$, there are two lines from $\begin{pmatrix} c \\ d \end{pmatrix}$ tangent to each of the parabolas. The points mapped to $\begin{pmatrix} c \\ d \end{pmatrix}$ by N_F are then the points of intersection between the vertical lines through the points of tangency of these lines with $y = x^2 + a$ and the horizontal lines through the points of tangency to $x = y^2 + b$. There are four such points, so N_F has degree 4. \square

We note that this extends nicely to show that a point on one of the parabolas has two inverse images, unless it is a root of F , in which case it has a single inverse image under N_F , the root itself.

Figure 2.5 shows the four inverse images of the black dot obtained by the method described above.

2.4 Making N a well-defined dynamical system

If the one wants make N a continuous mapping, one can blow-up at the points of indeterminacy p, q and r . After doing this, since we have blown-up at p , replacing p by the complex line (exceptional divisor) E_p , it is not clear to which point or points on E_p N_F should map (x, y) . To make $N_F(x, y)$ well-defined, we need to blow-up at (x, y) . (In fact, if (x, y) is a critical point, we will have to blow up two or more times above (x, y)). But doing this results in points of indeterminacy at each point that was mapped to (x, y) by N .

To make N_F well-defined at each of the repeated inverse images of the points of indeterminacy, p, q , and r we need to blow-up at every repeated inverse image of p, q , and r . (Formally this is achieved by an inverse limit.)

So long as there is no degeneracy (like one of the conics P or Q reducing to a pair of parallel lines), the points that one blows up accumulate in \mathbb{P}^2 . Without further work, these points of accumulation are terribly wild (for instance, every neighborhood has infinitely generated second homology.)

Chapter 3

General facts about the topology of the basins.

Given a root r_i of F , denote the basin of attraction under N_F by $W(r_i)$. In this chapter we will review the results that were proved by Hubbard and Papadopol about the topology of the $W(r_i)$ and we will then explain why it is necessary to consider these basins after the sequence of blow-ups mentioned in section 2.4 has been performed.

3.1 Facts proved by Hubbard and Papadopol about $W(r_i)$

In [35], Hubbard and Papadopol prove two surprising results about the topology of $W(r_i)$: $W(r_i)$ is path connected and $H_3(W(r_i), \mathbb{C}) = 0$.

Proposition 3.1.1. *The basin of attraction of each root r_i is path connected.*

Proof: The mapping N_F is locally four-to-one near the roots. So, we can choose a connected neighborhood U_0 of r_i such that $U_1 = N_F^{-1}(U_0)$ is connected. Define $U_k = N_F^{-1}(U_{k-1})$; we must prove that each of the U_k is path connected. Suppose that U_k is the first disconnected one, choose $\mathbf{x} \in U_k$, and choose a path γ in U_{k-1} connecting $N_F(\mathbf{x})$ to some point in U_0 . By a small perturbation of γ , we may assume that γ does not intersect the critical value locus $\Gamma_1 \cup \Gamma_2$, or the three double tangents L_1, L_2, L_3 . Then, the inverse image of γ consists of four arcs, all ending at points in U_1 . One such arc must lead to \mathbf{x} in U_k . Hence, we have connected every point in U_k to a point in U_1 , which is connected. This contradicts the assumption that U_k was disconnected. \square

Compare to Theorem 1.5.9, [35, p. 28].

Proposition 3.1.2. (Hubbard and Papadopol) *For any root r_i , $W(r_i)$ is a Stein domain.*

We refer the reader to [35, p. 122].

Theorem 3.1.3. *If M is a Stein Manifold of complex dimension n , then $H_i(M, \mathbb{C}) = 0$ for $n < i \leq 2n$.*

This is carried out in detail in Chapter 5 of Hörmander [29], culminating in Theorem 5.2.7 which states that if M is a Stein manifold of dimension n then $H^i(M, \mathbb{C}) = 0$ for $i > n$. Because we have \mathbb{C} coefficients, $H_i(M, \mathbb{C}) \cong \text{Hom}(H^i(M, \mathbb{C}), \mathbb{C}) = 0$, for $i > n$, as well. \square

Corollary 3.1.4. *For any root r_i , $H_3(W(r_i), \mathbb{C}) = 0$.*

3.2 Why do we use blow-ups?

In the proof that the basins of attraction are path connected, Hubbard and Papadopol used in an important way the fact that the path γ is one-dimensional. They were able to choose that γ is disjoint from the critical value locus and from the three double tangents L_1, L_2, L_3 . These double tangents are in the image of the exceptional divisors at the three points of

indeterminacy p , q , and r . By choosing that γ is disjoint from L_1, L_2, L_3 . we were able to completely ignore the blow-ups.

Our further considerations about the topology of $W(r_i)$ will be done after performing the sequence of blow-ups described in Section 2.4. For instance, in the remainder of this paper, we will study $H_1(W(r_i))$ for each of the basins of attraction. Suppose that we had not done blow-ups to resolve the points of indeterminacy and that we are working in \mathbb{C}^2 . In this case we can generate many homologically non-trivial loops in a basin of attraction, but the loops formed this way are in some sense tautological:

Choose one of the double tangents, say L_1 . One can find a small open ball U that intersects L_1 , is disjoint from the critical value locus of N , and entirely contained with in the basin of attraction of a single root $W(r_i)$.

Then $N^{-1}(U)$ consists of four disjoint open sets which are entirely contained in the basin $W(r_i)$, except for the point of indeterminacy p , which is not in any of the basins. Three of the components of $N^{-1}(U)$ intersect the three curves in $N^{-1}(L_1)$ and the remaining component contains the point of indeterminacy, p . Denote by \tilde{U} the component of $N^{-1}(U)$ containing p .

By construction, \tilde{U} is disjoint from the three curves $N^{-1}(L_1)$ because if there were an intersection, it would be in $N^{-1}(U)$, and \tilde{U} is disjoint from the other three components of $N^{-1}(U)$. Furthermore, because U is an open ball, there is a deformation retraction of U onto $U \cap L_0$. This deformation retraction lifts via N to a contraction of \tilde{U} to p .

Take a small closed curve γ within U that is linked with L_1 with linking number 1. By linked, we mean that γ is chosen such that any 2-chain σ having $\partial\sigma = \gamma$ must intersect L_1 with algebraic intersection number 1. Since γ is in U , $N^{-1}(\gamma)$ consists of four closed curves each in a different component of $N^{-1}(U) \subset W(r_i)$. Let $\tilde{\gamma}$ be the one that is in \tilde{U} . We will show that $\tilde{\gamma}$ corresponds to a non-trivial element in $H_1(W(r_i))$.

Because $\tilde{\gamma}$ is contained in the contractible set \tilde{U} , there is a 2-chain σ in \tilde{U} with $\partial\sigma = \tilde{\gamma}$. Since \tilde{U} is disjoint from the three curves in $N^{-1}(L_1)$ σ is as well, hence σ has algebraic intersection number 0 with each of these curves. The algebraic intersection number depends only on the homology class of σ , and since we are working in \mathbb{C}^2 (which has $H_2(\mathbb{C}^2) = 0$) every two chain τ with $\partial\tau = \tilde{\gamma}$ has algebraic intersection number 0 with each of the three curves in $N^{-1}(L_1)$.

This will imply that if $\partial\tau = \tilde{\gamma}$ then τ must contain the point of indeterminacy p . Since $\partial\tau = \tilde{\gamma}$, $N(\tau)$ is a 2 chain with $\partial N(\tau) = \gamma$. Because we chose γ to have linking number 1 with L_1 , $N(\tau)$ must have algebraic intersection number 1 with L_1 . Since τ has algebraic intersection number 0 with three curves in $N^{-1}(L_1)$, this can only happen if τ contains the point of indeterminacy p .

Since $p \notin W(r_i)$, τ is not entirely in $W(r_i)$ and hence $\tilde{\gamma}$ is non-trivial in $H_1(W(r_i))$. Figure 3.1 provides an illustration of this construction.

Similarly, after appropriately perturbing away from the critical value locus of N , curves in $N^{-2}(\gamma), N^{-3}(\gamma), \dots$ would all correspond to non-trivial elements of $H_1(W(r_i))$, and, in fact, one could easily prove that they correspond to an infinite set of generators of $H_1(W(r_i))$.

Within this paper we will do the sequence of blow-ups, avoiding loops of the form con-

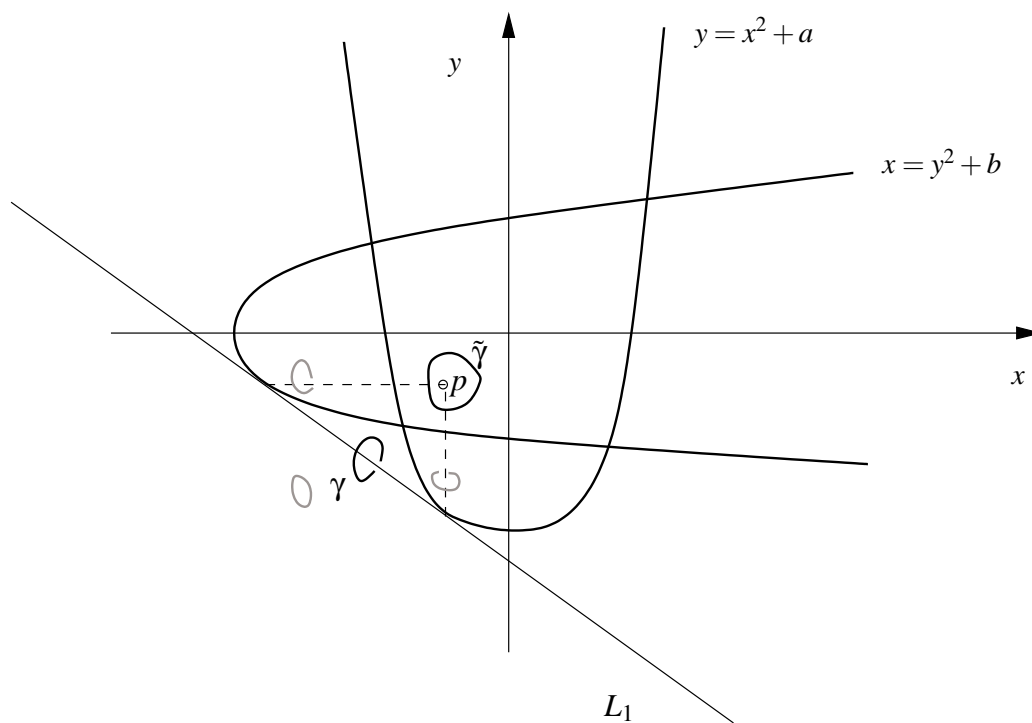


Figure 3.1: Without blow-ups, one can easily create non-trivial loops around the points of indeterminacy.



Figure 3.2: Does a curve surrounding this bubble correspond to a non-trivial loop in the orange basin? We will not be able to answer this question, but we will address a simpler but related question later in this dissertation.

structured above. We are interested in the much more subtle question: what is the topology of $W(r_i)$ within X^∞ , the space obtained from \mathbb{P}^2 after having performed the sequence of blow-ups. In particular, we will ask: within X^∞ what is $H_1(W(r_i))$. This is a much more difficult question.

By drawing slices in \mathbb{C}^2 through the basins, one finds many “bubbles” and other geometric objects which may or may not correspond to non-trivial elements of $H_1(W(r_i))$ and $H_2(W(r_i))$. See for instance the beautiful bubble shown in Figure 3.2.

The groups $H_1(W(r_i))$ and $H_2(W(r_i))$ are currently too difficult for our study, so in the remaining chapters of this dissertation, we will study $H_1(W(r_i))$ and $H_2(W(r_i))$ in the degenerate case where the parabola P becomes a pair of parallel lines. Hopefully some of the techniques developed in this degenerate case will be fruitful for some of the non-degenerate cases.

Chapter 4

The degenerate case, $A = 0$.

The case where the roots of F lie on two parallel lines is exceptional and presumably much simpler than the general case, because one variable evolves independently of the other. More precisely, if we set $A = 0$ in Normalization 1 we obtain $P(x, y) = x(1 - x)$ and $Q(x, y) = y^2 + Bxy - y$ and the roots lie on the parallel lines $x = 0$ and $x = 1$. The common roots of P and Q become $r_1 = (0, 0)$, $r_2 = (0, 1)$, $r_3 = (1, 0)$, and $r_4 = (1, 1 - B)$.

Equation 2.4 for the Newton map simplifies in the following way:

$$\begin{aligned} N_F \begin{pmatrix} x \\ y \end{pmatrix} &= \frac{1}{\Delta} \begin{pmatrix} x(Bx^2 + 2xy - x) \\ y(Bx^2 + 2xy - Bx - y) \end{pmatrix} \\ &= \begin{pmatrix} \frac{x^2}{2x-1} \\ \frac{y(Bx^2 + 2xy - Bx - y)}{(2x-1)(Bx+2y-1)} \end{pmatrix}. \end{aligned} \quad (4.1)$$

Using that when $A = 0$

$$\Delta = 2Bx^2 + 4xy - (2 + B)x - 2y + 1 = (2x - 1)(Bx + 2y - 1).$$

In the remainder of this dissertation we will drop the subscript F writing N for the Newton map with the understanding that we are always solving

$$F \begin{pmatrix} x \\ y \end{pmatrix} = \begin{pmatrix} x(1-x) \\ Q(x,y) \end{pmatrix} = \begin{pmatrix} 0 \\ 0 \end{pmatrix}.$$

4.1 Basic properties

The critical value locus is the union of the two parabolas going through the four roots. One of these coincides with $P(x, y) = x(1 - x)$, while the other is the non-degenerate parabola

$$C(x, y) = y^2 + Bxy + \frac{B^2}{4}x^2 - \frac{B^2}{4}x - y = 0 \quad (4.2)$$

We will often refer to the locus $C(x, y) = 0$ by C . Figure 4.1 shows the curves $P(x, y) = 0$ and $Q(x, y) = 0$, the critical value parabola C , and the four roots, r_1, r_2, r_3 , and r_4 .

Another property from Chapter 2 that continues to hold is that N has topological degree 4. One can also see this directly from Equation 4.1, since clearly every $x \neq 0, 1$ has two inverse images and the second component is an equation of degree two in y .

Recall from Proposition 2.3.3 that any line containing two of the roots is invariant under N . There are six such lines and, in this degenerate case, these lines have six points of intersection in \mathbb{C}^2 . Four of these intersections correspond to the roots r_1, r_2, r_3 , and r_4 , while the remaining two correspond to points of indeterminacy, which we label p and q . These are labeled as p and q in Figure 4.1.

The mapping governing the x coordinate is $x \mapsto \frac{x^2}{2x-1}$, which is itself the Newton Map corresponding to the polynomial $x(x-1)$, with Julia set consisting of the line $\operatorname{Re}(x) = 1/2$.

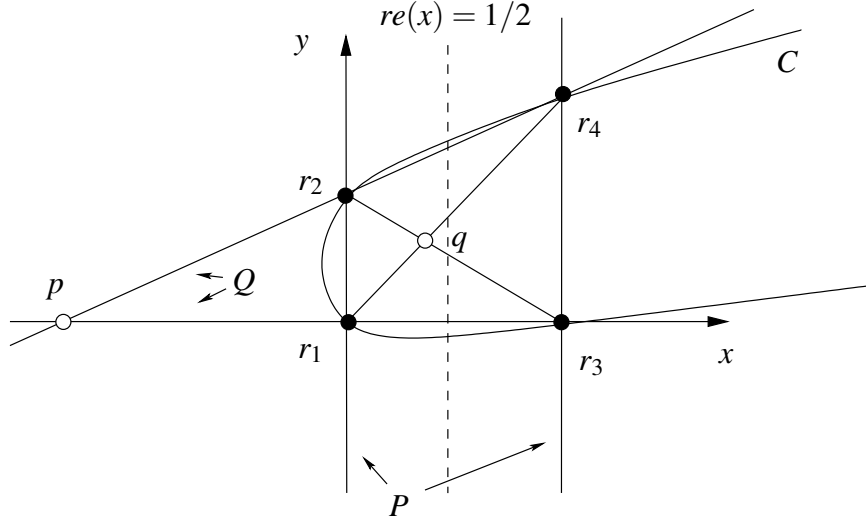


Figure 4.1: The degenerate case $A = 0$.

The dynamics of this one variable Newton map are easily understood, consequently, the dynamics of the Newton map in the form of Equation 4.1 is much easier to understand: all points in \mathbb{C}^2 with $\text{Re}(x) < 1/2$ are super-attracted to the line $x = 0$ and all points with $\text{Re}(x) > 1/2$ are super-attracted to the line $x = 1$. The vertical line at $x = m$ is mapped to the line at $x = m^2/(2m - 1)$ by the second coordinate of 4.1, which is in fact a rational map of degree 2, except at those values of m where the numerator and the denominator in the second coordinate of 4.1 have a common factor. This occurs exactly when $x = 1/B, x = 1/(2 - B)$, and $x = 1/2$. The first two correspond to the points of indeterminacy p and q .

Another way in which the dynamics simplifies for the degenerate case $A = 0$ is that one can compactify the space obtaining $N : \mathbb{P} \times \mathbb{P} \rightarrow \mathbb{P} \times \mathbb{P}$ since x evolves independently. In fact, we will only compactify in the y -direction obtaining $N : \mathbb{C} \times \mathbb{P} \rightarrow \mathbb{C} \times \mathbb{P}$, for reasons that will become apparent in the next chapter. In this simpler compactification, it is easy to see that the invariant circles in the lines at $x = 0$ and $x = 1$ are in fact super-attracting in the x -direction. We will denote these circles by S_0 and S_1 . (This is sharply in contrast with the non-degenerate case of Newton's Method in which the compactification to \mathbb{P}^2 resulted in a dense set of points on each of the invariant circles having multiplier exactly one.)

Notice that every point in $\mathbb{C} \times \mathbb{P}$ that is not above $\text{Re}(x) = 1/2$ is superattracted to the line $x = 0$ or the line $x = 1$, and consequently converges to one of the four roots, or to one of the two circles S_0 and S_1 . From this, we immediately know that N has no wandering domains and that there are no attracting periodic cycles, other than the fixed points themselves. *These are two questions that we have no idea how to answer, or even approach, in the non-degenerate case, $A, B \neq 0$, but which are easy to answer in this degenerate case.*

The points in $\mathbb{C} \times \mathbb{P}$ that are above $\text{Re}(x) = 1/2$ form a real 3-dimensional manifold that is invariant under N .

In Chapter 6 we will show that these circles have local superstable manifolds W_0^{loc} and W_1^{loc} . By pulling W_0^{loc} and W_1^{loc} back under the Newton map we generate superstable

“spaces” W_0 and W_1 , which are not generally manifolds, but real-analytic spaces. The space W_0 will form the boundary between the basin $W(r_1)$ and $W(r_2)$, and W_1 will form the boundary between the basin $W(r_3)$ and $W(r_4)$. For this reason, we will call W_0 and W_1 *superstable separatrices*. Figure 4.2 shows an illustration of these separatrices.

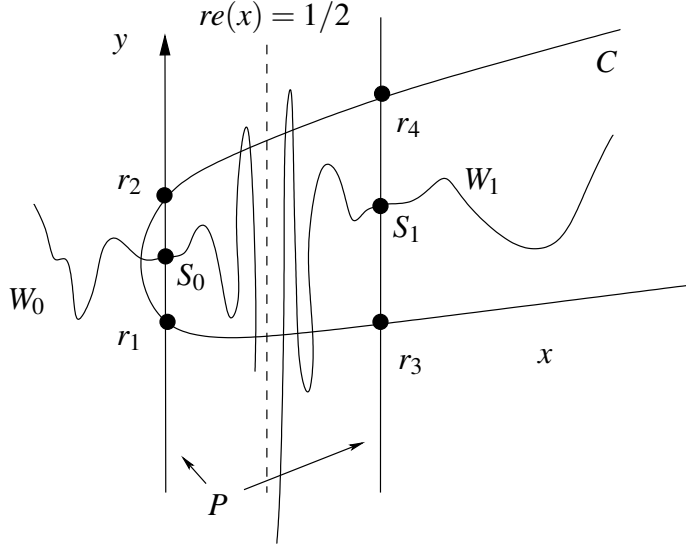


Figure 4.2: Superstable separatrices in the degenerate case, $A = 0$.

The following symmetry will play a surprisingly important role in the last chapter of this paper.

Proposition 4.1.1. (Axis of symmetry) *Let τ denote the vertical reflection about the line $Bx + 2y - 1 = 0$, that is: $\tau(x, y) = (x, 1 - Bx - y)$. Then, τ is a symmetry of N :*

$$\tau \circ N = N \circ \tau.$$

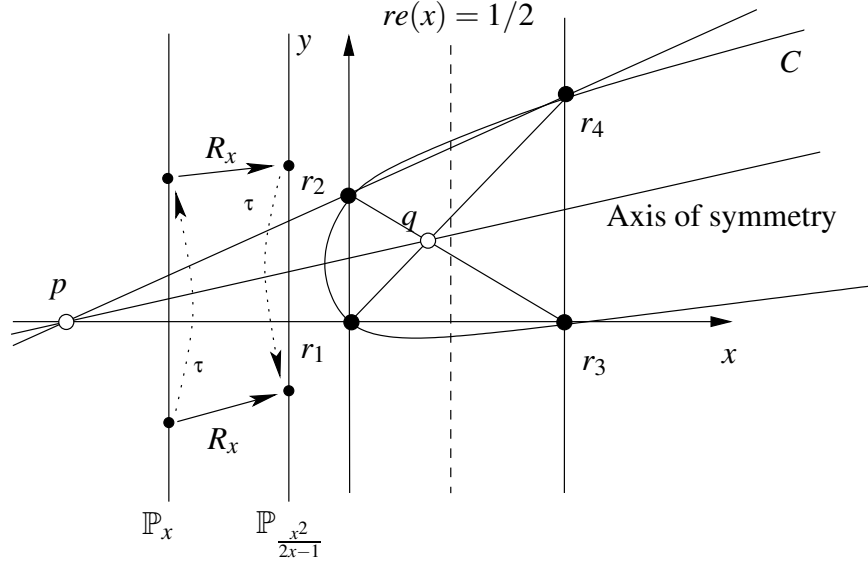
Furthermore, N maps this axis of symmetry to the line $y = \infty$.

Below it will be convenient to denote the second component of $N(x, y)$ by $R_x(y)$. This symmetry τ is illustrated by the dotted arrows in Figure 4.3.

Proof: This vertical symmetry about $2y + Bx - 1 = 0$ is exactly the affine map that interchanges r_1 with r_2 and interchanges r_3 with r_4 . Let $F \begin{pmatrix} x \\ y \end{pmatrix} = \begin{pmatrix} P(x, y) \\ Q(x, y) \end{pmatrix}$ so that r_1, r_2, r_3 , and r_4 are the roots of F . By Proposition 2.2.1, the Newton map $N_{F \circ \tau}$ for finding the roots of $F \circ \tau$ is the same as N , since they have the same roots. By the transformation, Proposition 2.1.1, $N_{F \circ \tau} = \tau^{-1} \circ N \circ \tau$. Hence:

$$\tau \circ N = \tau \circ N_{F \circ \tau} = \tau \circ \tau^{-1} \circ N \circ \tau = N \circ \tau$$

Alternatively, one can just check computationally. Since τ does not change the x -

Figure 4.3: The symmetry τ .

coordinate, only check that $\tau\left(\frac{x^2}{2x-1}, R_x(y)\right) = \left(\frac{x^2}{2x-1}, R_x(\tau(x, y))\right)$:

$$\begin{aligned}
 & 1 - B\left(\frac{x^2}{2x-1}\right) - R_x(y) \\
 = & \frac{(2x-1)(-Bx+1-2y)}{(2x-1)(-Bx+1-2y)} - B\left(\frac{x^2(-Bx+1-2y)}{(2x-1)(-Bx+1-2y)}\right) \\
 & \frac{y(Bx^2+2xy-Bx-y)}{(2x-1)(Bx+2y-1)} \\
 = & \frac{(1-Bx-y)(Bx^2-2x+2xy+1-y)}{(2x-1)(-Bx+1-2y)} \\
 = & \frac{(1-Bx+y)(Bx^2+2x(1-Bx+y)-Bx-(1-Bx+y))}{(2x-1)(Bx+2(1-Bx-y)-1)} \\
 = & R_x(1-Bx-y)
 \end{aligned}$$

The naturality mentioned above is the reason why this computation actually works.

The axis of symmetry $Bx+2y-1=0$ is mapped to the line $y=\infty$ by N because of the factor $Bx+2y-1=0$ in the denominator of R_x . Since $y=\infty$ is invariant under N and attracted to the points at infinity on the invariant circles it is in W_0 and W_1 , so $Bx+2y-1=0$ is also in W_0 and W_1 . \square

Because this symmetry swaps r_1 and r_2 and swaps r_3 and r_4 , it interchanges $W(r_1)$ with $W(r_2)$ and interchanges $W(r_3)$ with $W(r_4)$.

4.2 Computer exploration of N

In this section we will show computer images of the basins of attraction for the four common zeros of P and Q for $B = 0.769 - 0.625i$, and $B = 0.887 - .1371i$. The separatrices W_0 and W_1 are clearly visible in these images forming the smooth boundary between pairs of basins. The symmetry τ will also be evident, especially in slices along vertical lines.

According to our computer images, these two parameter values correspond to different types of dynamics: In the first, both of the superstable separatrices W_0 and W_1 intersect the critical value parabola C , and in the second case, the superstable separatrix W_0 intersects C , but W_1 appears not to intersect C . More specifically, for $B = 0.769 - 0.625i$ there are clearly clearly points in the green basin sharing a common boundary with points in the red basin in Figures 4.4 and 4.5. This common boundary is $W_1 \cap C$ and the common boundary between the blue basin and the gray basin is $W_0 \cap C$.

For $B = 0.887 - .1371i$, one cannot find any places where the green and red basins share a common boundary in Figures 4.8 and 4.9, so there appears to be no intersection between W_1 and C . We do see many places where the blue and the gray basins share a common boundary, corresponding to the intersection between W_0 and C .

Case 1: $B = 0.769 - 0.625i$

The first kind of slice that we will be looking is that of the critical value parabola C , i.e. $C(x, y) = y^2 + Bxy + \frac{B^2}{4}x^2 - \frac{B^2}{4}x - y = 0$. Figure 4.4 shows an example of such a slice and Figure 4.5 offers a zoomed in view of the region enclosed in the rectangle drawn in Figure 4.4. The center of the symmetry τ is in the center of Figure 4.4, but outside of Figure 4.5. Notice how reflection across the center of Figure 4.4 is a symmetry interchanging the basins of attraction.

The other type of one dimensional slice is along a vertical (complex) line, that is a complex line of constant x . Figure 4.6 shows the vertical line through the point a that is labeled from Figure 4.5, above, as well as the vertical lines through three inverse images of a . We have placed the center of the symmetry τ at the center of these images. Notice how reflection across this point is clearly a symmetry of these images that interchanges the basins.

Notice how the line $x = a_1$ is divided into two regions in $W(r_1)$ and two regions in $W(r_2)$. This is because we had chosen that a is a point on the superstable separatrix W_0 separating $W(r_1)$ from $W(r_2)$. The vertical line at $x = a_2$ and at $x = a_3$ are also shown. The line $x = a_2$ is divided into three regions in $W(r_1)$ and three regions in $W(r_2)$. The line $x = a_3$ is divided into five regions in $W(r_1)$ and five in $W(r_2)$. This behavior is expected and we describe it in detail in Chapter 8.

Figure 4.7 shows a similar sequence of vertical lines, but this time with the first line chosen to contain the point b in Figure 4.5. In these vertical lines W_1 forms a boundary between $W(r_3)$ and $W(r_4)$.

Case 2: $B = 0.8871 - 0.1371i$

Figure 4.8 shows the intersections of the basins of attraction for $W(r_1)$, $W(r_2)$, $W(r_3)$, and $W(r_4)$ with the critical value parabola C . Notice that there are clearly intersections of the superstable separatrix W_0 with C , these are just the boundary between blue and gray.

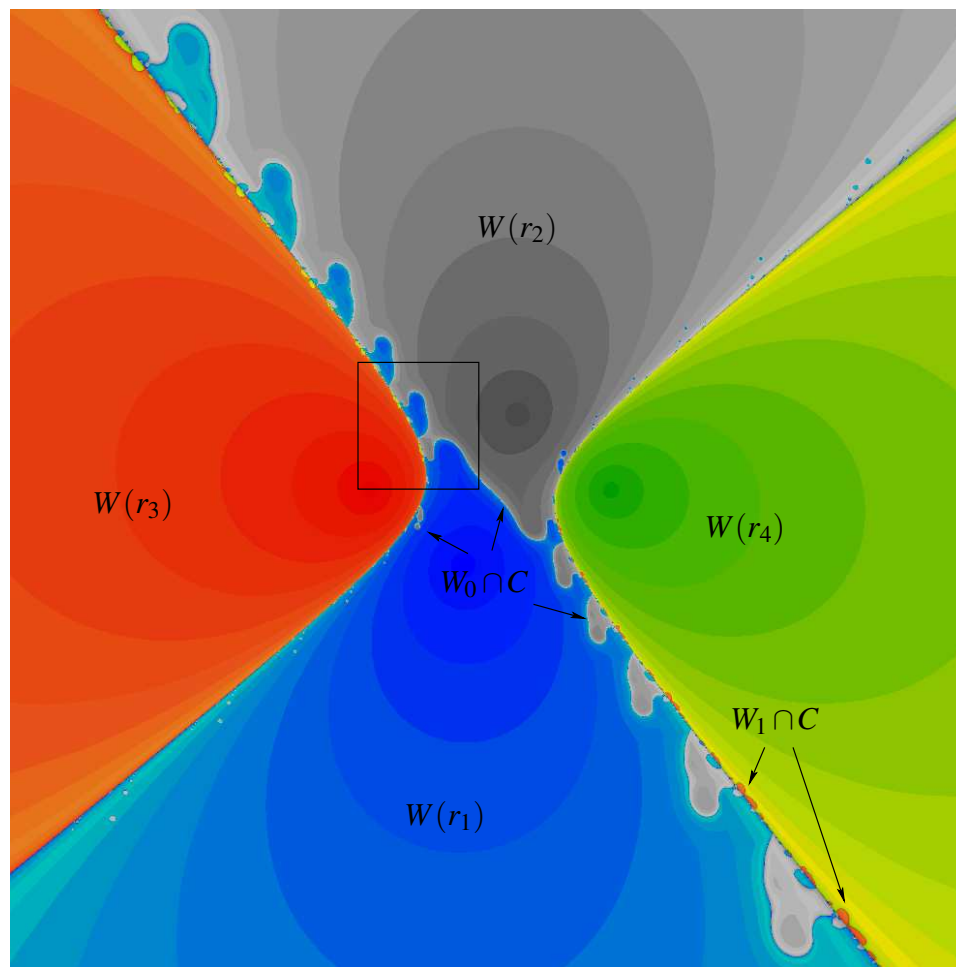


Figure 4.4: The critical value parabola C for $B = 0.769 - 0.625i$. The boundary between the green and red basins is $W_1 \cap C$ and the boundary between the blue and gray basins is $W_0 \cap C$.

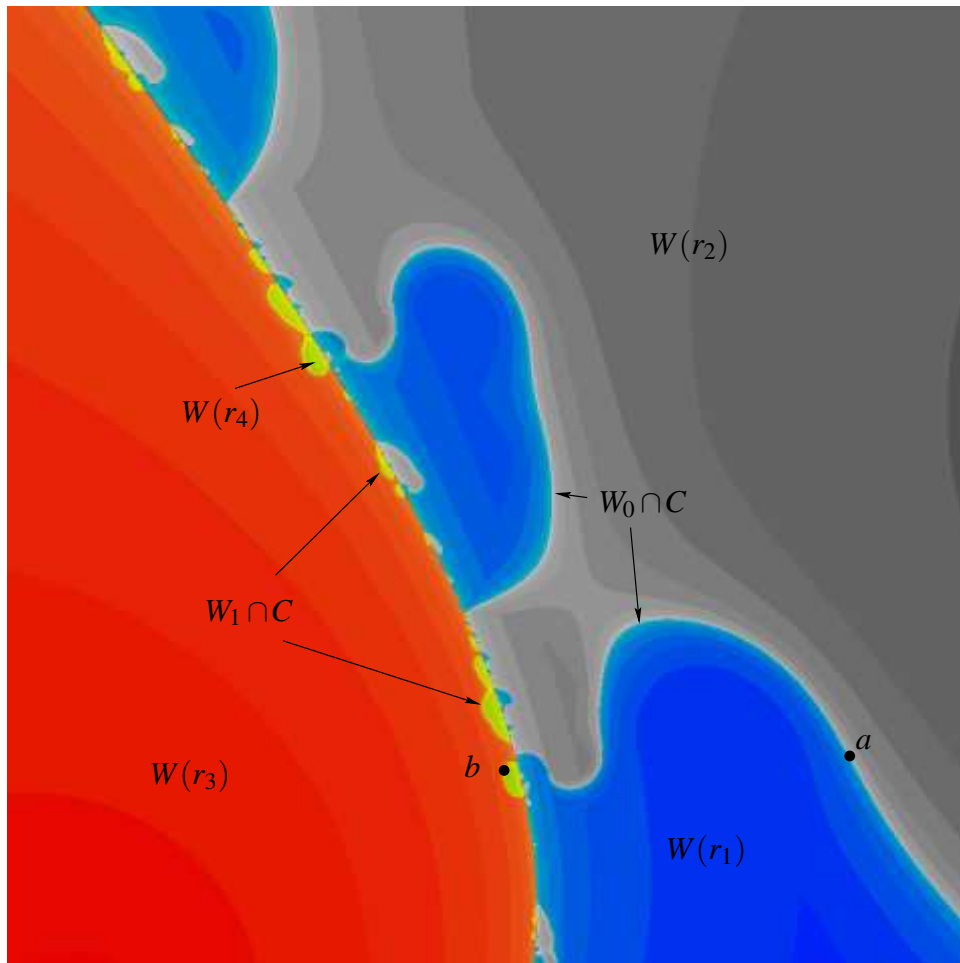


Figure 4.5: Zoomed in view from Figure 4.4.

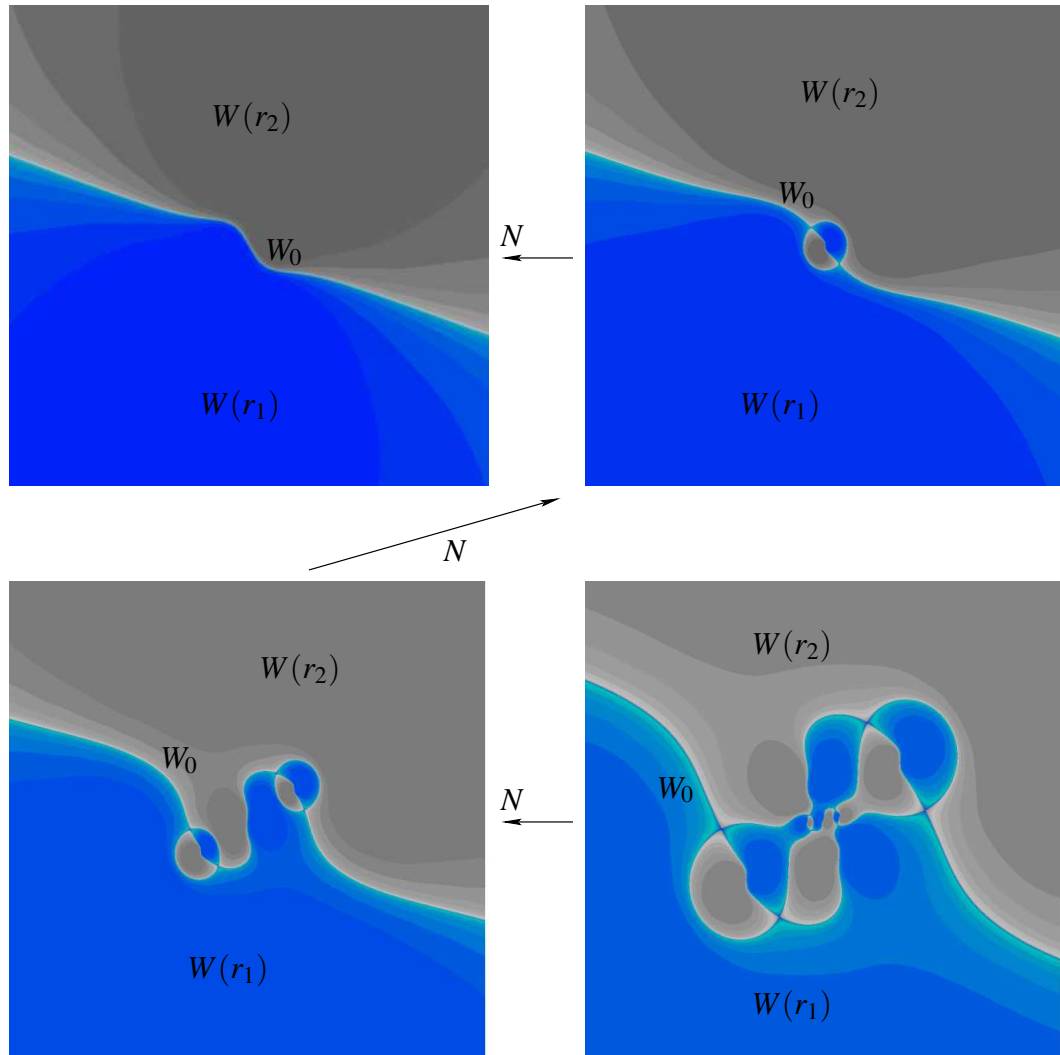


Figure 4.6: Vertical line through point a from Figure 4.5 and three inverse images of this line. The boundary between the blue and gray basins is the intersection of W_0 with these vertical lines. Notice that there are many closed loops in W_0 within these vertical lines. The center of the symmetry τ is at the center of these images.

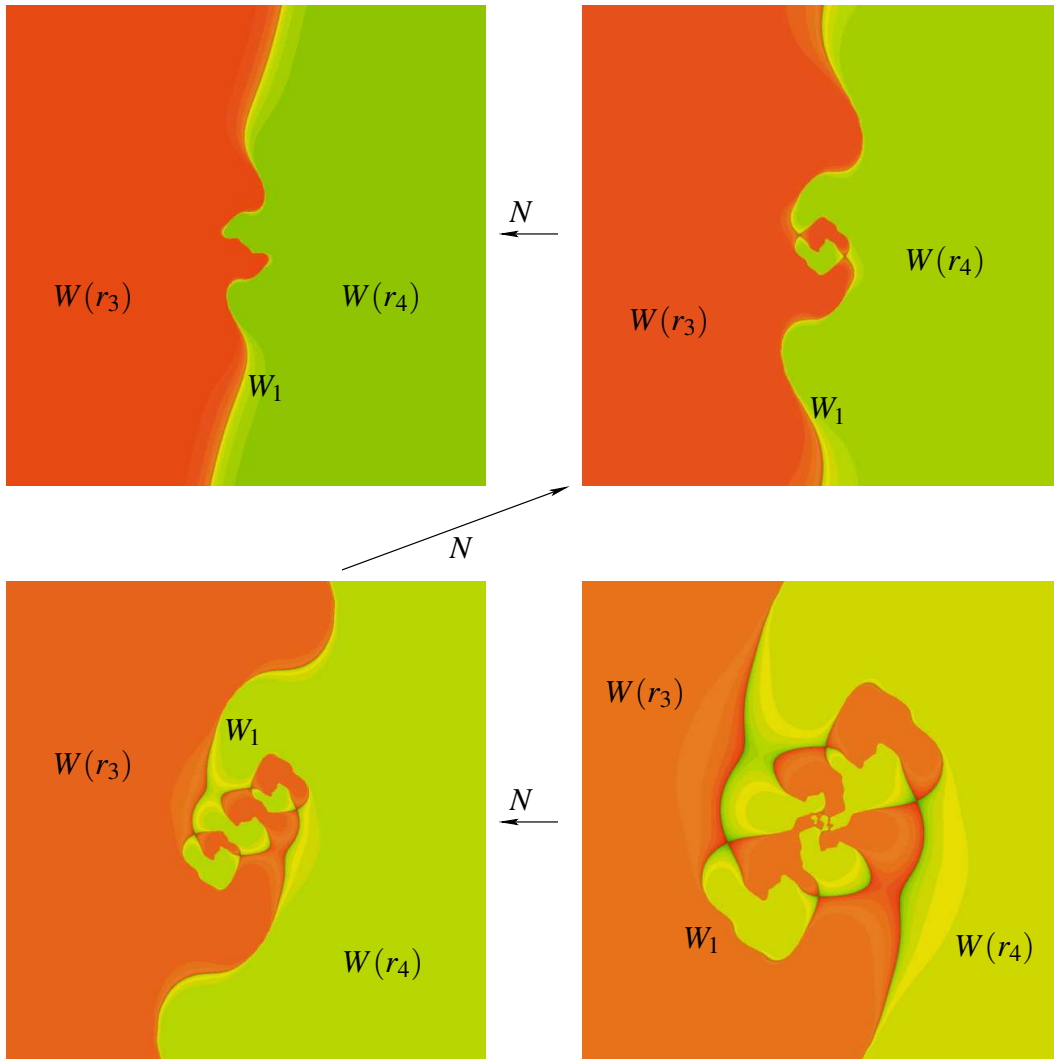


Figure 4.7: Vertical line through the point labeled b in Figure 4.5 and three consecutive inverse images of this line. The boundary between the green and red basins is the intersection of W_1 with these lines. Notice how there are an increasing number of closed loops in W_1 within the repeated inverse images of the vertical line through b .

However, we see no boundaries between the red basin and the green basin, indicating that W_1 might not intersect C . Figure 4.9 shows zoom-ins looking for intersections between W_1 and C .

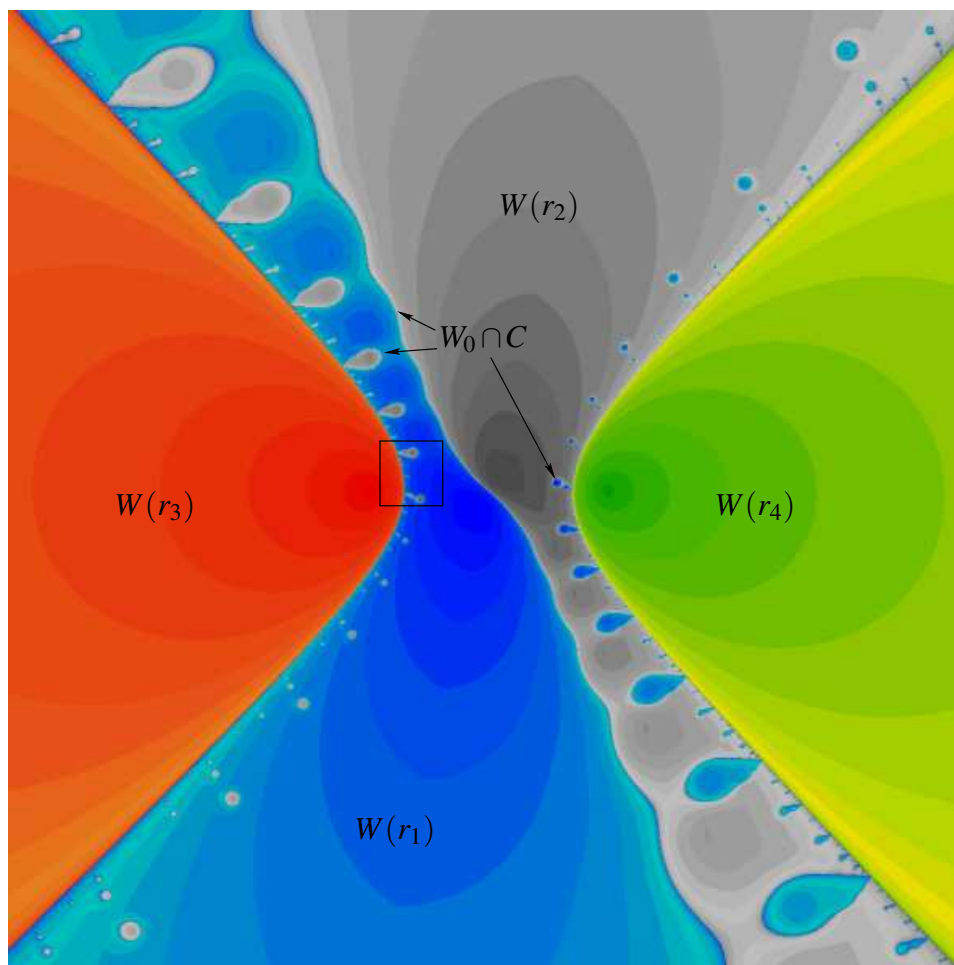


Figure 4.8: Critical value parabola C for $B = 0.8871 - 0.1371i$. The boundary between the blue and the gray basins is $W_0 \cap C$. We see no boundaries between the green and the red basins, indicating that W_1 might not intersect C .

As for the previous value of B , the vertical lines above points of intersection of W_0 with C and the vertical lines mapped to them by N contain many interestingly loops that are in W_0 .

We cannot find any intersections of W_1 with C , so in Figure 4.11 we display the intersections of 4 vertical lines with $W(r_3)$ and $W(r_4)$ above points very near to the separator, $\text{Re}(x) = 1/2$. Notice how W_1 appears very bumpy, almost fractal, and how there are no visible closed loops.

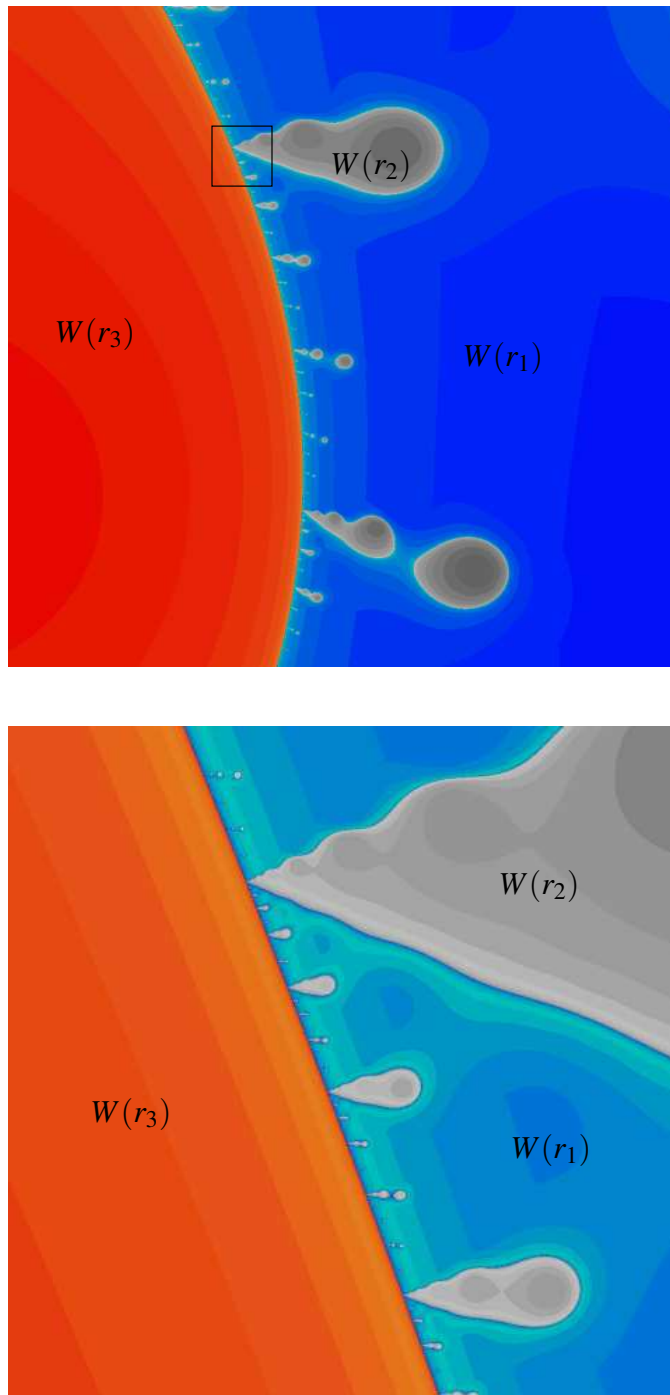


Figure 4.9: Zoomed in views of C . There is no evidence of any boundaries between the green and red basins, nor any points in the green basin at all, hence there is no evidence of intersections between W_1 and C .

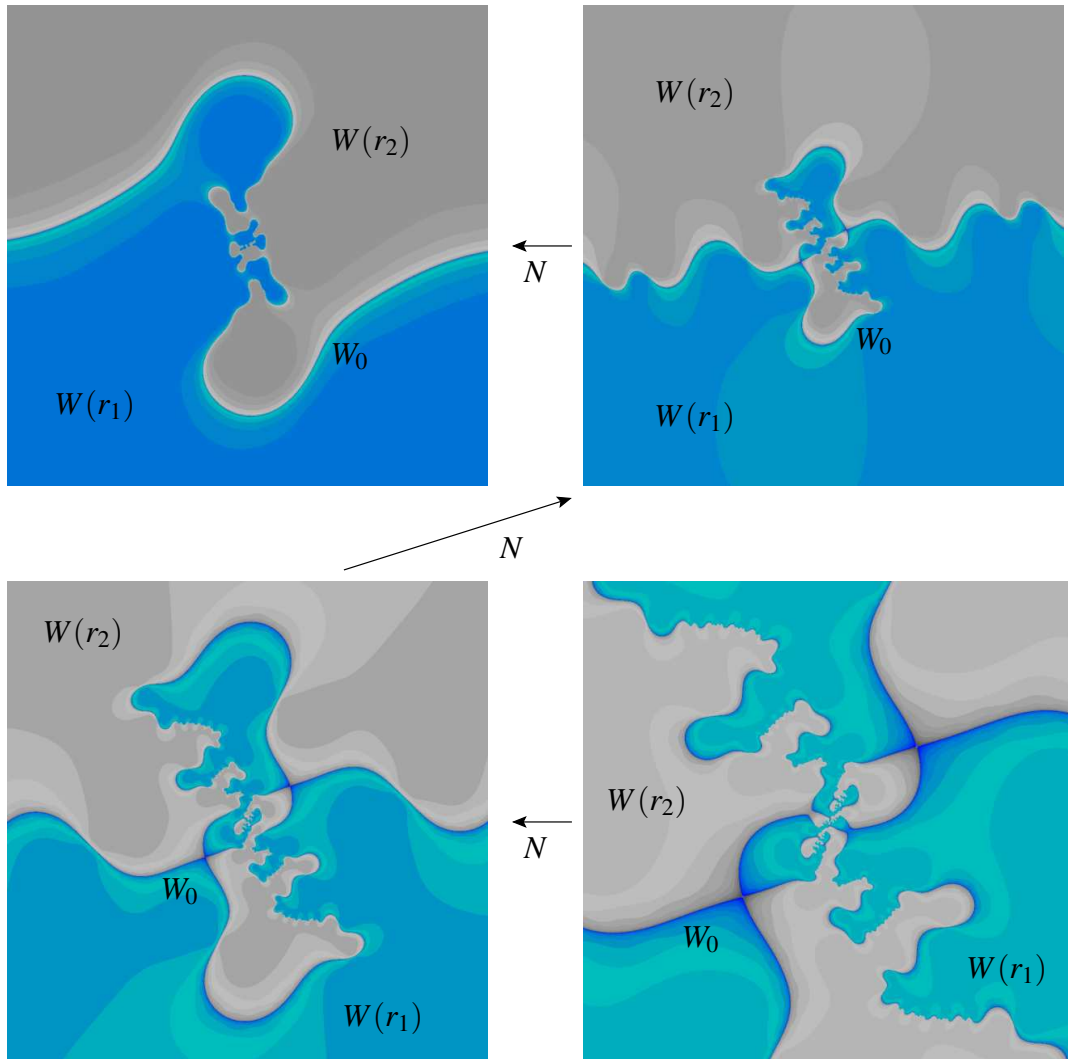


Figure 4.10: Vertical line through a point of intersection between W_0 and C , from Figure 4.8, and three inverse images of this line. As for the previous value of B , repeated inverse images of the vertical line through a point of intersection between W_0 and C lead to an increasing number of closed loops in W_0 in each of these lines.

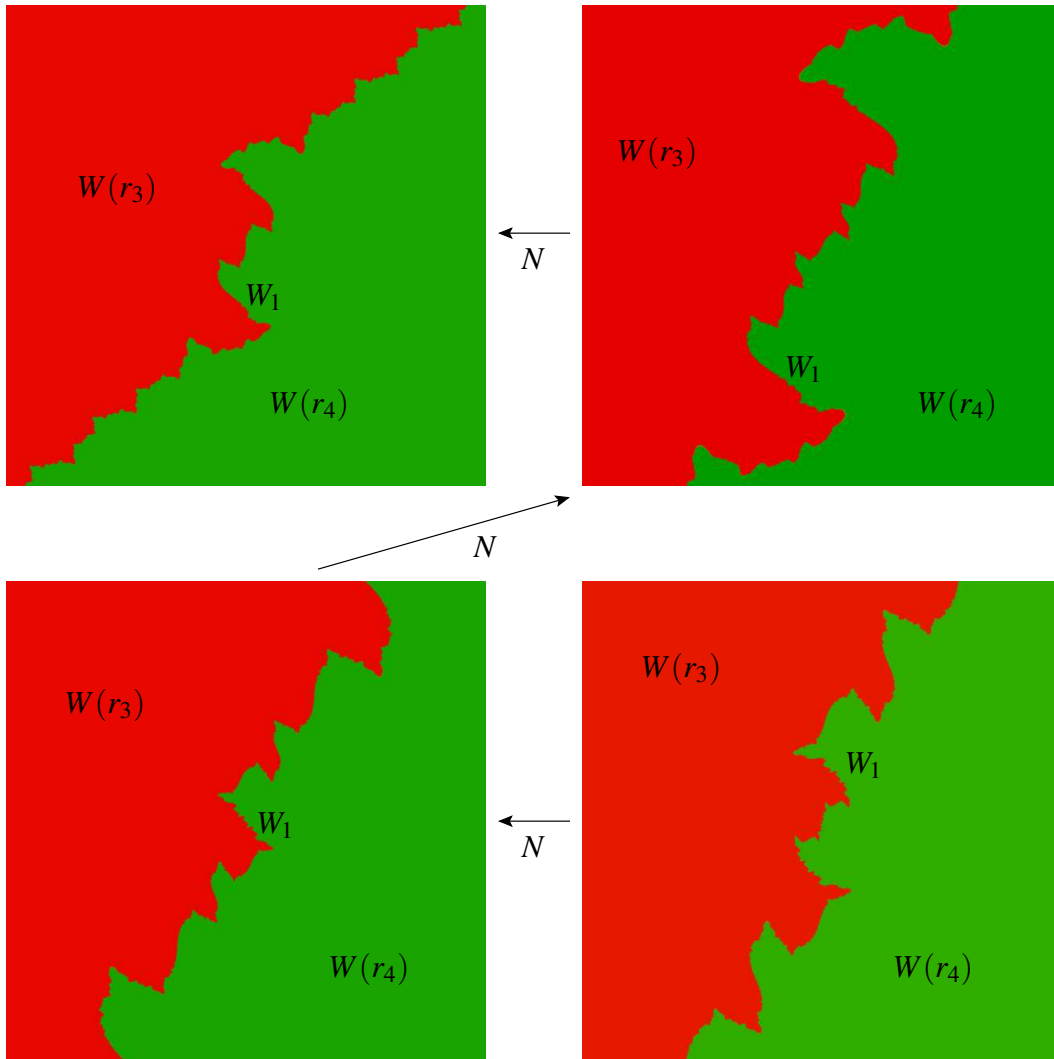


Figure 4.11: A vertical line through a point in the red basin, $W(r_3)$, within C , from Figure 4.8, and three inverse images of the vertical line. The common boundary between green and the red basins is W_1 . Notice that there are no closed loops in W_1 within any of these lines.

4.3 Parameter space Ω

Let $X_r = \{(x, y) \in \mathbb{C} \times \mathbb{P} : \operatorname{Re}(x) > 1/2\}$ and $X_l = \{(x, y) \in \mathbb{C} \times \mathbb{P} : \operatorname{Re}(x) < 1/2\}$. As mentioned earlier, both X_r and X_l are invariant under N . (The subscript r stands for “to the right of $1/2$ ” and the subscript l stands for “to the left of $1/2$ ”.)

Figure 4.1 shows the case when both points of indeterminacy p and q are in X_l . In terms of parameter B , the coordinates of p and q are $p = (\frac{1}{B}, 0)$ and $q = (\frac{1}{2-B}, \frac{1-B}{2-B})$. It is easy to check that p and q either are both in X_l , both in the separator $\operatorname{Re}(x) = 1/2$, or both in X_r . Let

$$\Omega = \{B \in \mathbb{C} : |1 - B| > 1\}.$$

If we assume that $B \in \Omega$ then both p and q are in X_l . Using the transformation properties of the Newton Map under affine changes of variables (Proposition 2.1.1) one can check that we can make this restriction without ignoring any conjugacy class of dynamics. Hence, from this point on we will always assume that $B \in \Omega$, so that $p, q \in X_l$.

There is a decomposition $\Omega = \Omega_{\text{reg}} \cup \Omega_{\text{bif}}$, where the “bifurcation locus”, Ω_{bif} , is the values of B for which there is a tangency between W_0 and C or between W_1 and C , and the “regular locus”, Ω_{reg} , is the complement of the bifurcation locus.

4.4 Statement of The Main Theorem

Let X_l^∞ be X_l after performing the sequence of blow-ups necessary to define N at p, q , and all inverse images of p and q . Let W_0 and W_1 be the superstable separatrices of the invariant circle in the lines $x = 0$ and $x = 1$.

The goal of this paper is to prove:

Theorem 4.4.1. *Let $\overline{W(r_1)}$ and $\overline{W(r_2)}$ be the closures in X_l^∞ of the basins of attraction of $r_1 = (0, 0)$ and $r_2 = (0, 1)$ under iteration of N and let $\overline{W(r_3)}$ and $\overline{W(r_4)}$ be the closures in X_r of the basins of attraction of $r_3 = (1, 0)$ and $r_4 = (1, 1 - B)$.*

- $H_1(\overline{W(r_1)})$ and $H_1(\overline{W(r_2)})$ are infinitely generated for every $B \in \Omega$.
- For $B \in \Omega$ if W_1 intersects the critical value parabola $C(x, y) = 0$ then both $H_1(\overline{W(r_3)})$ and $H_1(\overline{W(r_4)})$ are infinitely generated, otherwise $H_1(W(r_3))$ and $H_1(W(r_4))$ are trivial.

For $B \in \Omega_{\text{reg}}$, the separatrices are genuine manifolds, and, as we will see in Chapter 6 the basins and their closures in X_l^∞ and X_r have the some homotopy type. Hence:

Corollary 4.4.2. *For $B \in \Omega_{\text{reg}}$ Theorem 4.4.1 remains true when replacing the closures of each of the basins with the basins themselves.*

Indeed, for $B \in \Omega_{\text{reg}}$, $\overline{W(r_i)}$ is a manifold with boundary, hence the inclusion $W(r_i) \subset \overline{W(r_i)}$ is a homotopy equivalence.

Chapter 5

Compactification and resolution of points of indeterminacy

Because the variable x evolves independently from y , it is natural to first compactify the system as a rational map $\mathbb{P}^1 \times \mathbb{P}^1$, instead of the compactification to \mathbb{P}^2 that was used for the non-degenerate systems from the previous chapters. Unfortunately, this compactification is not the end of the story because N has points of indeterminacy at four points: $p = (1/B, 0)$, $q = (1/(2-B), (1-B)/(2-B))$, (∞, ∞) , and $(\infty, B/2)$.

We can ignore the points of indeterminacy at infinity by only considering N as a map from $\mathbb{C} \times \mathbb{P}^1$ to itself. We lose compactness, but are able to avoid many of the difficulties described in [35]. The Newton map naturally extends to the points at $y = \infty$ by $(x, \infty) \mapsto (x^2/(2x-1), \infty)$.

What do we do about the points of indeterminacy p and q in $\mathbb{C} \times \mathbb{P}^1$ and their inverse images? To make the Newton Map a well-defined dynamical system, we need to perform blow-ups at each of these points and at every inverse image of p and q .

To simplify notation, we will denote by X , the space $\mathbb{C} \times \mathbb{P}^1$. Before discussing points of indeterminacy, notice that we can partition X into three invariant subsets $X_l = \{(x, y) | \operatorname{Re}(x) < 1/2\}$, $X_{1/2} = \{(x, y) | \operatorname{Re}(x) = 1/2\}$, and $X_r = \{(x, y) | \operatorname{Re}(x) > 1/2\}$. (The subscripts “l” and “r” are meant to indicate “left of 1/2” and “right of 1/2”.) The invariance of the subsets follows directly from the invariance of the corresponding subsets in \mathbb{C} under $x \mapsto \frac{x^2}{2x-1}$, the first component of N .

We denote the space obtained by this infinite sequence of blow-ups by X_∞ . This space will presumably have a very complicated topology at any points where repeated inverse images of the points of indeterminacy, p and q , accumulate. In [35] elaborate techniques including *Farey Blow-ups* and *Real-oriented Blow-ups* are used to “tame” the topology at these points.

Using the invariance of the three subsets X_l , $X_{1/2}$, and X_r under N , we can think of N as giving separate dynamical systems on X_l and on X_r . Understanding each of these two systems is sufficient for a study of the topology of the basins of attraction for the four roots r_1, r_2, r_3 , and r_4 because none of the points in $X_{1/2}$ are in these basins.

Because we assume that $B \in \Omega$, the two points of indeterminacy $p, q \in X_l$ so all iterates of N are well-defined for every $(x_0, y_0) \in X_r$. The points of indeterminacy $p, q \in X_l$ do present a problem and we do need to do blow-ups at these points and all of their inverse images, obtaining the space X_l^∞ as the projective limit, on which we can iterate N .

The advantage of splitting up X this way is that in the space X_l , the inverse images of p and q do not accumulate, instead they go to the “Ends” of $X_l = \{\operatorname{Re}(x) < 1/2\} \times \mathbb{P}^1$ without accumulating. This makes the topology of X_l^∞ manageable.

(Note for the reader: those who have a sense of humor sometimes refer to X_l^∞ as the “bad side” and X_r as the “good side”.)

Most of the material in this section and in the following section closely follow the works of Hubbard and Papadopol [35] and Hubbard, Papadopol, and Veslov [30].

5.1 Construction of X_l^∞ and $N_\infty : X_l^\infty \rightarrow X_l^\infty$.

In this section we will describe the sequence of blow-ups necessary to make $N^{\circ k}$ well defined for each k and the inverse limit that is necessary to make a dynamical system, which we will call $N_\infty : X_l^\infty \rightarrow X_l^\infty$.

Substitution of the points p and q into $C(x, y)$ yields $\frac{1}{4}(B-1)$ and $\frac{B^2-7B+2}{4B-8}$, so values of B at which these expressions are non-zero, neither p nor q is a critical value.

More generally, let $S \subset \Omega$ be the subset of parameter space for which no inverse image of the point of indeterminacy p or of point of indeterminacy q is in the critical value locus C . It will be easiest to first describe the construction of X_l^∞ for parameter values $B \in S$, and then explain the necessary modifications for special circumstance when $B \notin S$.

It is relatively easy to show that the condition $B \in S$ is generic, in the sense of Baire's Theorem.

Theorem 5.1.1. *The set S is generic in the sense of Baire's Theorem, i.e. uncountable and dense in Ω .*

Because of its computational nature, we will leave it for Appendix B.

Construction of X_l^∞ when $B \in S$:

Proposition 5.1.2. *Let X_l^0 be the space X_l blown up at the points p and q and let $\pi_0 : X_l^0 \rightarrow X_l$ be the corresponding projection.*

- *The mapping N extends analytically to a mapping $N_0 : X_l^0 \rightarrow X_l$.*
- *N_0 maps the exceptional divisors E_p and E_q to the line $x = \frac{1}{B(2-B)}$ by isomorphisms.*

Proof: We will show the calculation in some detail for p and just state the extension for q . The definition of a blow-up and many examples are available in Appendix C.

We will work in the chart $(x, m) \mapsto (x, m(x - \frac{1}{B}), m) \in X_l \times \mathbb{P}^1$. Denote the components of the Newton map in Equation 4.1 by $N_1(x, y)$ and $N_2(x, y)$ so that $N(x, y) = (N_1(x, y), N_2(x, y))$.

In these coordinates we clearly have $N_1(x, m) = \frac{\frac{1}{B^2}}{2\frac{1}{B}-1} = \frac{1}{B(2-B)}$.

$$\begin{aligned} N_2(x, m) &= \frac{m(x - \frac{1}{B})(Bx^2 + 2xm(x - \frac{1}{B}) - Bx - m(x - \frac{1}{B}))}{(2x - 1)(Bx + 2m(x - \frac{1}{B}) - 1)} \\ &= \frac{\frac{m}{B}(Bx - 1)(Bx^2 + 2xm(x - \frac{1}{B}) - Bx - m(x - \frac{1}{B}))}{(2x - 1)(\frac{2m}{B} + 1)(Bx - 1)} \\ &= \frac{\frac{m}{B}(Bx^2 + 2xm(x - \frac{1}{B}) - Bx - m(x - \frac{1}{B}))}{(2x - 1)(\frac{2m}{B} + 1)} \end{aligned}$$

When restricted to the exceptional divisor E_p the mapping becomes

$$\begin{aligned} m \mapsto \frac{\frac{m}{B}(B\frac{1}{B^2} + 2\frac{1}{B}m(\frac{1}{B} - \frac{1}{B}) - B\frac{1}{B} - m(\frac{1}{B} - \frac{1}{B}))}{(\frac{2}{B} - 1)(\frac{2m}{B} + 1)} &= \frac{m(\frac{1}{B} - 1)}{(\frac{2}{B} - 1)(2m + B)} \\ &= \frac{m(1 - B)}{(2 - B)(2m + B)} \end{aligned}$$

If instead we had been working in the chart $(y, m') \mapsto (m'y + \frac{1}{B}, y, m')$, we would have obtained a similar extension and the mapping on the exceptional divisor is: $m' \mapsto \frac{(1-B)}{(2-B)(2+m'B)}$. This is consistent with the extension in terms of m since one is obtained from the other by the change of variables $m = \frac{1}{m'}$.

Both of the expressions for N restricted to E_p are linear-fractional transformations, hence N maps E_p to the line $y = \frac{1}{B(2-B)}$ by an isomorphism.

We now compute the blow-up at q in the coordinates $(x, m) \mapsto (x + \frac{1}{2-B}, m(x - \frac{1}{2-B}) + \frac{1-B}{2-B}, m)$. Just as for the point p , $N_1(x, m) = \frac{1}{B(2-B)}$. We also have $N_2(x, m) =$:

$$\begin{aligned} & \frac{(m(x - \frac{1}{2-B}) + \frac{1-B}{2-B})(Bx^2 + 2x(m(x - \frac{1}{2-B}) + \frac{1-B}{2-B}) - Bx - (m(x - \frac{1}{2-B}) + \frac{1-B}{2-B}))}{(2x - 1)(Bx + 2(m(x - \frac{1}{2-B}) + \frac{1-B}{2-B}) - 1)} \\ &= \frac{(m(x - \frac{1}{2-B}) + \frac{1-B}{2-B})((x - \frac{1}{2-B})(Bx + (1-B) + m(2x - 1))}{(2x - 1)(B + 2m)(x - \frac{1}{2-B})} \\ &= \frac{(m(x - \frac{1}{2-B}) + \frac{1-B}{2-B})(Bx + (1-B) + m(2x - 1))}{(2x - 1)(B + 2m)} \end{aligned}$$

On the exceptional divisor E_q , this map is:

$$m \mapsto \frac{(1-B)(m - 2 + 2B - B^2)}{B(2-B)(B + 2m)}$$

one can check that N also extends analytically to the one point on E_q that was not covered by this chart (corresponding to $m = \infty$.)

Both of the expressions for N restricted to E_p are linear-fractional transformations, hence N maps E_p to the line $x = \frac{1}{B(2-B)}$ by an isomorphism. \square

We will denote the vertical line $x = \frac{1}{B(2-B)}$ by V , since we use this line so frequently. This is the vertical line that is tangent to C at its ‘‘vertex’’.

Because we assume that $B \in \mathcal{S}$, we assume that neither p nor q are critical values, each has four inverse images under N_0 . Because we have blown-up at p and q , each of these inverse images becomes a point of indeterminacy for N_0 . We can then blow-up at each of these eight points obtaining the space X_l^1 and the projection $\pi_1 : X_l^1 \rightarrow X_l^0$. One can then extend N_0 to the exceptional divisors, obtaining $N_1 : X_l^1 \rightarrow X_l^0$.

To make iterates N^{ok} of N well-defined for all k we must repeat this process for the k -th inverse images, obtaining successive blow-ups $\pi_k : X_l^k \rightarrow X_l^{k-1}$ for every k . The following proposition describes the extension of N to these spaces:

Proposition 5.1.3. *Denote by X_l^k the space X_l^{k-1} blown-up at each of these $2 \cdot 4^k$ k -th inverse images of p and q .*

- *The mapping N_{k-1} extends analytically to a mapping $N_k : X_l^k \rightarrow X_l^{k-1}$.*
- *Suppose that z is one of the k -th inverse images of p or q and denote the exceptional divisor over z by E_z . Then, N_k maps E_z to $E_{N(z)}$ by isomorphism.*

Proof: This entire construction is done as Proposition C.4.1 in the appendix. We summarize the results here. As in Proposition 5.1.2 denote the first component of N by $N_1(x, y)$ and the second component by $N_2(x, y)$. Then, in the coordinates $(x, m) \mapsto (x, mx, m)$ in a neighborhood of E_z the mapping is given by:

$$m \mapsto \frac{\partial_x N_1 + \partial_y N_1 m}{\partial_x N_2 + \partial_y N_2 m}$$

which is just the linear-fractional transformation induced from DN at z . Since DN is non-singular at z , this gives an isomorphism from E_z to $E_{N(z)}$.

So long as $B \in S$, that is none of the k -th inverse images of p or of q are critical points, the extension works in this same way at each of these $2 \cdot 2^k$ points. \square

Hence, by repeated blow-ups we obtain a sequence of spaces and projections:

$$X_l \xleftarrow{\pi_0} X_l^0 \xleftarrow{\pi_1} X_l^1 \xleftarrow{\pi_2} X_l^2 \xleftarrow{\pi_3} X_l^3 \xleftarrow{\pi_4} X_l^4 \xleftarrow{\pi_5} X_l^5 \xleftarrow{\pi_6} \dots \quad (5.1)$$

The extensions of the Newton map N to these spaces that we calculated in Propositions 5.1.2 and 5.1.3 we obtain another sequence of spaces and mappings:

$$X_l \xleftarrow{N_0} X_l^0 \xleftarrow{N_1} X_l^1 \xleftarrow{N_2} X_l^2 \xleftarrow{N_3} X_l^3 \xleftarrow{N_4} X_l^4 \xleftarrow{N_5} X_l^5 \xleftarrow{N_6} \dots \quad (5.2)$$

However, we do not have a single space X_l^∞ , nor a single mapping N_∞ from this space to itself. However, there is a standard procedure using *Inverse Limits* to create such a space and mapping from a sequence of spaces 5.1 and the sequence of mappings like 5.2. That is, we will let X_l^∞ be the inverse limit of the blown-up spaces and projections in sequence 5.1 and then use the sequence of extensions of the Newton maps 5.2 to define a mapping $N_\infty : X_l^\infty \rightarrow X_l^\infty$ which naturally corresponds to an extension of N .

There are two ways to describe the inverse limit, the first via a universal property and the second via a construction. We will briefly describe both.

Definition 5.1.4. An **Inverse system**, denoted (M_i, σ_i) , is a family of objects M_i in a category C indexed by the natural numbers and for every i a morphism $\sigma_i : M_i \rightarrow M_{i-1}$.

The **Inverse Limit** of an inverse system (M_i, σ_i) , denoted by $\varprojlim (M_i, \sigma_i)$, is an object X in C together with morphisms $\alpha_i : X \rightarrow M_i$ satisfying $\alpha_{i-1} = \sigma_i \circ \alpha_i$ for each i satisfying the following universal property:

For any other pair $Y, \beta_i : Y \rightarrow M_i$ such that $\beta_{i-1} = \sigma_i \circ \beta_i$, we have a unique morphism $u : Y \rightarrow X$ so that for each i we have $\beta_i = \alpha_i \circ u$.

For our uses, the category will always be analytic spaces and the morphisms holomorphic maps. One should notice that we have restricted the objects M_i to be indexed by the natural numbers \mathbb{N} . Inverse systems and inverse limits are typically defined for objects M_i indexed by a filtering partially ordered set I , but we do not need this level of generality here.

The following proposition gives a construction of $\varprojlim (M_i, \sigma_i)$ as a subset of the product space $\prod_i M_i$.

Proposition 5.1.5. *Given an inverse system (M_i, σ_i) indexed by \mathbb{N} (i.e. $\sigma_i : M_i \rightarrow M_{i-1}$), we can construct the inverse limit as follows:*

$$\varprojlim (M_i, \sigma_i) = \{(m_0, m_1, m_2, m_3, \dots) | m_i \in M_i \text{ and } \sigma_i(m_i) = m_{i-1}\}.$$

We define $X_l^\infty = \varprojlim (X_l^k, \pi_k)$. Using Proposition 5.1.5 we can state more concretely that

$$X_l^\infty = \{(x_0, x_1, x_2, x_3, \dots) | x_i \in X_l^i \text{ and } \pi_i(x_i) = x_{i-1}\}.$$

We now need to extend the mappings N_k to a mapping $N_\infty : X_l^\infty \rightarrow X_l^\infty$ using the sequence of mappings 5.2.

We define $N_\infty : X_l^\infty \rightarrow X_l^\infty$ by

$$N_\infty((x_0, x_1, x_2, x_3, \dots)) = (N_1(x_1), N_2(x_2), N_3(x_3), \dots).$$

Notice that $N_i(x_i) \in X_l^{i-1}$ so that this definition makes sense.

Construction of X_l^∞ when $B \notin S$:

For parameter values $B \notin S$, the blow-ups done at p and q in Proposition 5.1.2 are exactly the same, since we have seen that N extends to these blow-ups for any value of B . (It is worth noticing that there is actually a critical point of N on both E_p and on E_q .)

However, special care needs to be taken when a k -th inverse image of p and of q is a critical point of N critical points. We describe the process here, although leave some of the details for the appendix.

The goal is to produce a space X_l^k and a projection $\pi_k : X_l^k \rightarrow X_l^{k-1}$ in such a way that N extends to a map (without singularities) $N_k : X_l^k \rightarrow X_l^{k-1}$. If we can create the spaces X_l^k and extensions N_k at every ‘‘level’’ k , we can use exactly the same process above to make X_l^∞ and $N_\infty : X_l^\infty \rightarrow X_l^\infty$.

So, suppose for the moment that z is a k -th inverse image of p and that none of the n -th inverse images of p for $n < k$ were in the critical locus $N^{-1}(C)$. In this case, there is a single exceptional divisor in X_l^{k-1} above $N(z)$. Because the z is critical, the extension of N to E_z will map all of E_z (except for one point) to a single point in $E_{N(z)}$. (See Appendix, section C.4). However, at the slope $m_{ker} \in E_z$ which is in the kernel of DN , the extension to E_z has another point of indeterminacy! Consequently, one has to blow-up this point on E_z , obtaining a second exceptional divisor E'_z above m_{ker} . In Proposition C.4.2 from Appendix C, we show that N extends to E'_z by an isomorphism from E'_z to $E_{N(z)}$. Figure 5.1 shows this situation.

These two blow-ups above z are sufficient to extend N .

However, the fact that there are two exceptional divisors above z results in a further complication at every point w that is mapped to z . Suppose that we have blown-up at w . The extension of N to E_w has a point of indeterminacy at point that is mapped to $m_{ker} \in E_z$. Because of this, one has to blow-up a second time above w to resolve this point of indeterminacy. In fact, at every repeated inverse image of z one will have to blow-up at least twice to resolve N .

There are further problems is an inverse image of z is again critical. At such a point, one will have to do even more blow-ups to resolve N . A detailed description of this process becomes rather tedious, and we will stop here.

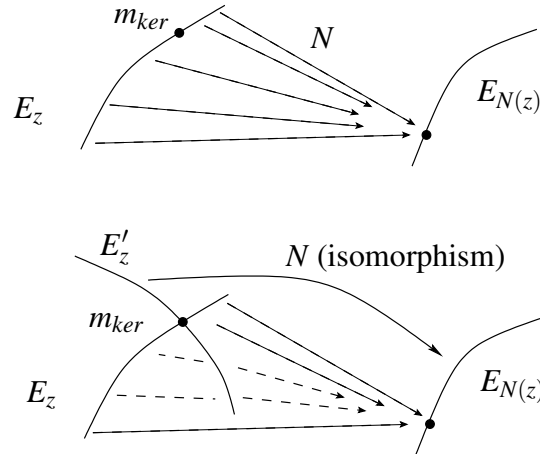


Figure 5.1: Blowing up a point on an exceptional divisor.

5.2 The mappings from E_z to V

We saw in the previous section that N maps each exceptional divisor that was newly created in X_l^k to one of the exceptional divisors newly created in X_l^{k-1} by either an isomorphism, or a constant map. Since N maps each E_p and E_q isomorphically to the line V the composition $N^{\circ k+1}$ maps each of the newly created exceptional divisors E_z in X_l^k to V either by an isomorphism, or a constant map. In summary:

Proposition 5.2.1. *Let E_z be one of the exceptional divisors newly created in X_l^k and let V be the line $x = 1/(B(2-B))$. Then $N^{\circ k+1}$ maps E_z to V by an isomorphism, or a constant map.*

5.3 Homology of X_r and of X_l^∞

Our eventual goal is to relate the homology of the basins of attraction for the four roots of F to the homology of the spaces X_r and X_l^∞ and to the homology of a “separator” which happen to be the superstable sets of the superattracting circles at $x = 0$ and $x = 1$. The next section is devoted to these superstable spaces. (We say spaces because they may have singularities for some values of the parameter B .) In this section, we will compute the homology of X_r and X_l^∞ .

Given a set S , we will denote by $\mathbb{Z}^{(S)}$ the submodule of the the product \mathbb{Z}^S where each element has at most finitely many non-zero components.

We will often find it necessary to encode information about the generators of these homology spaces within the notation describing them. For example, the module $\mathbb{Z}^{\{[K]\}}$ means the module \mathbb{Z} that is generated by the fundamental class of $[K]$.

Proposition 5.3.1. *We have:*

- $H_0(X_r) = \mathbb{Z}$

- $H_2(X_r) = \mathbb{Z}^{\{\mathbb{P}^1\}}$
- $H_i(X_r) = 0$, for $i \neq 0$ or 2 .

The homology of X_l^∞ is much more complicated. Unfortunately homology does not behave nicely under inverse limits.

Therefore, instead of directly using the fact that X_l^∞ is an inverse limit to compute it's homology, we will write X_l^∞ is a union of open subsets $U_0 \subset U_1 \subset U_2 \subset \dots$ in such a way that $H_2(U_i) = \mathbb{Z}^{(L_i \cup \{[V]\})}$ where L_i is the set of fundamental classes of exceptional divisors contained in U_i and $[V]$ is the fundamental class of the vertical line V given by $x = \frac{1}{B(2-B)}$.

Recall that the projection $\pi : X_l^\infty \rightarrow X_l$ is continuous, we will create an exhaustion of X_l^∞ by open sets $U_0 \subset U_1 \subset U_2 \subset \dots$ as inverse images of open subsets in X_l .

Let $V_k = X_l - \bigcup_{n=k}^\infty \{N^{-n}(p), N^{-n}(q)\}$. Clearly V_k is an open subset of X_l , so we will let $U_k = \pi^{-1}(V_k)$. It is also clear that $U_1 \subset U_2 \subset U_3 \subset \dots$ and that $\bigcup_{k=1}^\infty U_k = X_l^\infty$.

Lemma 5.3.2. *For each k , $H_2(U_k) \cong H_2(X_l^k)$*

Proof: Notice that U_k canonically isomorphic to $X_l^k - \bigcup_{n=k}^\infty \{N^{-n}(p), N^{-n}(q)\}$. Removing a discrete set of points from a 4 (real) dimensional manifold does not affect the second homology. Hence, $H_2(U_k) \cong H_2(X_l^k)$. \square

Lemma 5.3.3. $H_2(X_l^k) \cong \mathbb{Z}^{(L_k \cup \{[V]\})}$, where L_k is the set of fundamental classes of exceptional divisors in X_l^k .

Proposition 5.3.4. $H_2(X_l^\infty) \cong \mathbb{Z}^{(L \cup \{[V]\})}$, where L is the set of fundamental classes of exceptional divisors in X_l^∞ and $[V]$ is the fundamental class of the vertical line V .

Proof: Since $X_l^\infty = \bigcup_{k=1}^\infty U_k$ and $H_2(U_k) \cong H_2(X_l^k) \cong \mathbb{Z}^{(L \cup \{[V]\})}$, we have that $H_2(X_l^\infty) \cong \varinjlim \left(\mathbb{Z}^{(L_k \cup \{[V]\})} \right)$, which is clearly $\mathbb{Z}^{(L \cup \{[V]\})}$. \square

In the generic case where none of the inverse images of p or q under N are in the critical value parabola C , we can describe $H_2(X_l^\infty)$ somewhat more explicitly:

Proposition 5.3.5. *Let $p = (1/B, 0)$ and $q = (1/(2-B), (1-B)/(2-B))$ be the two points of indeterminacy for N . If none of the inverse images of p or q under N are in the critical value parabola C , we have*

- $H_0(X_l^\infty) = \mathbb{Z}$
- $H_2(X_l^\infty) = \mathbb{Z}^{\{[V]\}} \oplus \left(\bigoplus_{N^k(x)=p} \mathbb{Z}^{\{[E_x]\}} \right) \oplus \left(\bigoplus_{N^k(x)=q} \mathbb{Z}^{\{[E_x]\}} \right)$
- $H_i(X_l^\infty) = 0$, for $i \neq 0$ or 2 .

That is, the second homology of X_l^∞ is generated by the fundamental class $[V]$ of the vertical line $V := \{x = \frac{1}{B(2-B)}\}$, from the original product $\{\operatorname{Re}(x) < 1/2\} \times \mathbb{P}^1$, and by the fundamental classes of the exceptional divisors at the points of indeterminacy p and q and at every inverse image of p and q .

Proof: This is just a restatement of Proposition 5.3.4 using that when $B \in S$, only a single blow-up is necessary at each k -th inverse image of p and of q for every k . \square

We will need the following proposition about the intersection of classes in $H_2(X_1^\infty)$:

Proposition 5.3.6. *Let $[V]$ and $[E_z]$ be the fundamental classes of a vertical line V and an exceptional divisor E_z in $H_2(X_1^\infty)$ then:*

- $[V] \cdot [V] = 0$, and
- $[E_z] \cdot [E_z] \leq -1$.

Proof: We have chosen the vertical line V so that points on it are never blown-up, hence within X_1^∞ it has self-intersection number 0, just as it did in X_1 .

If no points on the the exceptional divisor E_z have been blown-up, then it is a classical result that $[E_z] \cdot [E_z] = -1$. Otherwise, if points in E_z have been blown-up, it is a classical result that each blow-up reduces $[E_z] \cdot [E_z]$ by 1, hence $[E_z] \cdot [E_z] \leq -1$. (See [24].)

\square

Chapter 6

Superstable separatrices W_0 and W_1 .

6.1 Superattracting invariant circles

Recall the invariant circles S_0 and S_1 in the lines $x = 0$ and $x = 1$ equidistant from r_1 and r_2 , equidistant from r_3 and r_4 respectively. Using that $r_1 = (0, 0)$, $r_2 = (0, 1)$, $r_3 = (1, 0)$, and $r_4 = (1, 1 - B)$ we have:

$$\begin{aligned} S_0 &= \{(x, y) \in X_l^\infty : x = 0, |y| = |1 - y|\} \\ S_1 &= \{(x, y) \in X_r : x = 0, |y| = |(1 - B) - y|\}. \end{aligned}$$

Proposition 6.1.1. *The invariant circles S_0 and S_1 have multiplier 0 in the x -direction and they have multiplier 2 in the direction normal to the circle, within the invariant vertical line.*

Proof: The vertical lines $x = 0$ and $x = 1$ are superattracting in the x -direction, hence the circles S_0 and S_1 within the lines are superattracting as well. Within these vertical lines, N is the Newton's method for finding the roots of the quadratic polynomial with roots r_1 and r_2 (or r_3 and r_4), so the invariant circle is repelling with multiplier 2. \square

In this next proposition we will show that these circles have local superstable manifolds.

Proposition 6.1.2. *The invariant circles S_0 and S_1 have local superstable manifolds W_0^{loc} and W_1^{loc} .*

More specifically, there are neighborhoods $U_0, U_1 \subset \mathbb{C}$ of $x = 0$ and $x = 1$ and subsets $W_0^{loc} \subset X_l^\infty$, $W_1^{loc} \subset X_r$ so that:

- $N(W_0^{loc}) \subset W_0^{loc}$ and $N(W_1^{loc}) \subset W_1^{loc}$
- W_0^{loc} is the image of some $\Phi_0 : U_0 \times S_0 \rightarrow X_l^\infty$ which is analytic in the first coordinate and quasiconformal in the second.
- W_1^{loc} is the image of some $\Phi_1 : U_1 \times S_1 \rightarrow X_r$ which is analytic in the first coordinate and quasiconformal in the second.

In the following proof we will use the theory of holomorphic motions and the λ -Lemma of Mañe, Sad, and Sullivan [40], instead of the more standard graph transformation approach. The following argument is due to Sebastien Krief. A somewhat different stable manifold theorem for the invariant circles in the non-degenerate case ($A \neq 0$) is proved using the λ -lemma in [35]. While points in the manifolds obtained in our proof are genuinely attracted to the circles S_0 and S_1 , the situation in [35] is much more complicated, with dense sets of points that are not attracted to the invariant circles.

Proof: To simplify computations we will make the change of variables $z(x) = \frac{x}{x-1}$ and $w(y) = \frac{y}{y-1}$ which conjugates the first coordinate of N to $z \mapsto z^2$ and places the invariant

circle S_0 at $\{z = 0, |w| = 1\}$. In the new coordinates (z, w) , the Newton map becomes:

$$N \begin{pmatrix} z \\ w \end{pmatrix} = \begin{pmatrix} z^2 \\ \frac{w^2 + (Bw - Bw^2)z - w^2 z^2}{1 + (B - Bw)z + (Bw^2 + B - 1 - 2Bw)z^2} \end{pmatrix}. \quad (6.1)$$

and the critical value locus of N in these coordinates is just the image of C under the change of variables, which we denote by C' . Because we are only interested in local properties of N , we can restrict our attention to $(z, w) \in D_\varepsilon \times \mathbb{P} \subset X_l^\infty$ where D_ε is an open disc of radius ε centered at 0.

Let

$$\Delta_{\varepsilon, \delta} = \{(z, y) \in X_l^\infty : |z| < \varepsilon \text{ and } 1 - \delta < |y| < 1 + \delta\}$$

so that $\Delta_{\varepsilon, \delta}$ is an open neighborhood of S_0 . The boundary of $\Delta_{\varepsilon, \delta}$ consists of the vertical boundary $\partial^V \Delta_{\varepsilon, \delta} = \{|z| = \varepsilon\}$ and the horizontal boundary $\partial^H \Delta_{\varepsilon, \delta} = \{|y| = 1 \pm \delta\}$.

We must choose ε and δ so that:

1. $\Delta_{\varepsilon, \delta}$ is disjoint from the critical value locus C' , and
2. N maps $\Delta_{\varepsilon, \delta}$ into $D \times \mathbb{P}$ so that $N(\partial^H \Delta_{\varepsilon, \delta})$ is entirely outside of $\Delta_{\varepsilon, \delta}$ and so that $N(\partial^V \Delta_{\varepsilon, \delta})$ is entirely inside of $|z| < \varepsilon$.

Figure 6.1 shows a depiction of the second condition for $(z, y) \in \mathbb{R} \times \mathbb{C}$.

The first condition is easy to ensure. The critical value locus C' intersects the vertical line $z = 0$ transversely at $w = 0$ and $w = \infty$. Because the intersection is transverse, we can choose ε sufficiently small so that C' intersects $D_\varepsilon \times \mathbb{P}$ outside of $\Delta_{\varepsilon, \frac{1}{2}}$.

Now, we must show that we can reduce ε and δ so that the second condition holds. Because the first coordinate of N is just $z \mapsto z^2$, we need not make any further restrictions to ensure that $N(\partial^V \Delta_{\varepsilon, \delta})$ is entirely inside of $|z| < \varepsilon$. In the line $z = 0$, $N(z, w) = w^2$, so by continuity we can clearly choose ε and δ small enough that $N(\partial^V \Delta_{\varepsilon, \delta})$ is entirely outside of $\Delta_{\varepsilon, \delta}$.

Let D_ε be the open disc $|z| < \varepsilon$ in \mathbb{C} for this ε . Conditions 1 and 2 on ε and δ are chosen so that the following lemma is true:

Lemma 6.1.3. *Suppose that $D \subset \Delta_{\varepsilon, \delta}$ is a complex disc which is the graph of an analytic function $\eta : D_\varepsilon \rightarrow \mathbb{P}$. Then $N^{-1}(D) \cap \Delta_{\varepsilon, \delta}$ is the union of two disjoint complex discs, each given as the graph of analytic functions $\zeta_1, \zeta_2 : D_\varepsilon \rightarrow \mathbb{P}$.*

Proof of Lemma 6.1.3: The locus $N^{-1}(D) \cap \Delta_{\varepsilon, \delta}$ satisfies the equation $N(z, w) \in D$, which is equivalent to $N_2(z, w) = \eta(z^2)$, because D is the graph of η . Because $D \subset \Delta_{\varepsilon, \delta}$, D is disjoint from C' , so $\partial_w N_2(z, w)$ is non-zero in a neighborhood of $N^{-1}(D)$, and we can use the implicit function theorem to solve for $w = \zeta_1(z)$ and $w = \zeta_2(z)$. There are exactly two branches because $N_2(z, w)$ is degree 2 in w .

The graphs of ζ_1 and ζ_2 form the two complex discs $N^{-1}(D) \cap \Delta_{\varepsilon, \delta}$.

□ Lemma 6.1.3.

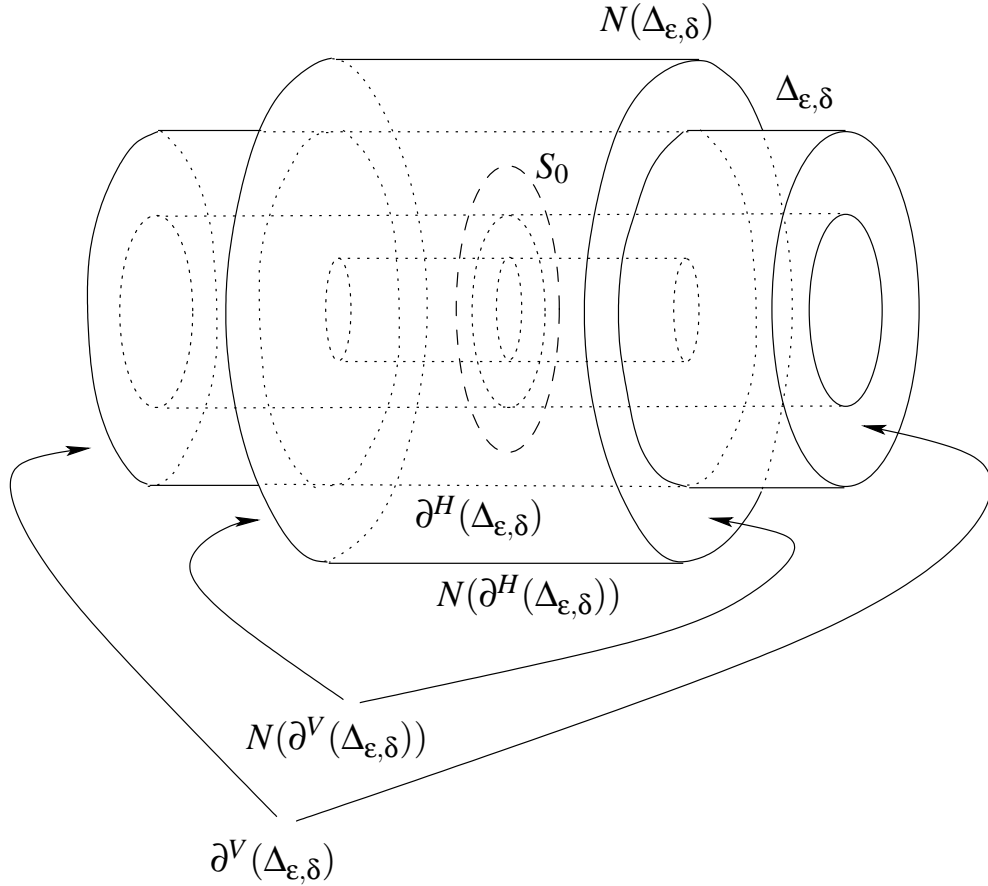


Figure 6.1: The Newton map N maps $\partial^H(\Delta_{\epsilon, \delta})$ outside of $\Delta_{\epsilon, \delta}$ and N maps $\partial^V(\Delta_{\epsilon, \delta})$ inside of inside of $|z| < \epsilon$.

In the old coordinates (x, y) , the line $y = \infty$ is invariant under N and attracted to the point $(0, \infty) \in S_0$. The image of this line under the coordinate change is $w = 1$, which is therefore invariant under N in the coordinates (z, w) and attracted to the point $(0, 1) \in S_0$. Let $D_0 = \{(z, w) : |z| < \epsilon, w = 1\}$. This disc will form the first part of W_0^{loc} .

Since $D_0 \subset \Delta_{\epsilon, \delta}$, satisfies the conditions of Lemma 6.1.3, letting $D_1 = N^{-1}(D_0) \cap \Delta_{\epsilon, \delta}$ we obtain two complex discs in $\Delta_{\epsilon, \delta}$ each of which is given by the graph of some analytic function $\eta : D_\epsilon \rightarrow \mathbb{P}$ and each of which is mapped within D_0 by N . These discs intersect S_0 and ∞ and the first inverse image of ∞ .

Because each of the discs in D_1 satisfies the hypotheses of Lemma 6.1.3 we can repeat this process, letting $D_2 = N^{-1}(D_1) \cap \Delta_{\epsilon, \delta}$, which this lemma guarantees is the union of four disjoint discs in $\Delta_{\epsilon, \delta}$, each of which is the graph of some analytic function $\eta : D_\epsilon \rightarrow \mathbb{P}$. These four discs intersect S_0 at the four inverse images of ∞ .

Of course we can repeat this process indefinitely, obtaining D_n consisting of 2^n disjoint complex discs in $\Delta_{\epsilon, \delta}$, each of which is given by the graph of an analytic function. These discs intersect S_0 at the 2^n inverse images of ∞ .

Let:

$$D_\infty = \bigcup_{n=0}^{\infty} D_n$$

which consists of a union of disjoint complex discs through each of the dyadic points \mathcal{D} on S_0 . Each of these discs is the graph of an analytic function from D_ε to \mathbb{P} , and every point in D_∞ is forward invariant to S_0 under N .

Looking at D_∞ a different way, D_∞ prescribes a *holomorphic motion*:

$$\phi : D_\varepsilon \times \mathcal{D} \rightarrow \mathbb{P}$$

where $\phi(z, \theta)$ is given by $\eta(z)$ where $\eta : D_\varepsilon \rightarrow \mathbb{P}$ is the analytic function whose graph is the disc in D_∞ containing $\theta \in S_0$.

By the λ -lemma of Mañé-Sad-Sullivan [40], ϕ extends continuously to a holomorphic motion on S_0 , the closure of \mathcal{D} .

$$\phi : D_\varepsilon \times S_0 \rightarrow \mathbb{P}$$

Then, the map $\Phi : S_0 \times D_\varepsilon \rightarrow D \times \mathbb{P} \subset X_f^\infty$ given by $(z, \theta) \mapsto (z, \phi(z, \theta))$ is holomorphic in z and quasi-conformal in θ . We let W_0^{loc} be the image of Φ . Clearly $N(W_0^{loc}) \subset W_0^{loc}$ and every point in W_0^{loc} is forward invariant to S_0 .

The existence of W_1^{loc} is an easy adaptation.

□ Proposition 6.1.2.

Because the local superstable manifolds W_0^{loc} and W_1^{loc} are forward invariant under N , we can define global invariant sets W_0 and W_1 by pulling back under N :

$$W_0 = \bigcup_{n=0}^{\infty} N^{-n}(W_0^{loc}), \quad W_1 = \bigcup_{n=0}^{\infty} N^{-n}(W_1^{loc}).$$

Recall from Chapter 4 that we defined the “bifurcation locus” $\Omega_{\text{bif}} \subset \Omega$ to be the set of parameter values for which there is a tangency between W_0 and C or a tangency between W_1 and C and that we defined the “regular locus” $\Omega_{\text{reg}} = \Omega - \Omega_{\text{bif}}$.

One might expect that W_0 and W_1 are manifolds, since the inverse function theorem gives that the pull-back of $N^{-k}(W_0^{loc})$ (or $N^{-k}(W_1^{loc})$) by N is “locally manifold” at points where $N^{-k}(W_0^{loc})$ (or $N^{-k}(W_1^{loc})$) is disjoint from or transverse to the critical value locus C . However, we do expect that there will be some values of the parameter B for which there is a tangency between $N^{-k}(W_0^{loc})$ (or $N^{-k}(W_1^{loc})$) and C . Therefore, at $B \in \Omega_{\text{bif}}$ W_0 (or W_1) will not be a manifold, but for $B \in \Omega_{\text{reg}}$ both W_0 and W_1 will be manifolds. Instead of calling W_0 and W_1 manifolds in general, we will call them *separatrices*, and only call them manifolds when $B \in \Omega_{\text{reg}}$.

Proposition 6.1.4. *The bifurcation locus Ω_{bif} is residual in Ω in the sense of Baire’s Theorem.*

Proof: This is relatively standard use of Baire's Theorem, so we omit the details. \square

Proposition 6.1.5. *For every B , the separatrices W_0 and W_1 are real analytic subspaces of X_1^∞ and X_r , each defined as the zero set of a single non-constant real-analytic equation in an neighborhood of W_0 and in a neighborhood of W_1 , respectively.*

Proof: As in the proof of Proposition 6.1.2, we make the change of variables $z = \frac{x}{x-1}$ and $w = \frac{y}{y-1}$ and in these coordinates

$$N \begin{pmatrix} z \\ w \end{pmatrix} = \begin{pmatrix} z^2 \\ \frac{w^2 + (Bw - Bw^2)z - w^2z^2}{1 + (B - Bw)z + (Bw^2 + B - 1 - 2Bw)z^2} \end{pmatrix}, \quad (6.2)$$

with S_0 is given by $\{z = 0, |w| = 1\}$. We will show that

$$\phi(z, w) = \lim_{n \rightarrow \infty} (N_2^n(z, w))^{1/2^n}$$

is well defined and converges on a neighborhood of W_0 so that $\omega(z, w) = \log |\phi(z, w)|$ is a non-constant real analytic function in a neighborhood of W_0 , vanishing on W_0 .

For every $(z, w) \in W_0$, $|N_2^n(z, w)|$ converges to 1 because $S_0 = \{|w| = 1\}$ and hence $\log |(N_2^n(z, w))^{1/2^n}|$ converges to 0. So, we only need to show that $\omega(z, w)$ is a non-constant real analytic function in a neighborhood of W_0 . The proof will be reminiscent of the proof of Böttcher's Theorem in one variable dynamics. (See Milnor [43, Section 9].)

Notice that ω is defined with the invariance property $\omega(N(z, w)) = 2 \cdot \omega(z, w)$. Therefore we can assume that $|x|$ is arbitrarily small.

With these restrictions, the second coordinate of N can be written as:

$$N_2(z, w) = w^2 + zg(z, w)$$

with $g(z, w)$ which is analytic in the neighborhood $|z| < \varepsilon$ for an appropriately small ε .

We can write $\phi(z, w) := \lim_{n \rightarrow \infty} (N_2^n(z, w))^{1/2^n}$ as a telescoping product:

$$\phi(z, w) = N_2(z, w)^{1/2} \cdot \frac{N_2^2(z, w)^{1/4}}{N_2(z, w)^{1/2}} \cdot \frac{N_2^3(z, w)^{1/8}}{N_2^2(z, w)^{1/4}} \cdots \quad (6.3)$$

so that the general term is of the form

$$\begin{aligned} \frac{N_2^{n+1}(z, w)^{1/2^{n+1}}}{N_2^n(z, w)^{1/2^n}} &= \left(\frac{(N_2^n(z, w))^2 + N_1^n(z, w) \cdot g(N_1^n(z, w), N_2^n(z, w))}{(N_2^n(z, w))^2} \right)^{1/2^{k+1}} \\ &= \left(1 + \frac{z^{2^n}}{(N_2^n(z, w))^2} \cdot g(z^{2^n}, N_2^n(z, w)) \right)^{1/2^{k+1}} \end{aligned}$$

using that $N_1^n(z, w) = z^{2^n}$.

In order to define the power $\frac{1}{2^{k+1}}$ we need to check that we can restrict, if necessary, the neighborhood of definition for $\phi(z, w)$ so that

$$\left| \frac{z^{2^n}}{(N_2^n(z, w))^2} \cdot g\left(z^{2^n}, N_2^n(z, w)\right) \right| \leq \frac{1}{2}. \quad (6.4)$$

The only real difficulty is when $(z, w) \in W(r_1)$ so that $(N_2^n(z, w))^2$ goes to 0. However, there is a neighborhood $U \subset W(r_1)$ of the line $z = 0$ in which the term in the numerator z^{2^n} will be sufficiently small to make the entire term 6.4 small:

In [35], the authors perform blow-ups at each of the four roots, and observe that the Newton map N induces rational functions of degree 2 on each of the exceptional divisors $E_{r_1}, E_{r_2}, E_{r_3}$, and E_{r_4} . Let's compute the rational function $s : E_{r_1} \rightarrow E_{r_1}$. In the coordinate chart $m = \frac{z}{w}$, the extension to E_{r_1} is obtained by:

$$\begin{aligned} s(m) &= \lim_{w \rightarrow 0} \frac{m^2 w^2 (1 + (B - Bw)mw + (Bw^2 + B - 1 - 2Bw)m^2 w^2)}{w^2 + (Bw - Bw^2)mw - w^2 m^2 w^2} \\ &= \frac{m^2}{1 + Bm}, \end{aligned}$$

since $w = 0$ on E_{r_1} .

The rational function $s(m)$ has $m = 0$ as a superattracting fixed point, so there is a neighborhood of $m = 0 \in E_{r_1}$ within $W(r_1)$ so that for any point (z, w) in this neighborhood, $\lim_{n \rightarrow \infty} \left| \frac{z^{2^n}}{N_2^n(z, w)} \right| = 0$. Pulling back this neighborhood under N we find a neighborhood $V \subset W(r_1)$ of the line $z = 0$ in which this limit is true.

So long as we restrict the points $(z, w) \in W(r_1)$ to be within this neighborhood V and restrict all other points (z, w) in X_l^∞ so that $\left| \frac{z}{w^2} \cdot g(z, w) \right|$ is less than $1/2$, we can assume that condition 6.4 holds.

Because Equation 6.4 is satisfied for every $(z, w) \in \Lambda$, we can use the binomial formula to define the factors in the product 6.3 in Λ :

$$(1 + u)^\alpha = \sum_{n=0}^{\infty} \frac{\alpha(\alpha - 1) \cdots (\alpha - n + 1)}{n!} u^n, \text{ when } |u| < 1.$$

Now that the terms in the product 6.3 are well defined, we check that the product converges on the neighborhood Λ of S_0 . For this product to converge it is sufficient to show that the corresponding series of logarithms converges. The general term in this series is:

$$\log \left| \left(1 + \frac{z^{2^n}}{(N_2^n(z, w))^2} \cdot g\left(z^{2^n}, N_2^n(z, w)\right) \right)^{1/2^{k+1}} \right| \leq \frac{\log 2}{2^{n+1}},$$

using Equation 6.4 and the triangle inequality so that

$$\left| 1 + \frac{z^{2^n}}{(N_2^n(z, w))^2} \cdot g\left(z^{2^n}, N_2^n(z, w)\right) \right| < 2.$$

This is clearly sufficient for the series of logarithms to converge and hence for the product 6.3 to converge to the analytic function on $\phi(z, w)$ on Λ . This way $\omega(z, w) = \log |\phi(z, w)|$ is a real analytic function on Λ , and by the invariance properties of ϕ on $\omega(z, w)$ is an analytic function on a neighborhood of W_0 .

The proof that W_1 is the zero locus of a non-constant analytic function is very similar. \square

Understanding the topology of W_0 and W_1 will become very important to us since knowing their topology helps us study the topology of the basins of attraction for the four roots. Two preliminary observations are:

Proposition 6.1.6. *Every point in X_l^∞ that is not attracted to r_1 or r_2 is on the separatrix W_0 , i.e. $X_l^\infty = W(r_1) \cup W(r_2) \cup W_0$.*

Similarly, every point in X_r that is not attracted to r_3 or r_4 is on the separatrix W_1 , i.e. $X_r = W(r_3) \cup W(r_4) \cup W_1$

Proof: Every point in X_l^∞ is attracted to the line $x = 0$. The only invariant sets on this line are the two roots, r_1, r_2 , and the invariant circle S_0 , hence the points that are not in $W(r_1)$ or $W(r_2)$ are in W_0 . Similarly, every point in X_r is attracted to the line $x = 1$, and the decomposition follows. \square

Proposition 6.1.7. *The fundamental classes $[S_0]$ and $[S_1]$ are non-zero in $H_1(W_0)$ and $H_1(W_2)$, respectively.*

Proof: The proof is the same for each circle, so we prove it for S_0 . If $[S_0] = 0$, then there is some 2-chain σ in W_0 with $\partial\sigma = W_0$. Every point in X_l^∞ is attracted to the line $x = 0$. Since σ is a compact subset of W_0 , one can choose k so that $N^k(\sigma)$ is within an arbitrarily small neighborhood of S_0 .

The Newton map N maps S_0 to itself by angle doubling, so $N^k(S_0) = 2^k S_0$. Since $\partial N^k(\sigma) = N^k(\partial\sigma) = 2^k S_0$, this would give that $[S_0]$ is torsion within this neighborhood. However, small neighborhoods of $S_0 \subset W_0$ are topologically $S_0 \times \mathbb{D}$ and $[S_0]$ is not torsion in $H_1(S_0 \times \mathbb{D}) \cong \mathbb{Z}^{\{[S_0]\}}$ \square

Proposition 6.1.8. (Neighborhoods of W_0 and W_1) *Within X_l^∞ and X_r there are neighborhoods $\mathcal{N}(W_0)$ and $\mathcal{N}(W_1)$ of W_0 and W_1 that deformation retract onto W_0 and W_1 .*

Proof: Any $A \subset M$ that is globally defined by the vanishing of a single non-constant real-analytic function $g : M \rightarrow \mathbb{R}$ has this property:

Since $g : M \rightarrow \mathbb{R}$ is non-constant and real-analytic, the critical points of g cannot accumulate, consequently we can choose a neighborhood $\mathcal{N}(A)$ so that the only critical points of g in $\mathcal{N}(A)$ are actually in A . Similarly, the only critical points of g^2 will have be on A . Hence, the vector field $-\nabla g^2$ will be zero on A , but it will have no zeros on $\mathcal{N}(A)$. Flow along this vector fields provides a deformation retraction of $\mathcal{N}(A)$ onto A . \square

6.2 Mayer-Vietoris computations

By Proposition 6.1.6 we have that $X_l^\infty = \overline{W(r_1)} \cup \overline{W(r_2)}$, and $W_0 = \overline{W(r_1)} \cap \overline{W(r_2)}$. Because of the neighborhood $\mathcal{N}(W_0)$ that deformation retracts onto W_0 , we can use the Mayer-Vietoris exact sequence to relate the homology of $\overline{W(r_1)}$ and $\overline{W(r_2)}$ to that of X_l^∞ and W_0 . For a reference about the Mayer-Vietoris exact sequence, we recommend [9] and [28].

Denote the inclusions $W_0 \hookrightarrow \overline{W(r_1)}$ and $W_0 \hookrightarrow \overline{W(r_2)}$ by i_1 and i_2 and the inclusions $\overline{W(r_1)} \hookrightarrow X_l^\infty$ and $\overline{W(r_2)} \hookrightarrow X_l^\infty$ by j_1 and j_2 . We have:

$$\begin{aligned}
0 &\rightarrow H_4(W_0) \xrightarrow{i_{1*} \oplus i_{2*}} H_4(\overline{W(r_1)}) \oplus H_4(\overline{W(r_2)}) \xrightarrow{j_{1*} - j_{2*}} H_4(X_l^\infty) \xrightarrow{\partial} \\
0 &\rightarrow H_3(W_0) \xrightarrow{i_{1*} \oplus i_{2*}} H_3(\overline{W(r_1)}) \oplus H_3(\overline{W(r_2)}) \xrightarrow{j_{1*} - j_{2*}} H_3(X_l^\infty) \xrightarrow{\partial} \\
0 &\rightarrow H_2(W_0) \xrightarrow{i_{1*} \oplus i_{2*}} H_2(\overline{W(r_1)}) \oplus H_2(\overline{W(r_2)}) \xrightarrow{j_{1*} - j_{2*}} H_2(X_l^\infty) \xrightarrow{\partial} \\
0 &\rightarrow H_1(W_0) \xrightarrow{i_{1*} \oplus i_{2*}} H_1(\overline{W(r_1)}) \oplus H_1(\overline{W(r_2)}) \xrightarrow{j_{1*} - j_{2*}} H_1(X_l^\infty) \xrightarrow{\partial} \\
0 &\rightarrow H_0(W_0) \xrightarrow{i_{1*} \oplus i_{2*}} H_0(\overline{W(r_1)}) \oplus H_0(\overline{W(r_2)}) \xrightarrow{j_{1*} - j_{2*}} H_0(X_l^\infty) \rightarrow 0
\end{aligned}$$

Recall from Proposition 5.3.4 that $H_2(X_l^\infty) = 0$ for $l \neq 2, 0$ from this we obtain:

$$H_4(\overline{W(r_1)}) \oplus H_4(\overline{W(r_2)}) \cong H_4(W_0), \quad H_3(\overline{W(r_1)}) \oplus H_3(\overline{W(r_2)}) \cong H_3(W_0).$$

and the exact sequence:

$$\begin{aligned}
0 &\rightarrow H_2(W_0) \xrightarrow{i_{1*} \oplus i_{2*}} H_2(\overline{W(r_1)}) \oplus H_2(\overline{W(r_2)}) \xrightarrow{j_{1*} - j_{2*}} \\
&H_2(X_l^\infty) \xrightarrow{\partial} H_1(W_0) \xrightarrow{i_{1*} \oplus i_{2*}} H_1(\overline{W(r_1)}) \oplus H_1(\overline{W(r_2)}) \rightarrow 0 \quad (6.5)
\end{aligned}$$

since we can truncate the 0-th homology from Exact Sequence 6.5 because each of these spaces is connected.

We can repeat these calculations in X_r . We denote the inclusions $W_1 \hookrightarrow \overline{W(r_3)}$ and $W_1 \hookrightarrow \overline{W(r_4)}$ by i_3 and i_4 and the inclusions $\overline{W(r_3)} \hookrightarrow X_r$ and $\overline{W(r_4)} \hookrightarrow X_r$ by j_3 and j_4 . Using that $H_2(X_r) = \mathbb{Z}^{\{\mathbb{P}^1\}}$ and $H_i(X_r) = 0$ for $i \neq 2, 0$, we get:

$$H_4(\overline{W(r_3)}) \oplus H_4(\overline{W(r_4)}) \cong H_4(W_0), \quad H_3(\overline{W(r_3)}) \oplus H_3(\overline{W(r_4)}) \cong H_3(W_0).$$

and the exact sequence:

$$\begin{aligned}
0 &\rightarrow H_2(W_1) \xrightarrow{i_{3*} \oplus i_{4*}} H_2(\overline{W(r_3)}) \oplus H_2(\overline{W(r_4)}) \xrightarrow{j_{3*} - j_{4*}} \\
&\mathbb{Z}^{\{\mathbb{P}^1\}} \xrightarrow{\partial} H_1(W_1) \xrightarrow{i_{3*} \oplus i_{4*}} H_1(\overline{W(r_3)}) \oplus H_1(\overline{W(r_4)}) \rightarrow 0
\end{aligned}$$

Lemma 6.2.1. *The boundary map $\partial : \mathbb{Z}^{\{\mathbb{P}^1\}} \rightarrow H_1(W_1)$ from exact sequence 6.6 satisfies $\partial([\mathbb{P}^1]) = [S_1]$. In particular, ∂ is injective.*

Proof: One can choose the vertical line $x = 1$ as the generator \mathbb{P} of $H_2(X_r)$. Since W_1 intersects this line transversely along S_0 , we have $\partial[\mathbb{P}^1] = [S_1]$. \square

In combination with exact sequence 6.6 we find:

Corollary 6.2.2. *The map*

$$H_2(W_1) \xrightarrow{i_{3*} \oplus i_{4*}} H_2(\overline{W(r_3)}) \oplus H_2(\overline{W(r_4)}) \quad (6.6)$$

is an isomorphism and the sequence

$$0 \rightarrow \mathbb{Z}\{\mathbb{P}\} \xrightarrow{\partial} H_1(W_1) \xrightarrow{i_{3*} \oplus i_{4*}} H_1(\overline{W(r_3)}) \oplus H_1(\overline{W(r_4)}) \rightarrow 0 \quad (6.7)$$

is exact.

6.3 Replacement of $\overline{W(r_i)}$ with $W(r_i)$.

In many cases one would prefer to make statements about the homology of the genuine basins of attraction $W(r_i)$, instead of the closures of the basins $\overline{W(r_i)}$.

Proposition 6.3.1. *For the parameter values B in which W_0 is a manifold, $W(r_1)$ is homotopy equivalent to $\overline{W(r_1)}$ and $W(r_2)$ is homotopy equivalent to $\overline{W(r_2)}$.*

Similarly, for parameter values B in which W_1 is a manifold, $W(r_3)$ is homotopy equivalent to $\overline{W(r_3)}$ and $W(r_4)$ is homotopy equivalent to $\overline{W(r_4)}$.

Proof: This follows from the relatively standard fact that if M is a manifold with boundary, then M and the interior of M are homotopy equivalent. \square

Recall that $\Omega_{\text{reg}} \subset \Omega$ is the set of parameters B for which there are no tangencies between W_0 and C and no tangencies between W_1 and C . For these parameter values, both W_0 and W_1 are manifolds and hence:

Corollary 6.3.2. *For every $B \in \Omega_{\text{reg}}$, $H_*(\overline{W(r_i)}) \cong H_*(W(r_i))$ for $i = 1, 2, 3$, and 4.*

Chapter 7

Morse Theory for W_1 and W_0

In this chapter we will use Morse Theory to prove that if $W_1 \cap C = \emptyset$, then W_1 is homotopy equivalent to S_1 and we will also see why the same method fails to work for W_0 .

In general, W_0 and W_1 are not manifolds but merely real-analytic spaces. However, we will only end up using Morse theory on W_1 in the special case where $W_1 \cap C = \emptyset$ and hence W_1 is a genuine manifold.

Recall Short Exact Sequence 6.7 from Corollary 6.2.2:

$$0 \rightarrow \mathbb{Z}^{\{\mathbb{P}\}} \xrightarrow{\partial} H_1(W_1) \rightarrow H_1(\overline{W(r_3)}) \oplus H_1(\overline{W(r_4)}) \rightarrow 0.$$

By Lemma 6.2.1 we have that $\partial([\mathbb{P}]) = [S_1]$, so that if W_1 is homotopy equivalent to S_1 , then $H_1(W_1) \cong \mathbb{Z}^{\{[S_1]\}} = \text{Image}(\partial)$. By exactness of the sequence, this will show that if $W_1 \cap C = \emptyset$, then $H_1(\overline{W(r_3)}) = 0 = H_1(\overline{W(r_4)})$. Since W_1 is a genuine manifold in this case, Proposition 6.3.1 will give that $H_1(W(r_3)) = 0 = H_1(W(r_4))$, as well, which is part of the third statement in Theorem 4.4.1.

7.1 Morse Theory for W_1 and W_0

Consider the function $h : \mathbb{C} \times \mathbb{P} \rightarrow \mathbb{R}$ given by

$$h \begin{pmatrix} x \\ y \end{pmatrix} = \left| \frac{x}{x-1} \right| \tag{7.1}$$

which is chosen so that

$$h \left(N \begin{pmatrix} x \\ y \end{pmatrix} \right) = \left| \frac{\frac{x^2}{2x-1}}{\frac{x^2}{2x-1} - 1} \right| = \left| \frac{x^2}{x^2 - 2x + 1} \right| = h \left(\begin{pmatrix} x \\ y \end{pmatrix} \right)^2. \tag{7.2}$$

The extension of h to the exceptional divisors is given by extending $\frac{x}{x-1}$ in the standard way (algebraically) then composing with the modulus $|\cdot|$. The result is a C^∞ function on $h : X_t^\infty \rightarrow \mathbb{R}$.

We will consider the restriction of h to the super-stable separatrix W_0 and W_1 and use it as a Morse function to study their topology.

There is a geometric description of the critical points of h : Notice that W_0 and W_1 intersect the critical value parabola C in real-analytic sets. Let K be the set of points in C where $W_0 \cap C$ (or $W_1 \cap C$) and the level curves of $h|_C$ are parallel. The critical points of h are inverse images of points in K and repeated inverse images of points in K under N .

It is relatively easy to search for points in K for specific parameter values. Figures 7.1 and 7.2 show the part of the critical value parabolas for two different values of B , with the level curves of $h|_C$ superimposed. Some of the points in K are marked for each of these parameter values.

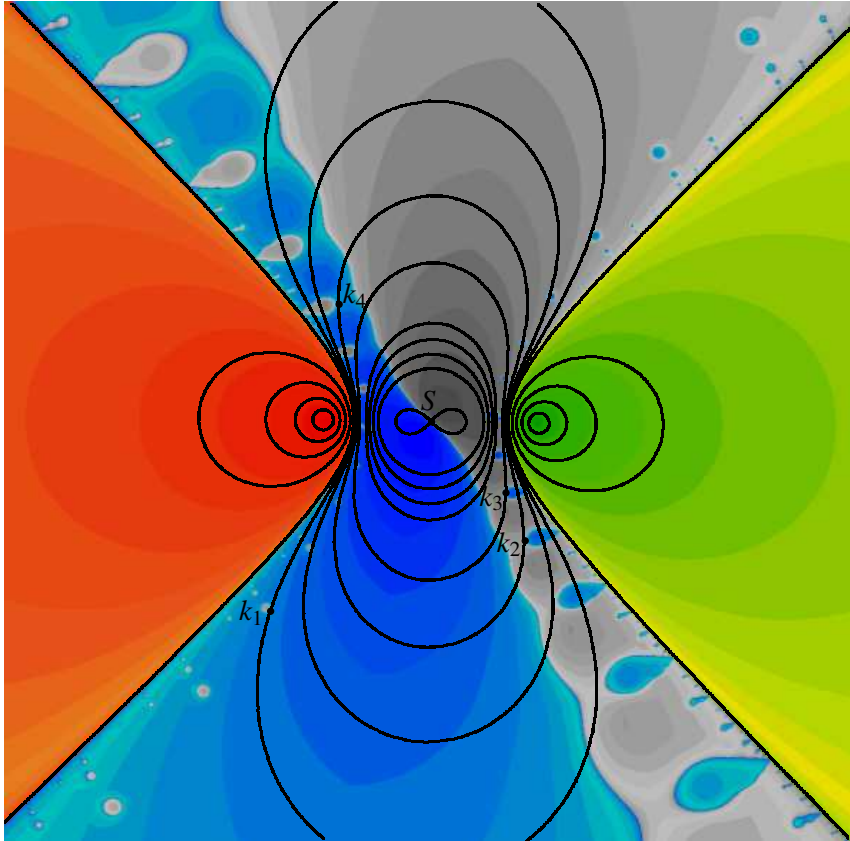


Figure 7.1: Level curves of the Morse function h within the critical value parabola C . The points labeled k_1, k_2, k_3 and k_4 are all in K , as well as any others. The critical point of $h|_C$ is labeled S .

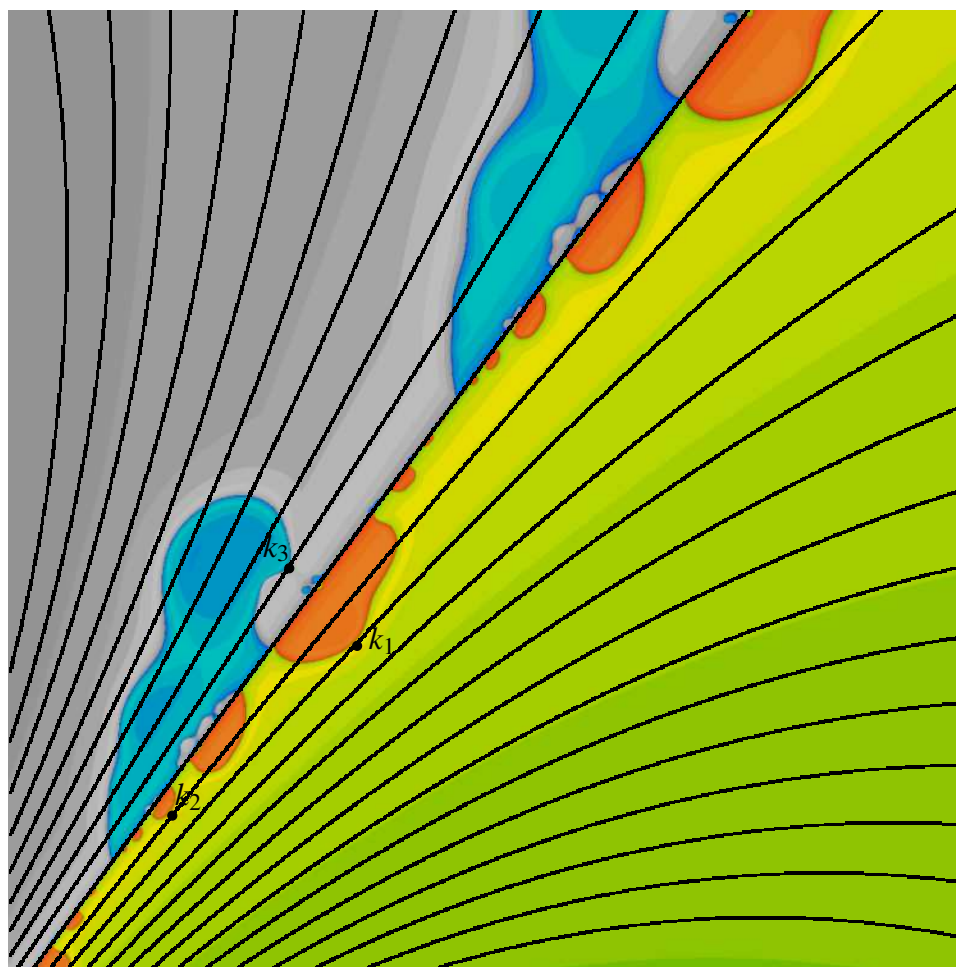


Figure 7.2: Level curves of the Morse function h within the critical value parabola C . The points labeled k_1, k_2 , and k_3 are all in K , as well as any others.

Proposition 7.1.1. *Let K be the set of points in C where $W_0 \cap C$ (or $W_1 \cap C$) is parallel to the level curves of $h|_C$. Then, the set of critical points of h on W_0 and W_1 is $\bigcup_{k=1}^{\infty} N^{-k}(K)$.*

Proof: Applying the chain rule to Equation 7.2 we find:

$$Dh \left(N \begin{pmatrix} x \\ y \end{pmatrix} \right) \cdot DN \begin{pmatrix} x \\ y \end{pmatrix} = 2h \begin{pmatrix} x \\ y \end{pmatrix} \cdot Dh \begin{pmatrix} x \\ y \end{pmatrix}. \quad (7.3)$$

Notice that $\left| h \begin{pmatrix} x \\ y \end{pmatrix} \right| = 0$ only when $x = 0$. Therefore, Equation 7.3 gives that if $Dh \begin{pmatrix} x \\ y \end{pmatrix} = 0$ for a point $\begin{pmatrix} x \\ y \end{pmatrix}$ on W_0 then either:

1. $Dh \left(N \begin{pmatrix} x \\ y \end{pmatrix} \right) = 0$ giving that $\begin{pmatrix} x \\ y \end{pmatrix}$ is an inverse image (possibly an n -th inverse image) of another critical point of h . Or,
2. $DN \begin{pmatrix} x \\ y \end{pmatrix}$ is singular and $Dh \left(N \begin{pmatrix} x \\ y \end{pmatrix} \right)$ is 0 within the image of DN .

The condition in the second case says that (x, y) is on the critical points locus of N , and that $Dh(N(x, y))$ is zero when restricted to the image of DN . Geometrically, this says that the curve $W_0 \cap C$ is tangent to the level curves of $h|_C$ at $N(x, y)$. \square

It is also possible that there may be critical points of $h|_{W_0}$ that are some of the exceptional divisors E_z that were introduced in the construction of X_1^∞ . We ignore this possibility for the moment, and eventually we will restrict our attention to Morse Theory in X_r .

Notice that if $h : W_0 \rightarrow \mathbb{R}$ has no critical points, or if $h : W_1 \rightarrow \mathbb{R}$ has no critical points (except at $x = 0$ and $x = 1$), then the negative gradient flow $-\nabla h$ gives a deformation retraction of W_0 to S_0 or the gradient flow ∇h gives a deformation retraction of W_1 to S_1 .

Although we cannot find any specific values of the parameter B for which we can prove that W_1 does not intersect C , our computer calculations indicate that this may often be the case. For example, this is probably the case in Figure 7.1, and clearly is not the case in Figure 7.2. If W_1 and C are disjoint, there are clearly no critical points of h :

Proposition 7.1.2. *If there are no points of intersection between W_1 and the parabola $C(x, y) = y^2 + Bxy + \frac{B^2}{4}x^2 - \frac{B^2}{4}x - y = 0$, then W_1 is homotopy equivalent to S_1 .*

Corollary 7.1.3. *If there are no points of intersection between W_1 and the parabola $C(x, y) = 0$, then the basins of attraction $W(r_3)$ and $W(r_4)$ for the roots $r_3 = (1, 0)$ and $r_4 = (1, 1 - B)$ have trivial first and second homology groups.*

Proof: For $H_1(W(r_3))$ and $H_1(W(r_4))$ this is a consequence of our discussion at the beginning of this chapter. For the second homology it is a consequence of the isomorphism 6.6.

We will never have this special situation in X_1^∞ for the following reason:

Proposition 7.1.4. *There are always critical points of $h : W_0 \rightarrow \mathbb{R}$.*

Proof: First, notice that there is a unique critical point of $h|C$: Implicit differentiation of $C(x, y) = 0$ gives

$$2y + B \frac{dx}{dy} y + Bx + \frac{B^2}{2} x \frac{dx}{dy} - \frac{B^2}{4} \frac{dx}{dy} - 1 = 0$$

which is equivalent to:

$$\left(By + \frac{B^2}{2} x - \frac{B^2}{4} \right) \frac{dx}{dy} = 1 - Bx - 2y$$

Therefore the unique point of intersection between the line $Bx + 2y - 1 = 0$ and the parabola $C(x, y) = 0$ is a vertical tangent to C and hence a critical point of $h|C$. This critical point is labeled S in Figures 7.1 and 7.2.

The line $L_\infty = \{y = \infty\}$ is clearly within W_0 , and the line $Bx + 2y - 1 = 0$ is mapped to L_∞ by N , hence it is in W_0 as well. Therefore, this critical point of $h|C$ is actually in W_0 . By Proposition 7.1.1, the inverse images of this point under N are critical points of $h|W_0$. \square

One might consider using further details about the critical points of h in order to study the topology of W_0 and W_1 when there are intersections with the critical value locus, C , but this seems like a difficult approach, especially since these spaces may have singularities, and we will avoid it.

Instead, in the next chapters we will use linking numbers to prove that if W_1 intersects the parabola $C(x, y) = 0$, then the basins of attraction for the roots $(1, 0)$ and $(1, 1 - B)$ have infinitely generated first homology. We will also prove that the basins of attraction for the roots at $(0, 0)$ and $(0, 1)$ always have infinitely generated first homology, as a consequence of the fact that W_0 always intersects the parabola $C(x, y) = 0$.

Chapter 8

Many loops in W_0 and W_1 .

In this chapter we will show that intersections between W_0 and the critical value locus C lead to an infinite number of closed loops in W_0 and that intersections between W_1 and C lead to an infinite number of closed loops in W_1 . In the chapter following this one we will show that infinitely many of them are homologically distinct, finishing the proof of Theorem 4.4.1.

8.1 The mapping on fibers

Denote the projective line in $\mathbb{C} \times \mathbb{P}$ above a fixed value of x by \mathbb{P}_x . Often we will informally call such a set a “vertical line”. Notice that if $x \neq 1/2$ then N_F maps \mathbb{P}_x to $\mathbb{P}_{x^2/(2x-1)}$ by the rational map:

$$R_x(y) = \frac{y(Bx^2 + 2xy - Bx - y)}{(2x - 1)(Bx + 2y - 1)}$$

It is worth noticing that when $x = \frac{1}{B}$ and when $x = \frac{1}{2-B}$, a common term cancels from the numerator and denominator of R_x , giving $R_x(y) = \frac{y}{2} + \frac{1-B}{2(2-B)}$ and $R_x(y) = \frac{y}{2}$, respectively.

In this section, we will use the details of R_x to understand the topology of intersections of W_0 with vertical lines \mathbb{P}_x having $\operatorname{Re}(x) < 1/2$ and the topology of intersections of W_1 with vertical lines \mathbb{P}_x having $\operatorname{Re}(x) > 1/2$.

Recall that X_l^∞ is the space $\mathbb{C} \times \mathbb{P}$ having $\operatorname{Re}(x) < 1/2$, after the infinite sequence of blow-ups that is necessary to resolve all iterates of N and that X_r is the space $\mathbb{C} \times \mathbb{P}$ having $\operatorname{Re}(x) > 1/2$, and that no blow-ups were necessary in X_r .

If a vertical line \mathbb{P}_x in X_l does not contain a point that we have blown-up, it naturally corresponds to a subset of X_l^∞ . Otherwise, if the vertical line \mathbb{P}_x does contain a point in X_l that we have blown-up, then by the vertical line \mathbb{P}_x in X_l^∞ we mean the proper transform of \mathbb{P}_x under the blow-ups. Hence, it is meaningful to discuss vertical lines X_l^∞ .

Proposition 8.1.1. *The critical values of R_x are the intersections of the critical value parabola C with the line \mathbb{P}_x . There are two distinct critical values, except when $x = \frac{1}{B(2-B)}$.*

Proof: The critical value curve $C(x, y) = 0$ for N is exactly the image of the locus where $\partial_y N_2(x, y) = 0$. Hence, the critical values of R_x are just the points of intersection between $C(x, y) = 0$ and \mathbb{P}_x . There are two such points of intersection, except when the discriminant $(Bx - 1)^2 - B^2(x^2 - x) = (B^2 - 2B)x + 1 = 0$, that is, when $x = \frac{1}{B(2-B)}$. This makes sense because the vertical lines containing p and q and the exceptional divisors E_p and E_q each map to the line $x = \frac{1}{B(2-B)}$ by isomorphisms. \square

Re-stating the previous proposition in somewhat more topological terms:

Corollary 8.1.2. *For vertical lines not at $x = \frac{1}{B}, x = \frac{1}{2-B}$, i.e. not containing p or q , the mapping $R_x : \mathbb{P}_x \rightarrow \mathbb{P}_{x^2/(2x-1)}$ is a ramified covering map of degree 2 with two distinct points of ramification.*

8.2 Intersection of W_0 and W_1 with vertical lines.

The goal of this section is to show that if there is an intersection of W_0 with the critical value parabola $C(x, y) = 0$ in X_l^∞ , then the super-stable separatrix W_0 divides certain sequences of vertical lines into arbitrarily many simply connected domains and, otherwise, if there is no such intersection then every vertical line in X_l^∞ is divided into exactly two simply connected domains by W_0 . We will also show that the same statement holds for X_r if we replace W_0 with W_1 . More formally:

Proposition 8.2.1. *Let x_i be the i -th iterate of x under $x \mapsto \frac{x^2}{2x-1}$. For x having $\operatorname{Re}(x) < 1/2$:*

- *If $W_0 \cap \{C(x_i, y) = 0\} = \emptyset$ for each i , then $W_0 \cap \mathbb{P}_x$ forms a simple closed curve dividing \mathbb{P}_x into two simply connected domains.*
- *If there is some k with $W_0 \cap \{C(x_k, y) = 0\} \neq \emptyset$, then $W_0 \cap \mathbb{P}_x$ forms a curve dividing \mathbb{P}_x into at least $2^k + 2$ distinct simply connected domains.*

Similarly, for x having $\operatorname{Re}(x) > 1/2$:

- *If $W_1 \cap \{C(x_i, y) = 0\} = \emptyset$ for each i , then $W_1 \cap \mathbb{P}_x$ forms a simple closed curve dividing \mathbb{P}_x into two simply connected domains.*
- *If there is some k with $W_1 \cap \{C(x_k, y) = 0\} \neq \emptyset$, then $W_1 \cap \mathbb{P}_x$ forms a curve dividing \mathbb{P}_x into at least $2^k + 2$ distinct simply connected domains.*

Figure 8.1 illustrates this proposition.

The closed loops generated in W_0 and W_1 bounding the simply connected domains guaranteed by Proposition 8.2.1 will be used the next chapter to show that $H_1(W_0)$ is always infinitely generated and to show that if W_1 intersects C , then $H_1(W_1)$ is infinitely generated.

We prove Proposition 8.2.1 for X_l^∞ , since it follows in a similar, although easier way for X_r . The proof will require some build-up.

Lemma 8.2.2. *For any choice of B , there are $\varepsilon_0 > 0$ and $\varepsilon_1 > 0$ so that if $|x - 0| < \varepsilon_0$, then $W_0 \cap \mathbb{P}_x$ forms a simple closed curve and so that if $|x - 1| < \varepsilon_1$, then $W_0 \cap \mathbb{P}_x$ forms a simple closed curve.*

Proof: This is a direct consequence of Proposition 6.1.2 where we prove the existence of W_0^{loc} and W_1^{loc} . \square

Lemma 8.2.3. *Let $R : \mathbb{P} \rightarrow \mathbb{P}$ be a ramified covering map of degree d and let $U \subset \mathbb{P}$ be a simply connected open subset of \mathbb{P} containing the image of at most one point of ramification of R . Then, $R^{-1}(U)$ consists of a finite number of disjoint simply connected domains.*

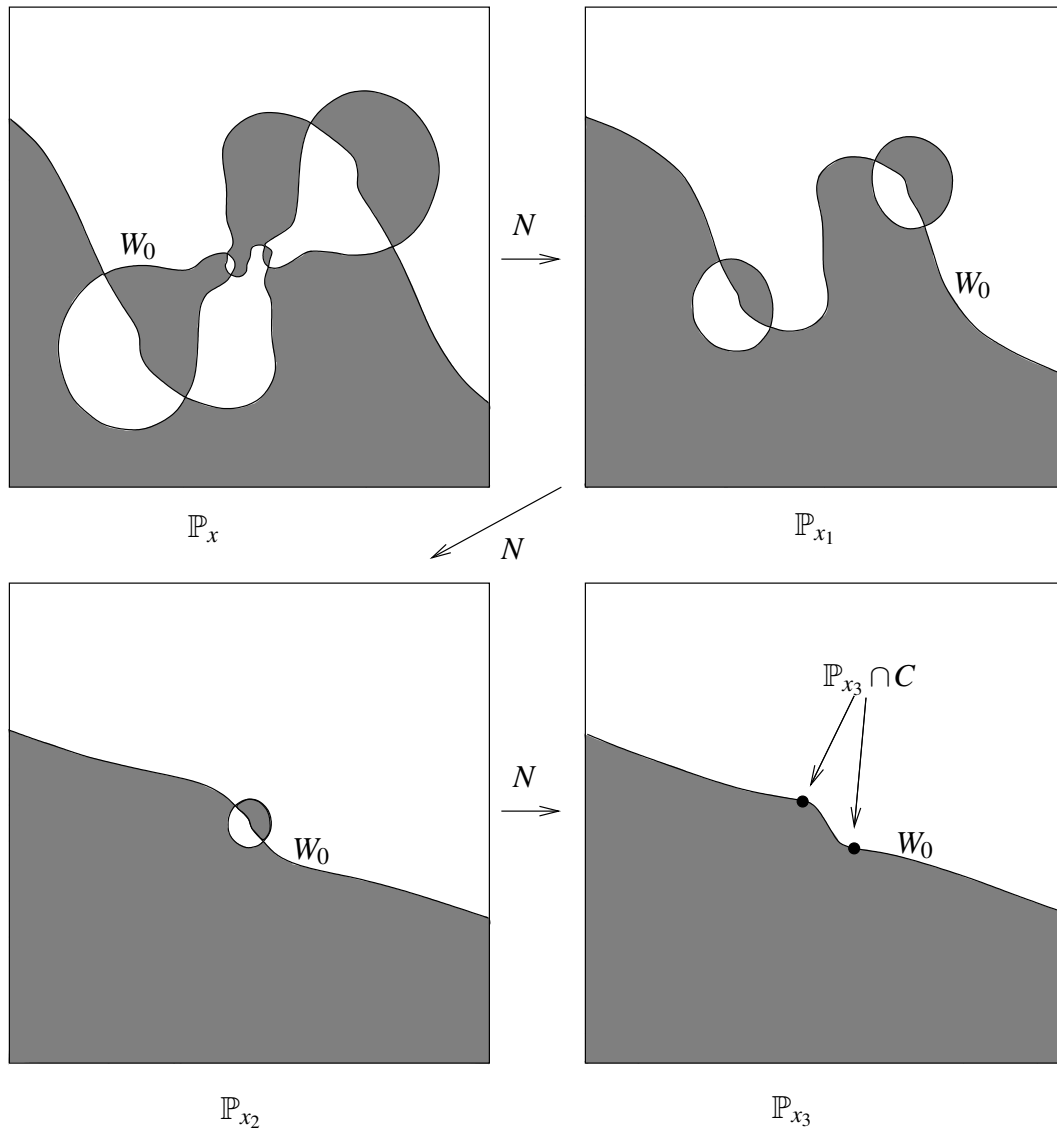


Figure 8.1: Forming many closed loops in W_0 . A sequence of vertical complex lines $\mathbb{P}_x, \mathbb{P}_{x_1}, \mathbb{P}_{x_2}$, and \mathbb{P}_{x_3} , one mapped to the next by N . Because W_0 intersects C in the line \mathbb{P}_{x_3} , Proposition 8.2.1 states that these vertical lines are divided by W_0 into at least 10, 6, 4, and 2 simply connected domains.

Proof: Because U is a simply connected open subset of \mathbb{P} , U is contractible. Let $c_t : U \times [0, 1] \rightarrow U$ be this contraction having $c_1(U) = u_0$, some base point in U . Recall that contractions satisfy $c_t(u_0) = u_0$ for all t .

If U does not contain the image of a ramification point, then $R : R^{-1}(U) \rightarrow U$ is a genuine covering map, and by the homotopy lifting property this contraction lifts, providing a contraction to $R^{-1}(U)$ to the points $R^{-1}(u_0)$.

Otherwise, if U contains a ramification point, we can modify our contraction c so that

the base point u_0 is this ramification point. Then, the mapping C lifts over $U - u_0$ and clearly extends by continuity over u_0 since $c_t(u_0) = u_0$ for all t .

Hence, $R^{-1}(U)$ consists of a collection of disjoint simply connected domains. The number of these domains is bounded above by the degree d .

□

Let $x_1 = \frac{x_0^2}{2x_0-1}$ so that we have $R_{x_0} : \mathbb{P}_{x_0} \rightarrow \mathbb{P}_{x_1}$. The symmetry 4.1.1 gives us two nice properties: First, since the critical values of R_{x_0} occur at symmetric points, either $W_0 \cap \mathbb{P}_{x_1}$ contains both critical values or neither of them.

Second, Since the symmetry interchanges $W(r_1)$ with $W(r_2)$, any simply connected domain in $\mathbb{P}_{x_1} - W_0$ and its image under the symmetry are disjoint. Since the two critical values of R_{x_0} are at symmetric points, such a domain can contain at most one of these critical values. Therefore, the inverse image of a simply connected domain will be some finite number of simply connected domains. The following lemma counts this number:

Lemma 8.2.4. *Let $x_1 = x_0^2/(2x_0 - 1)$ and suppose that U is a simply connected domain in \mathbb{P}_{x_1} .*

- *If U contains one of the critical values of R_{x_0} , then $R_{x_0}^{-1}(U)$ is a single simply connected domain.*
- *If U contains does not contain a critical value of R_{x_0} , then $R_{x_0}^{-1}(U)$ is two simply connected domains.*

Proof: Notice that $R_{x_0} : R_{x_0}^{-1}(U) \rightarrow U$ is a ramified covering map of degree 2, so the Riemann-Hurwitz formula applies giving, $\chi(R_{x_0}^{-1}(U)) = 2\chi(U) - k$ where k is the number of critical values of R_{x_0} in U . (Here, $k = 0$ or $k = 1$.) Since U is a single simply connected domain and $R_{x_0}^{-1}(U)$ is a finite union of simply connected domains, the Euler characteristic just counts the number of domains. Hence, if U contains a critical value, $k = 1$, and there are $2 - 1 = 1$ domains in $R_{x_0}^{-1}(U)$. Otherwise, if U does not contain a critical value, $k = 0$ and there are $2 - 0 = 2$ domains in $R_{x_0}^{-1}(U)$. □

Corollary 8.2.5. *Let $x_1 = \frac{x_0^2}{2x_0-1}$. If W_0 divides \mathbb{P}_{x_1} into m simply connected domains then*

- *If $W_0 \cap \mathbb{P}_{x_1}$ contains the critical values of R_{x_0} then W_0 divides \mathbb{P}_{x_0} into exactly $2m$ simply connected domain.*
- *If $W_0 \cap \mathbb{P}_{x_1}$ does not contain the critical values of R_{x_0} then W_0 divides \mathbb{P}_{x_0} into exactly $2m - 2$ simply connected domains.*

Proof: If $W_0 \cap \mathbb{P}_{x_1}$ contains the critical values of R_{x_0} , then none of the m domains in \mathbb{P}_{x_1} contain a critical value. By Lemma 8.2.4, each of these domains has two domains as inverse image under R_{x_0} , and hence W_0 divides \mathbb{P}_{x_0} into exactly $2m$ simply connected domain.

Otherwise, at most two of the domains in \mathbb{P}_{x_1} contain critical values of R_{x_0} . Each of these two domains has a single domain as inverse image under R_{x_0} , while each of the

remaining $m - 2$ domains has 2 domains as inverse image, giving a total of $2 + 2(m - 2) = 2m - 2$ domains in \mathbb{P}_{x_0}

□

Proof of Proposition 8.2.1: Let x_k be the k -th iterate of x_0 under $x \mapsto \frac{x^2}{2x-1}$. Suppose that W_0 divides the vertical line \mathbb{P}_{x_0} into m pieces. Because the line $x = 0$ is globally attracting in X_I^∞ , there is some k so that $|x_k - 0| < \varepsilon_0$. Using Lemma 8.2.2, $W_0 \cap \mathbb{P}_{x_k}$ forms a simple closed curve in \mathbb{P}_{x_k} and hence divides \mathbb{P}_{x_k} into only two simply connected domains.

Let x_n be the last point in the sequence x_1, x_2, \dots, x_k having $W_0 \cap \{C(x_n, y) = 0\} \neq \emptyset$. Repeated use of Lemma 8.2.5 gives the lower bound $m \geq 2^{n+1} - 2^{n-1} - 2^{n-2} - \dots - 2 = 2^{n+1} - 2^n + 2 = 2^n + 2$. The upper bound on the number of simply connected domains is clearly 2^{n+1} , so we have $2^n + 2 < m < 2^{n+1}$.

This proves Proposition 8.2.1 for X_I^∞ . The proof is virtually identical for X_r . □

8.3 Sizes

Suppose that $W_0 \cap \mathbb{P}_x$ divides \mathbb{P}_x into $2m$ simply connected domains. By the symmetry, m of these domains are in the basin $W(r_1)$ and m of them are in $W(r_2)$. Denote the domains in $W(r_1)$ by U_1, \dots, U_m and the domains in $W(r_2)$ by V_1, \dots, V_m . Let k be chosen so that W_0 forms a simple closed curve in \mathbb{P}_{x_k} (where x_k is the k -th iterate of x under $x \mapsto \frac{x^2}{2x-1}$.) Denote by U the domain in \mathbb{P}_{x_k} within $W(r_1)$ and by V the domain in \mathbb{P}_{x_k} within $W(r_2)$.

Under the mapping N^k , each of the domains U_1, \dots, U_m covers U with some degree l_1, \dots, l_m and each of the domains V_1, \dots, V_m covers V with degree p_1, \dots, p_m . Then, the following is true:

Proposition 8.3.1.

$$\sum_{i=1}^m l_i = 2^k, \quad \sum_{i=1}^m p_i = 2^k$$

Proof: The sum $\sum_{i=1}^m l_i$ counts the number of times that U is covered by $\cup_{i=1}^m U_i \subset \mathbb{P}_x$. Since \mathbb{P}_x covers \mathbb{P}_{x_k} with degree 2^k we must have $\sum_{i=1}^m l_i = 2^k$. The proof for the second sum is the same. □

Given a region U_i in $W(r_1)$ we will can assign $\text{size}(U_i) = -\frac{l_i}{2^k}$ and given a region V_i in $W(r_2)$ we can assign $\text{size}(U_i) = \frac{p_i}{2^k}$. Where k, l_i , and p_i are as in the above proposition. This is well defined because given k_1 and k_2 as above, the l_i corresponding to k_1 and the l_i corresponding to k_2 will differ by $2^{k_1-k_2}$.

Corollary 8.3.2. *Suppose that $W_0 \cap \mathbb{P}_x$ divides \mathbb{P}_x into $2m$ simply connected domains: $U_1, \dots, U_m \subset W(r_1)$ and $V_1, \dots, V_m \subset W(r_1)$. Then:*

$$\sum_{i=1}^m \text{size}(U_i) = -1, \quad \sum_{i=1}^m \text{size}(V_i) = 1$$

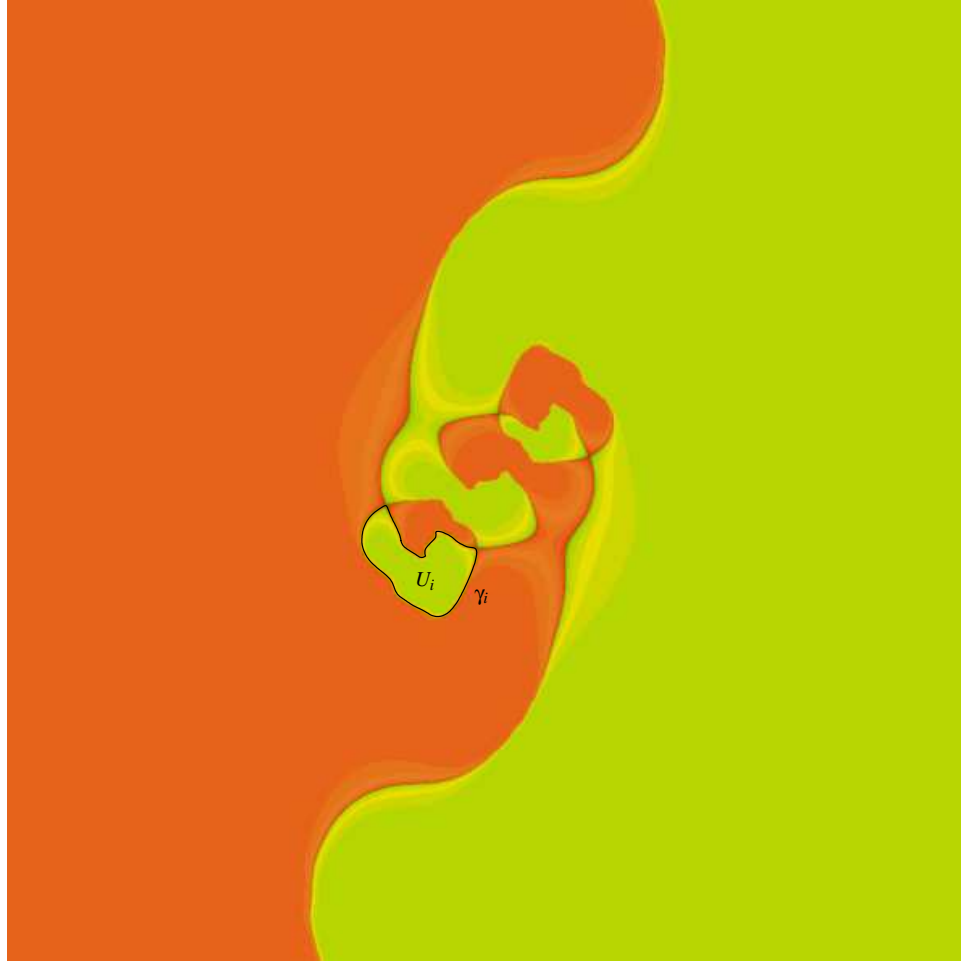


Figure 8.2: Example of a curve γ_i surrounding a simply connected domain U_i in some vertical line. In the next chapter we will prove that curves of this form are non-trivial in $H_1(W_0)$ (or $H_1(W_1)$) by linking these curves with an object that is disjoint from W_0 (or from W_1 .)

8.4 Many loops in W_0 and W_1

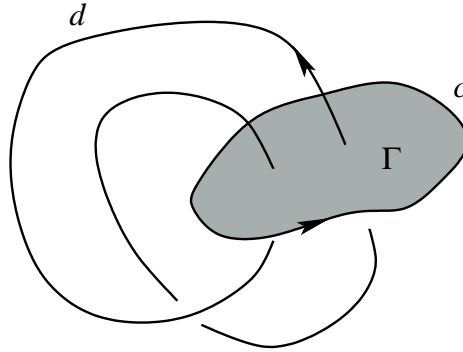
Given a region U_i or V_i in some vertical line \mathbb{P}_x let γ_i be the curve in W_0 bounding U_i . Since γ_i is a subset of $W_0 \cap \mathbb{P}_x$, it is a piecewise smooth curve. (This will be useful later when we want to consider the class $[\gamma_i] \in H_1(W_0)$.)

In the next chapter we will see that $\text{size}(U_i)$ for such a region equals the linking number for γ_i with an appropriate geometric object in X_1^∞ . (This object will remain mysterious for the moment.) These linking numbers will descend to the homology $H_1(W_0)$, which will allow us to show that if there is an intersection between W_0 and $C(x, y) = 0$, then $H_1(W_0)$ is infinitely generated. The similar statement about simply connected domains in vertical lines in X_r will be true as well.

Chapter 9

Linking numbers

The classical scenario is the linking of two oriented loops c and d in \mathbb{S}^3 . The linking number $lk(c, d) \in \mathbb{Z}$ is found by taking any oriented surface Γ with oriented boundary c and defining $lk(c, d)$ to be the signed intersection number of Γ with d . For example, in the following diagram $lk(c, d) = +2$.



To see that $lk(c, d)$ is well-defined in \mathbb{S}^3 , we can express this computation in terms of homology, letting c and d be one-cycles and Γ a 2-chain with $\partial\Gamma = c$. (Because $H_1(\mathbb{S}^3) = 0$, $[c] = 0$, so the existence of Γ is guaranteed.) We can then consider $[d] \in H_1(\mathbb{S}^3, c)$ and $[\Gamma] \in H_2(\mathbb{S}^3, c)$. We define $lk(c, d) = [\Gamma] \cdot [d]$, where \cdot indicates the intersection product on $H_*(\mathbb{S}^3, c)$.

Suppose that Γ' is some other 2-chain with $\partial\Gamma' = c$, then $\partial(\Gamma - \Gamma') = [c] - [c] = 0$, and so $(\Gamma - \Gamma')$ forms a homology class in $H_2(\mathbb{S}^3)$. Since $H_2(\mathbb{S}^3) = 0$ we must have that $[\Gamma - \Gamma'] = 0$ and so the intersection number is $[\Gamma - \Gamma'] \cdot [d] = 0$. Therefore: $[\Gamma] \cdot [d] = [\Gamma'] \cdot [d]$, giving that $lk(c, d)$ is well defined.

The two properties that we used were that $[c] = 0$, so that there are 2-chains Γ with $\partial\Gamma = c$ and that $H_2(\mathbb{S}^3) = 0$ to check that the linking number is independent of the choice of Γ .

To summarize: if M is a 3-dimensional manifold with $H_2(M) = 0$, let $Z_1(M)$ be the 1-cycles in M and $B_1(M) \subset Z_1(M)$ be the 1-boundaries in M . Given a 1-cycle d , let $B_1^d(M)$ be the 1-boundaries in M that are disjoint from d . Then, we have homomorphism, which we write

$$lk(\cdot, b) : B_1^d(M) \rightarrow \mathbb{Z}$$

defined by $lk(c, d) = [\Gamma] \cdot [d]$, where Γ is a 2-chain with $\partial\Gamma = c$. Since we require that c be disjoint from d , there is no ambiguity about this intersection number.

In this chapter we will build up the tools necessary to define some notion of linking in X_1^∞ , which has an infinitely generated $H_2(X_1^\infty)$. *Making linking numbers well defined in this space will be a major difficulty that we overcome in the next few sections.*

9.1 Linking in manifolds M with non-trivial intermediate homology.

Suppose that $M = \mathbb{S}^2 \times \mathbb{S}^1$, so that $H_2(M) = \mathbb{Z}\{[\mathbb{S}^2]\}$. Let c be the equator of \mathbb{S}^2 crossed with some point on $p \in \mathbb{S}^1$ and let d be the copy of \mathbb{S}^1 above say the north pole of \mathbb{S}^2 . Figure 9.1 shows these curves in $\mathbb{S}^2 \times [-1, 1]$, and it is left to the reader to identify the endpoints of each interval, in order to visualize $\mathbb{S}^2 \times \mathbb{S}^1$.

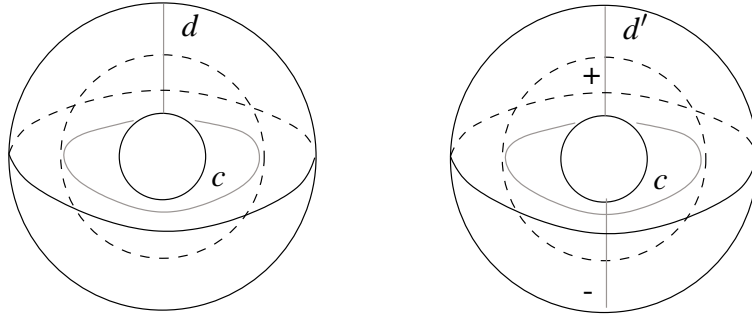


Figure 9.1: Linking in a weird space.

Let's see that $lk(c, d)$ is not well defined: Suppose that Γ_1 is the northern hemisphere of \mathbb{S}^2 crossed with p and that Γ_2 is the southern hemisphere of \mathbb{S}^2 crossed with p . Choose orientations for $\partial\Gamma_1 = c$ and $\partial\Gamma_2 = c$.

Since Γ_1 has intersection number 1 with d and Γ_2 has intersection number 0 with d , we see that $lk(c, d)$ is not well-defined! This follows from the simple reason $[\mathbb{S}^2] \cdot [d] = 1$.

Let d' be the copy of \mathbb{S}^1 above say the north pole of \mathbb{S}^2 minus the copy of \mathbb{S}^1 above the south pole of \mathbb{S}^2 . This way, $[d'] \cdot [\mathbb{S}^2] = 0$ so that $\Gamma_1 \cdot [d'] = \Gamma_2 \cdot [d']$ for any Γ_1 and Γ_2 having boundary c . In this case, $lk(c, d') = +1$.

This is the same as showing that the curve c is homologically non-trivial in $\mathbb{S}^2 \times \mathbb{S}^1$ with the two curves forming $[d']$ removed: $[c] \neq 0 \in H_1(\mathbb{S}^2 \times \mathbb{S}^1 - d')$.

Linking kernel: $\mathcal{LZ}_p(M)$

Suppose that M is a 3-dimensional manifold with $H_2(M) \neq 0$. As in the previous example, we can define a linking number, so long as the second argument d has $[d] \cdot \sigma = 0$ for every $\sigma \in H_2(M)$. We define $\mathcal{LZ}_1(M) \subset Z_1(M)$ to be the sub-module of $Z_1(M)$ with this property. As before, given $d \in \mathcal{LZ}_1(M)$, we denote by $B^d(M)$ the 1-boundaries in M that are disjoint from d . Then, the map:

$$lk(\cdot, d) : B_1^d(M) \rightarrow \mathbb{Z}$$

given by $lk(c, d) = \Gamma \cdot d$ is well-defined, i.e. independent of Γ .

In a manifold M of dimension m , one can define a linking number between boundaries c of dimension n and cycles d of dimension p so long as $n + p = m - 1$. If $H_{n+1}(M) = 0$, $lk(c, d) = \Gamma \cdot d$ for an $n + 1$ -chain Γ with $\partial\Gamma = c$ provides a well-defined linking number.

Otherwise, one must make a similar restriction as above restricting to $d \in \mathcal{LZ}_p(M)$ satisfying $[d] \cdot \sigma = 0$ for every $\sigma \in H_{p+1}(M)$. We will then denote by $B_n^d(M)$ the n -boundaries

in M that are disjoint from d . We get

$$lk(\cdot, d) : B_n^d(M) \rightarrow \mathbb{Z}.$$

9.2 Linking kernel for X_l^∞

Recall from Chapter 4 that except in the exceptional situation when one of the inverse images of the points of indeterminacy is on the critical locus,

$$H_2(X_l^\infty) = \mathbb{Z}^{\{[V]\}} \oplus \left(\bigoplus_{N^k(x)=p} \mathbb{Z}^{\{[E_x]\}} \right) \oplus \left(\bigoplus_{N^k(x)=q} \mathbb{Z}^{\{[E_x]\}} \right)$$

Recall from Proposition 5.3.6 that each exceptional divisor $[E_i]$ has $[E_i] \cdot [E_i] \leq -1$ and that $[V] \cdot [V] = 0$ so that if $\omega = a_0[V] + a_1[E_1] + \cdots + a_n[E_n]$, and satisfies $\omega \cdot \sigma = 0$ for every $\sigma \in H_2(X_l^\infty)$ $a_i = 0$ for all $i \neq 0$, that is, $\omega = a_0[V]$.

In summary, $\mathcal{L}Z_2(X_l^\infty)$ consists of only the 2-cycles that are homologous to multiples of $[V]$. The particular curves that we will consider here, i.e. the γ_i , have linking number 0 with $[V]$, since each of these curves is entirely within some vertical line. So, to show that all of these curves are non-trivial, we will need to look elsewhere for something to link with. We will do this by extending the definition of linking to linking with “positive closed currents”.

9.3 Linking with currents

Just as distributions are defined as the topological dual of smooth functions with compact support, currents are the topological dual of smooth differential forms of compact support. In fact, naturally, the dual of $A_c^0(M)$ is the space of n -currents (or generalized n -forms), not generalized functions as is usually stated.

More precisely, if we let $A_c^{n-q}(M)$ denote the $(n-q)$ -forms with compact support on a smooth manifold M , the linear maps $T : A_c^{n-q}(M) \rightarrow \mathbb{C}$ that are continuous are the **currents of degree q** (or, as some say, the currents of **dimension $n-q$**) and are denoted by $\mathcal{D}^q(M)$. If M has a complex structure, one defines the currents of bi-degree (p, q) , denoted $\mathcal{D}^{p,q}(M)$ as the topological dual of the $(n-p, n-q)$ -forms with compact support $A_c^{n-p, n-q}(M)$.

The reader who would like more background on currents should consult [24, section 3.1 and 3.2], or one articles on complex dynamics which outlines the basic properties of currents and their use in dynamics, [36, 48, 47].

Throughout the remainder of this section we will only be interested in currents on 2-dimensional complex surfaces and complex curves.

We will be interested in a very small sub-space of currents, the **closed, positive (1,1) currents** T which, according to the dd^c -Poincaré Lemma, are locally expressed as $T = dd^c \phi$ for a plurisubharmonic function ϕ .

Reminder: An upper semicontinuous function $g : U \rightarrow \mathbb{R} \cup \{-\infty\}$ is said to be *subharmonic* if for every $x \in U$ and every $r > 0$ for which $\bar{B}(x, r) \subset U$, and for every real valued function h on $\bar{B}(x, r)$ that is harmonic on $B(x, r)$ and satisfies $h \geq g$ on $\partial B(x, r)$, it holds that $h \geq g$ on $B(x, r)$. Given a domain $\Lambda \subset \mathbb{C}^n$, an upper semicontinuous function $g : \Lambda \rightarrow \mathbb{R} \cup \{-\infty\}$ is said to be *plurisubharmonic* if for every line L , $f|_L$ is subharmonic on $\Lambda \cap L$.

We will try to avoid using many details about plurisubharmonic functions, but we will occasionally need to use them to describe the geometry of closed-positive currents. Denote by $Z_+^{1,1}(M)$ the closed-positive $(1, 1)$ currents on M . Given a current $T \in Z_+^{1,1}(M)$, and a piecewise smooth 2-chain σ having $\partial\sigma$ disjoint from the support of T , we have the pairing:

$$C_2(M) \times Z_+^{1,1}(M) \rightarrow \mathbb{R}$$

defined by $(\sigma, T) = \int_\sigma T$. It is a well known result that this depends only on the homology class of σ .

Denote by $\mathcal{L}Z_+^{1,1}(M)$ the space of positive closed currents T having $\int_\sigma T = 0$ for every $\sigma \in H_2(M)$. Given $T \in \mathcal{L}Z_+^{1,1}(M)$, let $B_1^T(M)$ be the 1-boundaries in M that are disjoint from the support of T . We can define a linking number with respect to T by:

$$lk(\cdot, T) : B_1^T(M) \rightarrow \mathbb{R}$$

by $lk(c, T) = \int_\Gamma T$, where Γ is any 2-chain with $\partial\Gamma = c$. Since $T \in \mathcal{L}Z_+^{1,1}(M)$, we have that $\int_\Gamma T = \int_{\Gamma'} T$ for any other Γ' with $\partial\Gamma' = c$ since $\int_{\Gamma-\Gamma'} T = 0$. Since c is disjoint from the support of T , there are no problems.

9.4 Finding an element of $\mathcal{L}Z_+^{1,1}(X_l^\infty)$

In this section, we will find an element of $\mathcal{L}Z_+^{1,1}(X_l^\infty)$ by successively determining elements of $\mathcal{L}Z_+^{1,1}(X_l)$, $\mathcal{L}Z_+^{1,1}(X_l^0)$, $\mathcal{L}Z_+^{1,1}(X_l^1)$, $\mathcal{L}Z_+^{1,1}(X_l^2)$, \dots where X_k^j is the space X_k after having completed the blow-ups at level j . In the limit, we will find an element of $\mathcal{L}Z_+^{1,1}(X_l^\infty)$, which in the next section will be useful for linking.

Let L_1 be the invariant line that goes through $(0, 0)$ and $(1, 0)$, i.e. $y = 0$ and L_2 be the invariant line that goes through $(0, 1)$ and $(1, 1 - B)$, i.e. $y + Bx - 1 = 0$. (To remember the indexing, think that L_1 contains r_1 and L_2 contains r_2 .) Note that we can use the Poincaré-Lelong formula (see for example [24, p. 388] or [48]) to express the fundamental classes of these lines as positive-closed currents:

$$[L_1] = \frac{1}{2\pi} dd^c \log |y|, \quad [L_2] = \frac{1}{2\pi} dd^c \log |y + Bx - 1|$$

Notice that each of these lines intersects any given vertical line \mathbb{P} with intersection number 1, or equivalently that

$$\int_{\mathbb{P}} [L_1] = 1 = \int_{\mathbb{P}} [L_2]$$

Hence, because $[V]$ is the sole generator of $H_2(X_I)$ we have that $[L_2] - [L_1] \in \mathcal{LZ}_+^{1,1}(X_I)$.

Now, suppose that we want to find an element of $\mathcal{LZ}_+^{1,1}(X_I^0)$, that is, a positive-closed 1-1 current that evaluates to 0 on every element of $H_2(X_I^0) \cong \mathbb{Z}^{\{[V],[E_p],[E_q]\}}$. In fact, we also have that:

$$\begin{aligned} \int_{E_p} [L_1] &= 1 = \int_{\mathbb{E}_1} [L_2] \\ \int_{E_q} [L_1] &= 0 = \int_{\mathbb{E}_1} [L_2] \end{aligned}$$

So, in fact $[L_2] - [L_1] \in \mathcal{LZ}_+^{1,1}(X_I^0)$

However, this luck will not continue. Let z be one of the two preimages-images of p that is in the invariant line L_1 . Since L_1 and L_2 intersect at the single point p , $z \notin L_2$. This results in the fact that

$$\int_{E_z} [L_1] = 1 \neq 0 = \int_{E_z} [L_2].$$

So that $[L_2] - [L_1] \notin \mathcal{LZ}_+^{1,1}(X_I^1)$.

Consider the inverse images under N of the lines L_1 and L_2 . The Poincaré-Lelong formula gives

$$\begin{aligned} [N^{-1}(L_1)] &= \frac{1}{2\pi} dd^c \log |N_2(x,y)|, \\ [N^{-1}(L_2)] &= \frac{1}{2\pi} dd^c \log |N_1(x,y) + B \cdot N_2(x,y) - 1| \end{aligned}$$

where $N_1(x,y)$ and $N_2(x,y)$ are the first and second components of the Newton map N . Let's check that $[N^{-1}(L_2)] - [N^{-1}(L_1)] \in \mathcal{LZ}_+^{1,1}(X_I^1)$.

This is slightly easier to prove if we instead work with $[N^{-2}(L_1)]$ and $[N^{-2}(L_2)]$, the second inverse images of L_1 and L_2 .

In general, if we denote by $N_1^k(x,y)$ and $N_2^k(x,y)$ are the first and second coordinates of N^2 , then:

$$\begin{aligned} [N^{-k}(L_1)] &= \frac{1}{2\pi} dd^c \log |N_2^k(x,y)|, \\ [N^{-k}(L_2)] &= \frac{1}{2\pi} dd^c \log |N_1^k(x,y) + B \cdot N_2^k(x,y) - 1| \end{aligned}$$

Before proceeding, we will need the following lemma:

Lemma 9.4.1. *For every $k \geq 0$ we have*

$$\int_V [N^{-k}(L_1)] = \int_V [N^{-k}(L_2)]$$

Proof: The k -th inverse images $N^{-k}(L_1)$ and $N^{-k}(L_2)$ both have degree 2^k in y , so they each intersect a generic vertical line exactly 2^k times. This intersection number coincides with the integrals. \square

Suppose that E_z is one of the exceptional divisors in X_l^1 . From Proposition 5.2.1 we know that N^l induces a ramified covering from E_z to $V = \mathbb{P}_{1/(B(2-B))}$ of some degree d (which is possibly 0) where $l = 1$ or $l = 2$. Then we can compute the following:

$$\begin{aligned}\int_{E_z} [N^{-2}(L_1)] &= \int_{N^l(E_z)} [N^{2-l}L_1] = d \int_V [N^{2-l}L_1] \\ \int_{E_z} [N^{-2}(L_2)] &= \int_{N^l(E_z)} [N^{2-l}L_2] = d \int_V [N^{2-l}L_2]\end{aligned}$$

and these are both equal because $\int_V [N^{2-l}L_1] = \int_V [N^{2-l}L_2]$ by Lemma 9.4.1

Since $H_2(X_l^1)$ is generated by the fundamental classes of V , E_p , E_q , and those introduced at the inverse images of p and of q , we conclude that $[N^{-2}(L_2)] - [N^{-2}(L_1)] \in \mathcal{LZ}_+^{1,1}(X_l^1)$.

There was nothing special about this situation; it generalizes to give the following proposition.

Proposition 9.4.2. $[N^{-(k+1)}(L_2)] - [N^{-(k+1)}(L_1)] \in \mathcal{LZ}_+^{1,1}(X_l^k)$

Proof Let E_z any one of the exceptional divisors in X_l^k . Using Proposition 5.2.1, there is some d and some $l \leq k+1$ so that N^l maps E_z to V by a ramified cover of degree d (possibly with $d = 0$.) Then, just as in the discussion above:

$$\begin{aligned}\int_{E_z} [N^{-(k+1)}(L_1)] &= \int_{N^l(E_z)} [N^{-(k+1)+l}L_1] = d \int_V [N^{-(k+1)+l}L_1] \\ \int_{E_z} [N^{-(k+1)}(L_2)] &= \int_{N^l(E_z)} [N^{-(k+1)+l}L_2] = d \int_V [N^{-(k+1)+l}L_2]\end{aligned}$$

and these are both equal, using Lemma 9.4.1.

Since $H_k(X_l^1)$ is generated by the fundamental classes of V and the fundamental classes of each of the exceptional divisors E_z we conclude that $[N^{-(k+1)}(L_2)] - [N^{-(k+1)}(L_1)] \in \mathcal{LZ}_+^{1,1}(X_l^k)$. \square

Fundamental classes such as $[N^{-k}(L_2)]$ and $[N^{-k}(L_1)]$ probably seem quite abstract at the moment. Because the inverse images of these lines are varieties in X_l^∞ , which is a rather complicated 2 complex-dimensional manifold, they are rather difficult to visualize. One can actually see something in \mathbb{R}^2 : In the top of Figure 9.2 we show $N^{-1}(L_1)$ (in gray) and $N^{-1}(L_2)$ (in black) in \mathbb{R}^2 , with $B = -0.3$. In the bottom of Figure 9.2 we show $N^{-2}(L_1)$ (in gray) and $N^{-2}(L_2)$ (in black). The points where these two curves cross are at the points in indeterminacy, which are labeled. We hope that this will give the reader some idea about these inverse images.

Since $X_l^\infty = \varprojlim (X_l^k, \pi)$ and because $([N^{-(k+1)}(L_2)] - [N^{-(k+1)}(L_1)]) \in \mathcal{LZ}_+^{1,1}(X_l^k)$ it seems that a limit as $k \rightarrow \infty$ of $[N^{-(k+1)}(L_2)] - [N^{-(k+1)}(L_1)]$ will be an element of $\mathcal{LZ}_+^{1,1}(X_l^\infty)$. We must be careful to make clear what limit we are taking, but we do so below.

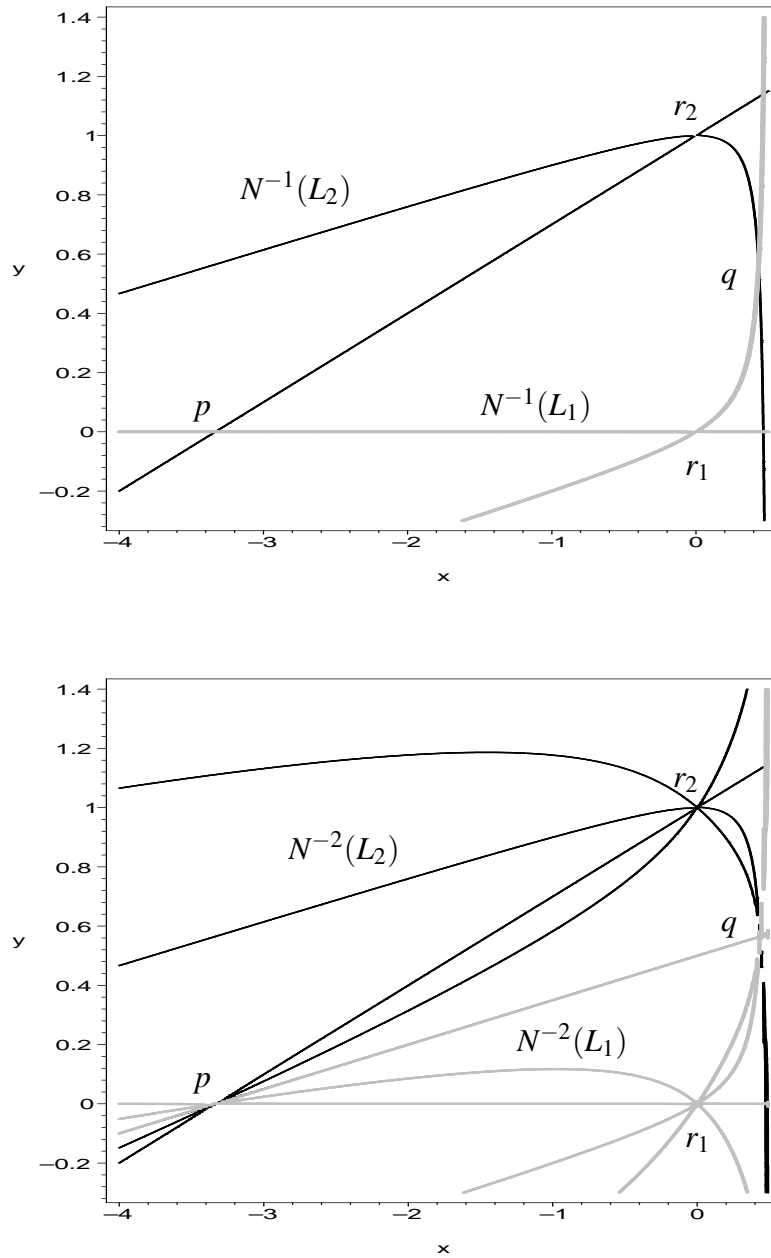


Figure 9.2: Newton map in \mathbb{R}^2 , $B = -0.3$. Top: $N^{-1}(L_2)$ in black and $N^{-1}(L_1)$ in gray. Bottom: $N^{-2}(L_2)$ in black and $N^{-2}(L_1)$ in gray.

First, we choose to normalize $[N^{-(k+1)}(L_2)]$ and $[N^{-(k+1)}(L_1)]$ so that their integrals over V are 1. By dividing by the degrees, we define:

$$\begin{aligned}\lambda_1^k &= \frac{1}{2^k}[N^{-k}(L_1)] = \frac{1}{2\pi}dd^c \frac{1}{2^k} \log |N_2^k(x,y)|, \\ \lambda_2^k &= \frac{1}{2^k}[N^{-k}(L_2)] = \frac{1}{2\pi}dd^c \frac{1}{2^k} \log |N_1^k(x,y) + B \cdot N_2^k(x,y) - 1|\end{aligned}$$

Both λ_1^k and λ_2^k are still positive closed currents because we have only divided by 2^k . We let

$$\begin{aligned}\lambda_1 &= \lim_{k \rightarrow \infty} \lambda_1^k = \frac{1}{2\pi}dd^c \lim_{k \rightarrow \infty} \frac{1}{2^k} \log |N_2^k(x,y)|, \\ \lambda_2 &= \lim_{k \rightarrow \infty} \lambda_2^k = \frac{1}{2\pi}dd^c \lim_{k \rightarrow \infty} \frac{1}{2^k} \log |N_1^k(x,y) + B \cdot N_2^k(x,y) - 1|.\end{aligned}$$

We will first check that these limits exist and define positive-closed 1-1 currents, and then we will show that $\lambda_2 - \lambda_1 \in \mathcal{LZ}_+^{1,1}(X_I^\infty)$.

Proposition 9.4.3. *The limits*

$$\begin{aligned}G_1(x,y) &= \lim_{k \rightarrow \infty} \frac{1}{2^k} \log |N_2^k(x,y)| \\ G_2(x,y) &= \lim_{k \rightarrow \infty} \frac{1}{2^k} \log |N_1^k(x,y) + B \cdot N_2^k(x,y) - 1|\end{aligned}$$

exist and are plurisubharmonic functions in the basins of attraction $W(r_1)$ and $W(r_2)$, respectively. Hence, $\lambda_1 = \frac{1}{2\pi}dd^c G_1(x,y)$ and $\lambda_2 = \frac{1}{2\pi}dd^c G_2(x,y)$ are positive closed 1-1 currents on X_I^∞ , that is: $\lambda_1, \lambda_2 \in \mathcal{Z}_+^{1,1}(X_I^\infty)$.

Proof: To see that $G_1(x,y)$ and $G_2(x,y)$ are well-defined and plurisubharmonic, we will show that $G_1(x,y)$ and $G_2(x,y)$ coincide with the potential functions that were described in [35, p. 21] and [36]. We will do this for $G_1(x,y)$, and leave necessary modifications for $G_2(x,y)$ to the reader.

Supposing that $(0,0)$ is a root, Hubbard and Papadopol [35] consider the limit

$$G_{HP}(x,y) = \lim_{k \rightarrow \infty} \frac{1}{2^k} \log ||N^k(x,y)||$$

which they show exists and is a plurisubharmonic function on the basin of $(0,0)$. The reader should notice that G_{HP} does not depend on the choice of the norm $|| \cdot ||$ that is used to define it because any two different norms on a finite dimensional vector space are equivalent by a finite multiplicative constant, which is eliminated by the multiplicative factor of $\frac{1}{2^k}$. Therefore, we can use the supremum norm.

We will show that $G_1 = G_{HP}$ on $W(r_1)$, to see that G_1 is plurisubharmonic.

If $|N_2^k(x,y)| \geq |N_1^k(x,y)|$ for all (x,y) as $k \rightarrow \infty$, then the supremum norm coincides with $|N_2^k(x,y)|$ giving $G_1(x,y) = G_{HP}(x,y)$. This condition is equivalent to the condition:

$$\lim_{k \rightarrow \infty} \frac{1}{2^k} \log \left| \frac{N_2^k(x,y)}{N_1^k(x,y)} \right| \geq 0. \quad (9.1)$$

which will now show is a consequence of a standard result from the dynamics of one complex variable.

In [35], the authors perform blow-ups at each of the four roots, and observe that the Newton map N induces rational functions of degree 2 on each of the exceptional divisors $E_{r_1}, E_{r_2}, E_{r_3}$, and E_{r_4} . Let's compute the rational function $s : E_{r_1} \rightarrow E_{r_1}$. In the coordinate chart $m = \frac{y}{x}$, the extension to E_{r_1} is obtained by:

$$\begin{aligned} s(m) &= \lim_{x \rightarrow 0} \frac{mx(Bx^2 + 2mx^2 - Bx - mx)}{x^2(Bx + 2mx - 1)} \\ &= \lim_{x \rightarrow 0} \frac{m(Bx + 2mx - B - m)}{Bx + 2mx - 1} = m(B + m) \end{aligned}$$

since $x = 0$ on E_{r_1} .

Since condition 9.1 is a limit, it suffices to check it in an arbitrarily small neighborhood of the origin. In a small enough neighborhood, we can replace $\frac{N_2^k(x,y)}{N_1^k(x,y)}$ with $s\left(\frac{x}{y}\right)$ obtaining

$$\lim_{k \rightarrow \infty} \frac{1}{2^k} \log \left| \frac{N_2^k(x,y)}{N_1^k(x,y)} \right| = \lim_{k \rightarrow \infty} \frac{1}{2^k} \log |s^k(m)| = G_s(m). \quad (9.2)$$

where $G_s(m)$ is the standard Green's function from one variable complex dynamics associated to the polynomial $s(m)$. This last equality is actually a delicate but well-known result that was proved by Brodin [12]. A more friendly proof is available in [48, Section 9].

Having the last equality, it is a standard result, for example see Milnor [43] pages 95 and 96, that $G_s(m) = 0$ on the filled Julia set $K(s)$ and that $G_s(m) > 0$ outside of $K(s)$.

This justifies the replacement of the supremum norm from G_{HP} by $|N_2^k(x,y)|$, and hence gives that $G_1(x,y) = G_{HP}(x,y)$. \square

Corollary 9.4.4. *Let $s : E_{r_1} \rightarrow E_{r_1}$ be the polynomial induced by the Newton map N and let $G_s : E_{r_1} \rightarrow \mathbb{R}$ be its Green's function. We have:*

$$G_1(x,y) = G_s\left(\frac{y}{x}\right) - \log \left| \frac{1}{x} \right|.$$

Proof: This just comes from the algebra:

$$\begin{aligned} G_1(x,y) &= \lim_{k \rightarrow \infty} \frac{1}{2^k} \log |N_2^k(x,y)| \\ &= \lim_{k \rightarrow \infty} \frac{1}{2^k} \left(\log \left| \frac{N_2^k(x,y)}{N_1^k(x,y)} \right| + \log |N_1^k(x,y)| \right) \\ &= G_s\left(\frac{y}{x}\right) + \lim_{k \rightarrow \infty} \frac{1}{2^k} \log |N_1^k(x,y)| \\ &= G_s\left(\frac{y}{x}\right) + \log |x| = G_s\left(\frac{y}{x}\right) - \log \left| \frac{1}{x} \right| \end{aligned}$$

Because $N_1^k(x,y) = \frac{x^2}{2x-1}$ is conjugate to $x \mapsto x^2$ near $x = 0$. \square

9.5 Nice properties of λ_2 and λ_1 :

In this section, we will prove some of the nice properties of λ_2 and λ_1 . We will finish the section by showing that $\lambda_2 - \lambda_1 \in \mathcal{LZ}_{1,1}^+$.

Lemma 9.5.1. (Normalization) *Suppose that \mathbb{P}_x is a vertical line that is divided into exactly two simply connected domains $U \subset W(r_1)$ and $V \subset W(r_2)$ by W_0 . Then:*

$$\int_V \lambda_2 = 1 = \int_U \lambda_1 \text{ and } \int_U \lambda_2 = 0 = \int_V \lambda_1$$

Proof: Because $N_2^k(x, y)$ and $BN_1^k(x, y) + N_2^k(x, y) - 1$ are of degree 2^k in y , both λ_1^k and λ_2^k are normalized to that $\int_V \lambda_1^k = 1$ and $\int_V \lambda_2^k = 1$. Since the potential for λ_1^k and λ_2^k converge uniformly on compact subsets to λ_1 and λ_2 , we have

$$\int_U \lambda_1 = \int_U \lim_{k \rightarrow \infty} \lambda_1^k = \lim_{k \rightarrow \infty} \int_U \lambda_1^k = \lim_{k \rightarrow \infty} 1 = 1.$$

and similarly for λ_2 . The proof that $\int_U \lambda_2 = 0 = \int_V \lambda_1$ is identical. \square

Corollary 9.5.2. *Suppose that \mathbb{P}_x is vertical line, then $\int_{\mathbb{P}_x} \lambda_2 = 1 = \int_{\mathbb{P}_x} \lambda_1$.*

The currents λ_1 and λ_2 have nice invariance properties:

Lemma 9.5.3. (Invariance) *Suppose that $\Gamma \in Z_2(X_1^\infty)$, then*

$$\int_{N(\Gamma)} \lambda_1 = 2 \cdot \int_\Gamma \lambda_1 \quad \int_{N(\Gamma)} \lambda_2 = 2 \cdot \int_\Gamma \lambda_2$$

Proof The proof is the same for λ_1 and λ_2 , so will show it for λ_1 :

$$\begin{aligned} \int_{N(\Gamma)} \lambda_1 &= \int_{N(\Gamma)} \lim_{k \rightarrow \infty} \frac{1}{2^k} \log |N_1^k(x, y)| = \int_\Gamma \lim_{k \rightarrow \infty} \frac{1}{2^k} \log |N_1^{k+1}(x, y)| \\ &= \int_\Gamma 2 \lim_{(k+1) \rightarrow \infty} \frac{1}{2^{k+1}} \log |N_1^{k+1}(x, y)| = 2 \cdot \int_\Gamma \lambda_1 \end{aligned}$$

\square

Proposition 9.5.4. (Support disjoint from W_0) *There is a neighborhood Θ of W_0 in X_1^∞ which is disjoint from the support of λ_1 and disjoint from the support of λ_2 .*

Proof: By construction, λ_1 has support in $\overline{W(r_1)}$ and λ_2 has support in $\overline{W(r_2)}$. We will find a neighborhood, which we also call Θ , of W_0 in $\overline{W(r_1)}$ that is disjoint from the support of λ_1 . Clearly similar methods will work in $\overline{W(r_2)}$ and the desired neighborhood is the union of the two.

Recall from Corollary 9.4.4 that

$$G_1(x, y) = G_s\left(\frac{y}{x}\right) - \log \left| \frac{1}{x} \right|,$$

where G_s is the Green's function associated to the polynomial $s : E_{r_1} \rightarrow E_{r_1}$ induced by N at r_1 . Recall that $s(m) = m(B + m)$ in the coordinates $m = \frac{x}{y}$ on E_{r_1} , so that $m = \infty$ is a superattracting fixed point. (This is the standard situation for a quadratic polynomial.)

It is a standard result from one-variable dynamics, for example see [43] p. 96, that G_s is harmonic outside of the Julia set $J(s)$. In particular, G_s is harmonic in a neighborhood of ∞ (not including ∞). A related standard result that G_s has the singularity

$$G(m) = \log |m| + O(1) \text{ as } m \rightarrow \infty$$

We check that this singularity exactly cancels with $-\log \left| \frac{1}{x} \right|$ coming from $G_1(x, y) = G_s \left(\frac{y}{x} \right) - \log \left| \frac{1}{x} \right|$:

$$\begin{aligned} G_1(x, y) &= \log \left| \frac{y}{x} \right| - \log \left| \frac{1}{x} \right| + O(1) \text{ as } \left| \frac{y}{x} \right| \rightarrow \infty \\ &= \log |y| + O(1) \text{ as } \left| \frac{y}{x} \right| \rightarrow \infty \end{aligned}$$

Therefore, $G_1(x, mx)$ is harmonic on a neighborhood U of $m = \infty$, including the point ∞ . Choose $\theta > 0$ so that if $\frac{|m|}{|x|} > \theta$, then $G_1(x, mx)$ is harmonic.

Let $\Theta_0 = \{(x, y) \in W(r_1) \text{ such that } \left| \frac{y}{x} \right| > \theta\}$. This is the open cone of points in $W(r_1)$ with slope to the origin greater than θ . Since the invariant circle S_0 is above $m = \infty$, Θ_0 is a neighborhood of S_0 (within $W(r_1)$.)

By construction,

$$\Theta = \bigcup_{n=0}^{\infty} N^{-n}(\Theta_0)$$

will be invariant under N and open. Because Θ_0 is disjoint from the support of λ_1 , the invariance properties for λ_1 from Lemma 9.5.3 give that all of Θ must be disjoint from the support of λ_1 .

Finally, since Θ_0 contains a neighborhood of S_0 , and both W_0 and Θ are invariant under N , Θ forms an open neighborhood of W_0 . \square

Corollary 9.5.5. *Given any piecewise smooth chain $\sigma \in W_0$, we have that $\int_{\sigma} \lambda_1 = 0$ and $\int_{\sigma} \lambda_2 = 0$.*

Proposition 9.5.6. $\lambda_1 - \lambda_2 \in \mathcal{L}Z_+^{1,1}(X_l^{\infty})$

Proof: This proof will be along the lines of the proof from Proposition 9.4.2, but will be even simpler, using the invariance of λ_1 and λ_2 shown in Lemma 9.5.3.

An element of $H_2(X_l^{\infty})$ is a linear combination of the fundamental class $[V]$ with a finite number of fundamental classes of exceptional divisors E_z . By Corollary 9.5.2, we have $\int_V \lambda_1 = \int_V \lambda_2$.

Any exceptional divisor E_z was created during the blow-ups at some level k , and using Proposition 5.2.1 there is some l so that $N^{\circ(k+1)}$ maps E_z to $V = \mathbb{P}_1/(B(2-B))$ by a ramified covering mapping of degree l , (possibly $l = 0$). Then:

$$\int_{E_z} \lambda_1 = \frac{l}{2^k} \int_V \lambda_2 = \frac{l}{2^k} \int_V \lambda_2 = \int_{E_z} \lambda_1$$

using that $\int_V \lambda_1 = \int_V \lambda_2$. Hence $\int_{E_z} (\lambda_2 - \lambda_1) = 0$ for any exceptional divisor E_z .

Since an element of $H_2(X_I^\infty)$ is a linear combination of the fundamental class $[V]$ with a finite number of fundamental classes of exceptional divisors E_z , we have shown that $\lambda_2 - \lambda_1 \in \mathcal{LZ}_+^{1,1}(X_I^\infty)$. \square

9.6 Linking with currents in X_I^∞

We have infinitely many cycles γ_i in W_0 and we now have $(\lambda_2 - \lambda_1) \in \mathcal{LZ}_+^{1,1}(X_I^\infty)$ with which we can try to link them.

Proposition 9.6.1. *Suppose that γ_i is a curve in a vertical line bounded by a simply connected domain U_i . Then:*

$$lk(\gamma_i, \lambda_2 - \lambda_1) = \text{size}(U_i)$$

Proof of Proposition 9.6.1:

This will follow easily from Lemma 9.5.1 and the invariance properties of λ_2 and λ_1 that were proved in Lemma 9.5.3.

Recall that $\text{size}(U_i)$ is defined as $\pm \frac{l_i}{2^k}$ where k is such that N^k maps to a vertical line \mathbb{P}_x that is divided by W_0 into only two domains $U \subset W(r_1)$ and $V \subset W(r_2)$ and where l_i is the degree of this mapping to U or V . The sign $-$ if U_i is mapped to U and $+$ if U_i is mapped to V . Without loss in generality, suppose that U_i is mapped to U , and hence $\text{size}(U_i) < 0$. Using Lemma 9.5.3 we have that:

$$\begin{aligned} \int_{U_i} \lambda_2 - \lambda_1 &= \frac{1}{2^k} \int_{N^k(U_i)} \lambda_2 - \lambda_1 = \\ \frac{1}{2^k} \int_{l_i U} -\lambda_1 &= -\frac{l_i}{2^k} \int_{U_i} \lambda_1 = -\frac{l_i}{2^k} = \text{size}(U_i) \end{aligned}$$

where we are using that $\int_U \lambda_2 = 0$ and $\int_U \lambda_1 = 1$. \square

Recall from Chapter 7 that W_0 always intersects the critical value parabola C and from Chapter 8 that such an intersection leads to sequences of vertical lines that are divided into arbitrarily many simply connected domains. Hence, there are always regions U_i having $|\text{size}(U_i)|$ arbitrarily small, but non-zero. Consequently, there are always $\gamma_i \in B_1(W_0)$ having $|lk(\gamma_i, \lambda_2 - \lambda_1)|$ arbitrarily small, but non-zero:

Proposition 9.6.2. *The image of the homomorphism:*

$$lk(\cdot, \lambda_2 - \lambda_1) : B_1^{\lambda_2 - \lambda_1}(X_I^\infty) \rightarrow \mathbb{R}$$

contains elements of arbitrarily small, but non-zero, absolute value.

9.7 $H_1(W_0)$ is infinitely generated.

Since $H_1(X_I^\infty) = 0$, every 1-cycle in X_I^∞ is in fact a 1-boundary in X_I^∞ . In particular, $Z_1(W_0) \subset B_1(X_I^\infty)$. By Lemma 9.5.4, the support of $\lambda_2 - \lambda_1$ is disjoint from W_0 , giving that $Z_1(W_0) \subset B_1^{\lambda_2 - \lambda_1}(X_I^\infty)$. Hence, we can restrict $lk(\cdot, \lambda_2 - \lambda_1)$ to 1-cycles in W_0 :

$$lk(\cdot, \lambda_2 - \lambda_1) : Z_1(W_0) \rightarrow \mathbb{R}$$

Proposition 9.7.1. *For every $\gamma \in Z_1(W_0)$, $lk(\gamma, \lambda_2 - \lambda_1)$ depends only on $[\gamma] \in H_1(W_0)$. In other words, the linking number descends to $H_1(W_0)$:*

$$lk(\cdot, \lambda_2 - \lambda_1) : H_1(W_0) \rightarrow \mathbb{R}$$

Proof: Suppose that $\gamma_1 - \gamma_2 = \partial\sigma$, with $\sigma \in C_2(W_0)$. since the support of $\lambda_2 - \lambda_1$ is disjoint from W_0 , $\int_\sigma \lambda_2 - \lambda_1 = 0$. Hence, $lk(\gamma_1, \lambda_2 - \lambda_1) = lk(\gamma_2, \lambda_2 - \lambda_1)$. \square

Corollary 9.7.2. *The image of the homomorphism*

$$lk(\cdot, \lambda_2 - \lambda_1) : H_1(W_0) \rightarrow \mathbb{R}$$

contains elements of arbitrarily small, but non-zero, absolute value.

This gives us our desired result:

Corollary 9.7.3. *The homology group $H_1(W_0)$ is infinitely generated.*

Recall the Mayer-Vietoris exact sequence 6.5 from Chapter 6:

$$H_2(\overline{W(r_1)}) \oplus H_2(\overline{W(r_2)}) \rightarrow H_2(X_I^\infty) \xrightarrow{\partial} H_1(W_0) \rightarrow H_1(\overline{W(r_1)}) \oplus H_1(\overline{W(r_2)}) \rightarrow 0$$

If $\text{Image}(\partial) = 0$, or even if we knew that $|\text{size}(\partial(\sigma))|$ were bounded away from 0 for every $\sigma \in H_2(X_I^\infty)$, we would be able to conclude that $H_1(\overline{W(r_1)})$ and $H_1(\overline{W(r_2)})$ are infinitely generated. However, this is not the case.

Proposition 9.7.4. *There are $\sigma \in H_2(X_I^\infty)$ with $|lk(\partial(\sigma), \lambda_2 - \lambda_1)|$ arbitrarily small, but non-zero.*

Proof: For every k , there exists some exceptional divisor E having $N^k : E \rightarrow V$ an isomorphism. This is easy to see for generic parameter values $B \in S$. In this case, any exceptional divisor at a $(k-1)$ -st inverse image of p will have this property, since, for generic B there is a single exceptional divisor above each point that we have blown up, and $N : E_z \rightarrow E_{N(z)}$ is always an isomorphism.

For the values of $B \notin S$, which are non-generic, there may be many blow-ups done at each $(k-1)$ -st inverse image of p . So, we take a detailed look at the sequence of blow-ups from section 5.1 that was used to create X_I^{k-1} from X_I^{k-2} . One must check that for each exceptional divisor $E_{N(z)}^i$ that occurs in the sequence of blow-ups at $N(z)$, there is

an exceptional divisor in the sequence of blow-ups at z that maps isomorphically to $E_{N(z)}^i$. Using this fact, one can always choose a sequence of exceptional divisors starting with E_p , and working backward to find an exceptional divisor E above some $(k-1)$ -st inverse image of p with the property that $N^{k-1} : E \rightarrow E_p$ is an isomorphism. Since $N : E_p \rightarrow V$ is always an isomorphism, E is the desired exceptional divisor.

Because N^k maps E isomorphically to V , it maps $\partial([E])$ to $\partial([V])$. We can use the invariance property from Lemma 9.5.3 to check that

$$lk(\partial([E]), \lambda_2 - \lambda_1) = \frac{1}{2^k} lk(\partial([V]), \lambda_2 - \lambda_1) = \frac{1}{2^k}.$$

□ Proposition 9.7.4.

9.8 $H_1(\overline{W(r_1)})$ and $H_1(\overline{W(r_2)})$ are infinitely generated.

The following idea will allow us to show that $H_1(\overline{W(r_1)})$ and $H_1(\overline{W(r_2)})$ are infinitely generated, despite the fact that $|lk(\partial(\sigma), \lambda_2 - \lambda_1)|$ can be arbitrarily small, but non-zero, for $\sigma \in H_2(X_I^\infty)$.

Recall from Proposition 4.1.1 that N has a symmetry of reflection about the line $Bx + 2y - 1 = 0$ which exchanges the basins of attraction. Denote this involution by $\tau : X_I^\infty \rightarrow X_I^\infty$.

Even and odd parts of Homology:

Notice that τ induces an involution τ_* on $H_*(X_I^\infty)$, $H_*(W_0)$, and $H_*(W(r_1)) \oplus H_*(W(r_2))$. Every homology class σ will have $\tau_*^2(\sigma) = \sigma$ and consequently the eigenvalues of σ are ± 1 .

We say that a homology class σ is *even* if it is in the eigenspace of τ_* corresponding to eigenvalue $+1$, and we say that σ is *odd* if it is in the eigenspace of τ_* corresponding to eigenvalue -1 .

Because the Mayer-Vietoris exact sequence commutes naturally with induced maps, we have a decomposition of the sequence 6.5 into even and odd parts:

$$(H_2(\overline{W(r_1)}) \oplus H_2(\overline{W(r_2)}))^{ev} \rightarrow H_2^{ev}(X_I^\infty) \xrightarrow{\partial} H_1^{ev}(W_0) \rightarrow (H_1(\overline{W(r_1)}) \oplus H_1(\overline{W(r_2)}))^{ev} \rightarrow 0$$

$$(H_2(\overline{W(r_1)}) \oplus H_2(\overline{W(r_2)}))^{od} \rightarrow H_2^{od}(X_I^\infty) \xrightarrow{\partial} H_1^{od}(W_0) \rightarrow (H_1(\overline{W(r_1)}) \oplus H_1(\overline{W(r_2)}))^{od} \rightarrow 0$$

We will only need the odd part of the homology.

The involution τ exchanges the currents λ_2 and λ_1 :

Lemma 9.8.1. *If σ is some piecewise smooth chain, then:*

$$\int_{\sigma} \lambda_2 = \int_{\tau(\sigma)} \lambda_1 \text{ and } \int_{\sigma} \lambda_1 = \int_{\tau(\sigma)} \lambda_2. \quad (9.3)$$

Proof:

Recall the definition of λ_2 and λ_1 :

$$\begin{aligned}\lambda_1 &= \frac{i}{\pi} \partial \bar{\partial} \lim_{k \rightarrow \infty} \frac{1}{2^k} \log |N_2^k(x, y)|, \\ \lambda_2 &= \frac{i}{\pi} \partial \bar{\partial} \lim_{k \rightarrow \infty} \frac{1}{2^k} \log |N_1^k(x, y) + B \cdot N_2^k(x, y) - 1|.\end{aligned}$$

Since precomposition with τ exchanges the line $Bx + y - 1$ with the line $y = 0$, clearly Equation 9.8.1 holds. \square

Corollary 9.8.2. *For every $[\gamma] \in H_1(W_0)$ we have:*

$$lk(\gamma, \lambda_2 - \lambda_1) = -lk(\tau(\gamma), \lambda_2 - \lambda_1)$$

Proof:

Suppose that σ is a piecewise smooth 2-chain with $\partial\sigma = \gamma$. Then we certainly have $\partial(\tau(\sigma)) = \tau(\gamma)$. Lemma 9.8.1 gives:

$$\begin{aligned}lk(\gamma, \lambda_2 - \lambda_1) &= \int_{\sigma} \lambda_2 - \lambda_1 = \int_{\tau(\sigma)} \lambda_1 - \lambda_2 \\ &= - \int_{\tau(\sigma)} \lambda_2 - \lambda_1 = -lk(\tau(\gamma), \lambda_2 - \lambda_1)\end{aligned}$$

\square

Proposition 9.8.3. *If $\gamma \in H_1^{\text{od}}(W_0)$ is in the image of the boundary map $\partial : H_2^{\text{od}}(X_1^{\infty}) \rightarrow H_1^{\text{od}}(W_0)$, then $lk(\gamma, \lambda_2 - \lambda_1) = 0$.*

We will need the following lemma:

Lemma 9.8.4. *For any exceptional divisor E_z we have*

$$\partial(\tau_*[E_z]) = -\tau_*(\partial([E_z])) \tag{9.4}$$

Proof: This proof will depend *essentially* on the explicit interpretation of the boundary map ∂ from the Mayer-Vietoris sequence. In the following paragraph we closely paraphrase Hatcher [28], p. 150:

The boundary map $\partial : H_n(X) \rightarrow H_{n-1}(A \cap B)$ can be made explicit. A class $\alpha \in H_n(X)$ is represented by a cycle z . By appropriate subdivision, we can write z as a sum $x + y$ of chains in A and B , respectively. While it need not be true that x and y are cycles individually, we do have $\partial x = -\partial y$ since $z = x + y$ is a cycle. The element $\partial\alpha$ is represented by the cycle $\partial x = -\partial y$.

The details of the next two paragraphs depend heavily on Figure 9.3.

We use this explicit interpretation of ∂ to check Equation 9.4. Notice that $\tau_*[E_z] = [E_{\tau(z)}]$ consistent with the orientation that E_z and $E_{\tau(z)}$ have as Riemann surfaces. Therefore we

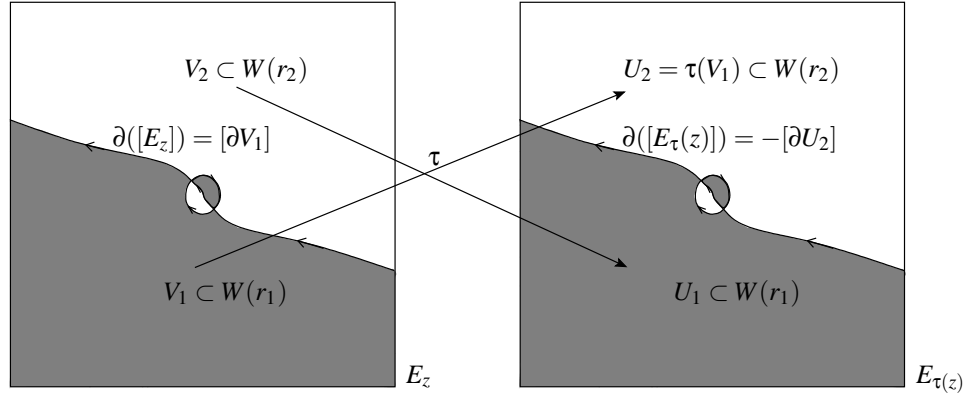


Figure 9.3: Showing that $\partial(\tau_*[E_z]) = -\tau_*(\partial([E_z]))$.

have that $\partial(\tau_*[E_z]) = \partial([E_{\tau(z)}]) = [\partial U_1] = -[\partial U_2]$, where U_1 is the oriented region of $E_{\tau(z)}$ that is in $\overline{W(r_1)}$ and U_2 is the oriented region of $E_{\tau(z)}$ that is in $\overline{W(r_2)}$.

Similarly $\partial([E_z]) = [\partial V_1] = -[\partial V_2]$, where V_1 and V_2 are $E_z \cap \overline{W(r_1)}$ and $E_z \cap \overline{W(r_2)}$. Because τ maps E_z to $E_{\tau(z)}$ swapping $\overline{W(r_1)}$ with $\overline{W(r_2)}$ we have:

$$\tau_*(\partial([E_z])) = [\partial U_2] = -\partial(\tau_*[E_z])$$

□

Proof of Proposition 9.8.3:

Since elements of the form $[E_z] - [\tau(E_z)]$ span $H_2^{\text{od}}(X_l^\infty)$, we need only check that the images of differences like this under ∂ have 0 linking number:

$$\begin{aligned} lk(\partial([E_z] - [\tau(E_z)]), \lambda_2 - \lambda_1) &= lk(\partial([E_z]) - \partial(\tau_*([E_z])), \lambda_2 - \lambda_1) \\ &= lk(\partial([E_z]) + \tau_*(\partial([E_z])), \lambda_2 - \lambda_1) = 0 \end{aligned}$$

The last term is 0 by Lemma 9.8.4. □

Proposition 9.8.5. *The image of $lk(\cdot, \lambda_2 - \lambda_1) : H_1^{\text{od}}(W_0) \rightarrow \mathbb{R}$ contains elements of arbitrarily small, but non-zero absolute value.*

Proof of Proposition 9.8.5:

Recall from Proposition 9.7.2 that we can find 1-cycles γ that have $lk(\gamma, \lambda_2 - \lambda_1)$ arbitrarily small, but non-zero. Notice that $[\gamma - \tau(\gamma)]$ is obviously odd, and using Lemma 9.8.4:

$$\begin{aligned} lk(\gamma - \tau(\gamma), \lambda_2 - \lambda_1) &= lk(\gamma, \lambda_2 - \lambda_1) - lk(\tau(\gamma), \lambda_2 - \lambda_1) \\ &= lk(\gamma, \lambda_2 - \lambda_1) + lk(\gamma, \lambda_2 - \lambda_1) = 2lk(\gamma, \lambda_2 - \lambda_1). \end{aligned}$$

Hence, by choosing γ so that $lk(\gamma, \lambda_2 - \lambda_1)$ is arbitrarily small, but non-zero, we can make $lk(\gamma - \tau(\gamma), \lambda_2 - \lambda_1)$ arbitrarily small, but non-zero with $[\gamma - \tau(\gamma)] \in H_1^{\text{od}}(W_0)$. □

Figure 9.4 illustrates the proof Proposition 9.8.5.

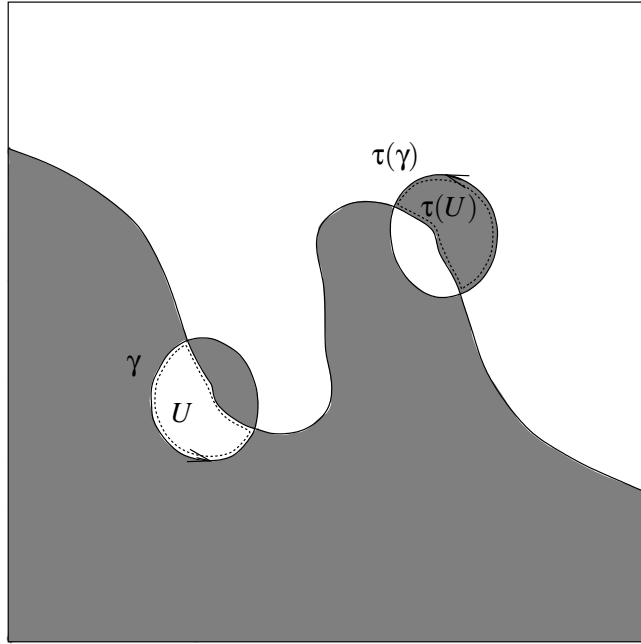


Figure 9.4: Diagram illustrating the proof of Lemma 9.8.5.

Recall the last part of the exact sequence on the odd parts of homology:

$$\rightarrow H_2^{\text{od}}(X_l^\infty) \xrightarrow{\partial} H_1^{\text{od}}(W_0) \xrightarrow{i_{1*} \oplus i_{2*}} \left(H_1(\overline{W}(r_1)) \oplus H_1(\overline{W}(r_2)) \right)^{\text{od}} \rightarrow 0$$

where i_1 and i_2 are the inclusions $W_0 \hookrightarrow \overline{W}(r_1)$ and $W_0 \hookrightarrow \overline{W}(r_2)$ respectively.

As a consequence of Proposition 9.8.3, given any $\tau \in \left(H_1(\overline{W}(r_1)) \oplus H_1(\overline{W}(r_2)) \right)^{\text{od}}$ we can define $lk(\tau, \lambda_2 - \lambda_1) = lk(\gamma, \lambda_2 - \lambda_1)$ for any $\gamma \in H_1^{\text{od}}(W_0)$ whose image under $i_{1*} \oplus i_{2*}$ is τ . As a consequence of Proposition 9.8.5 we know that there are $\tau \in \left(H_1(\overline{W}(r_1)) \oplus H_1(\overline{W}(r_2)) \right)^{\text{od}}$ with arbitrarily small $|lk(\tau, \lambda_2 - \lambda_1)|$. This proves the the desired result:

Theorem 9.8.6. *Let $\overline{W}(r_1)$ and $\overline{W}(r_2)$ be the the closures in X_l^∞ of the basins of attraction of the roots $r_1 = (0,0)$ and $r_2 = (0,1)$ under the Newton Map N . Then $H_1(\overline{W}(r_1))$ and $H_1(\overline{W}(r_2))$ are infinitely generated.*

Recall also:

Corollary 9.8.7. *For parameter values $B \in \Omega_r$, we can replace $\overline{W}(r_1)$ and $\overline{W}(r_2)$ with $W(r_1)$ and $W(r_2)$ finding that $H_1(W(r_1))$ and $H_1(W(r_2))$ are also infinitely generated.*

9.9 Linking with currents in X_r

Much of the work in the previous few sections was to overcome the fact that $H_2(X_l^\infty)$ is infinitely generated in order to develop well-defined linking numbers. In contrast, $H_2(X_r) \cong$

$\mathbb{Z}^{\{\mathbb{P}\}}$, so it is relatively easy to find elements in $\mathcal{LZ}_2(X_r)$.

However, one can also just mimic the work in the previous sections for X_r . If we define λ_3 and λ_4 in a similar way as λ_1 and λ_2 were defined, then:

Proposition 9.9.1. *Suppose that γ_i is a curve in a vertical line bounded by a simply connected domain U_i . Then:*

$$lk(\gamma_i, \lambda_4 - \lambda_3) = \text{size}(U_i)$$

If W_1 intersects the critical value locus C , then W_0 divides vertical lines in X_r to arbitrarily many simply connected domains, and hence to domains of arbitrarily small size. As in X_1^∞ , these linking numbers descend to the homology $H_1(W_1)$ showing:

Proposition 9.9.2. *If W_1 intersects the critical value locus $C(x, y) = y^2 + Bxy + \frac{B^2}{4}x^2 - \frac{B^2}{4}x - y = 0$, then $H_1(W_1)$ is infinitely generated.*

Since there is only one generator of $H_2(X_r)$, without going to odd and even parts, this directly gives:

Theorem 9.9.3. *If W_1 intersects the critical value locus $C(x, y) = y^2 + Bxy + \frac{B^2}{4}x^2 - \frac{B^2}{4}x - y = 0$, then $H_1(\overline{W}(r_3))$ and $H_1(\overline{W}(r_4))$ are infinitely generated.*

where $\overline{W}(r_3)$ and $\overline{W}(r_4)$ are the closures in X_r of the basins of attraction of roots $r_3 = (1, 0)$ and $r_4 = (1, 1 - B)$ under N .

Corollary 9.9.4. *For parameter values $B \in \Omega_r$, we can replace $\overline{W}(r_1)$ and $\overline{W}(r_2)$ with $W(r_1)$ and $W(r_2)$ finding that $H_1(W(r_1))$ and $H_1(W(r_2))$ are also infinitely generated.*

This is the last part of the ‘‘Main Theorem’’ from Chapter 4 that we needed to prove. \square
Theorem 4.4.1.

Appendix A

The extension of N_F to \mathbb{CP}^2

Many of the methods used in [35] and some of the details from Chapter 1 of this dissertation rely upon extending N_F to \mathbb{P}^2 , the complex projective plane. This is easy to do in either normalization, here we extend in Normalization 2.7. Let (X, Y, Z) be homogeneous coordinates on \mathbb{P}^2 . The extension must satisfy the following for $Z = 1$

$$N_F(X, Y, 1) = \left(\frac{2YX^2 + Y^2 - 2aY - b}{4XY - 1}, \frac{2XY^2 + X^2 - 2Xb - a}{4XY - 1}, 1 \right) = \\ (2YX^2 + Y^2 - 2aY - b, 2XY^2 + X^2 - 2Xb - a, 1(4XY - 1))$$

which we can write in homogeneous coordinates as:

$$N_F(X, Y, Z) = \\ (2YX^2 + Y^2Z - 2aYZ^2 - bZ^3, 2XY^2 + X^2Z - 2XZ^2b - aZ^3, 4XYZ - Z^3)$$

where the subscripts indicate the first and second coordinates. To check that an extension makes sense, one must see that this defines a continuous map in the two other coordinate charts $(1, y, z)$ and $(x, 1, z)$ on \mathbb{P}^2 . We divide by the first coordinate and by the second coordinate respectively to find how the mapping 2.8 is defined in these coordinates:

$$\left(1, \frac{2XY^2 + X^2Z - 2XZ^2b - aZ^3}{2YX^2 + Y^2Z - 2aYZ^2 - bZ^3}, \frac{4XYZ - Z^3}{2YX^2 + Y^2Z - 2aYZ^2 - bZ^3} \right) = \\ = \left(1, \frac{2\left(\frac{y}{x}\right)^2 + \left(\frac{z}{x}\right) - 2\left(\frac{z}{x}\right)b - a\left(\frac{z}{x}\right)^3}{2\left(\frac{y}{x}\right) - \left(\frac{y}{x}\right)^2\left(\frac{z}{x}\right) - 2\left(\frac{y}{x}\right)\left(\frac{z}{x}\right)^2 - b\left(\frac{z}{x}\right)^3}, \frac{4\left(\frac{y}{x}\right)\left(\frac{z}{x}\right) - \left(\frac{z}{x}\right)^3}{2\left(\frac{y}{x}\right) - \left(\frac{y}{x}\right)^2\left(\frac{z}{x}\right) - 2\left(\frac{y}{x}\right)\left(\frac{z}{x}\right)^2 - b\left(\frac{z}{x}\right)^3} \right).$$

Therefore, in the (y, z) coordinates, we have:

$$N_F \left(\begin{array}{c} y \\ z \end{array} \right) = \frac{1}{2y + y^2z - 2ayz^2 - bz^3} \left(\begin{array}{c} 2y^2 + z - 2z^2b - az^3 \\ 4yz - z^3 \end{array} \right)$$

Similar work can be done to express N_F in the coordinates (x, z) , where $x = \frac{X}{Y}$ and $z = \frac{Z}{Y}$ obtaining

$$N_F \left(\begin{array}{c} x \\ z \end{array} \right) = \frac{1}{2x + x^2z - 2xz^2b - az^3} \left(\begin{array}{c} 2x^2 + z - 2az^2 - bz^3 \\ 4xz - z^3 \end{array} \right).$$

Appendix B

Proof of Theorem 5.1.1

Let $S \subset \Omega$ be the set of parameter values B for which no inverse image of the point of indeterminacy p or the point of indeterminacy q is in the critical value locus C . Recall that we are especially interested in $B \in S$ because for these parameter values the sequence of blow-ups described in section 5.1 is especially easy to describe.

Theorem 5.1.1 states:

Theorem. *The set S is generic in the sense of Baire's Theorem, i.e. uncountable and dense in Ω .*

This will follow as a corollary to:

Theorem. (Baire) *Let X be either a complete metric space, or a locally compact Hausdorff space. Then, the intersection of any countable family of dense open sets in X is dense.*

See Bredon [9], Theorem 17.1 and Corollary 17.3, for example, for a proof.

Proof of Theorem 5.1.1:

Let $S_n \subset \mathbb{C}$ be the subset of parameter values B for which none of the n -th inverse images of p or q under N are in the critical value locus C .

Lemma B.0.5. *S_n is a dense open set in \mathbb{C}*

Proof: Let R_n be the set of B for which an n -th inverse image of p is in C and let T_n be the set of B for which an n -th inverse image of q is in C . We will show that R_n and T_n are finite, showing that $S_n = \Omega - (R_n \cup T_n)$ is a dense open set.

Lemma B.0.6. *For each n , T_n is a finite set.*

Proof: In terms of equations, $B \in T_n$ if:

$$y^2 + Bxy + \frac{B^2}{4}x^2 - \frac{B^2}{4}x - y = 0, \quad N_1^n(x, y) = \frac{1}{2-B}, \quad N_2^n(x, y) = \frac{1-B}{2-B} \quad (\text{B.1})$$

has a solution. Here, as in other parts of this paper, N_1^n and N_2^n denote the first and second coordinates of N^n . By clearing the denominators in the second and third equations, condition B.1 can be expressed as the common zeros of 3 polynomials $P_1(x, y, B)$, $P_2(x, y, B)$, and $P_3(x, y, B)$ in the three variables x, y , and B . We will check that there are only finitely many solutions to these three polynomials. It is sufficient to check that there is no common divisor of $P_1(x, y, B)$, $P_2(x, y, B)$, and $P_3(x, y, B)$.

First, notice that $P_1(x, y, B) = y^2 + Bxy + \frac{B^2}{4}x^2 - \frac{B^2}{4}x - y = 0$ is irreducible. There are many ways to see this, we used the computer algebra system Maple [13].

Hence P_1 has a factor in common with P_2 or P_3 if and only if P_1 divides P_2 or P_3 . We will show that this is impossible by examining the lowest degree terms of P_2 and P_3 . If P_1 divides P_2 or P_3 , then the lowest degree term, $-y$, of P_1 must divide the lowest degree term of P_2 or the lowest degree term of P_3 .

Let's check by induction that the lowest degree term of P_2 is ± 1 for every n . To simplify notation, let $a_n(x, y, B)$ be the polynomial obtained by clearing the denominators from the second equation in Equation B.1, specifically for the n -th iterate of N . (I.e. a_n is P_2 for this specific n .)

By clearing denominators of $N_1(x, y) = \frac{1}{2-B}$, we find $a_1(x, y, B) = x^2(2-B) - 1(2x-1) = 2x^2 - Bx^2 - 2x + 1$, so $a_1(x, y, B)$ has constant term ± 1 . Now suppose that $a_n(x, y, B)$ has constant term ± 1 . By definition, $a_{n+1}(x, y, B)$ is obtained by clearing the denominators of $a_n(N_1(x, y), N_2(x, y), B) = 0$. Because the denominators of both $N_1(x, y)$ and $N_2(x, y)$ have constant term ± 1 and because $a_n(x, y, B)$ has constant term 1 we find that $a_{n+1}(x, y, B)$ has constant term ± 1 .

So, P_2 has constant term ± 1 for every n , hence P_1 cannot divide P_2 , and we conclude that there are no common factors between P_1 and P_2 .

A nearly identical proof by induction shows that lowest degree term of P_3 is also ± 1 for each n . Hence P_1 does not divide P_3 , and we conclude that P_1 and P_3 have no common divisors.

To see that P_2 and P_3 have no common divisors, notice that $P_2(x, y, B) = 0$ is an equation for many disjoint vertical lines, while $P_3(x, y, B) = 0$ stipulates that the n -th image of this locus has constant $y = 0$. Since vertical lines are mapped to vertical lines by N , P_2 and P_3 can have no common factors.

Hence, P_1, P_2 , and P_3 are algebraically independent, so they have a finite number of common zeros, giving that T_n is a finite set. \square Lemma B.0.6.

Lemma B.0.7. R_n is a finite set.

Proof: Now we show that R_n , the set of B so that an n -th inverse image of p under N is in C , is finite. In terms of equations, R_n is the set of B so that:

$$y^2 + Bxy + \frac{B^2}{4}x^2 - \frac{B^2}{4}x - y = 0, \quad N_1^n(x, y) = \frac{1}{B}, \quad N_2^n(x, y) = 0 \quad (\text{B.2})$$

has a solution. Let Q_1, Q_2 , and Q_3 be the polynomials equations resulting from clearing the denominators in Equation B.2.

The proof is the same as for T_n except that a different proof is needed to see that Q_1 does not divide Q_3 . An adaptation of the proof that P_1 does not divide P_3 fails because the lowest degree term of Q_3 has positive degree in y . We will check that Q_1 does not divide Q_3 and leave the remainder of the proof to the reader.

The x -axis, $y = 0$, is one of the invariant lines of N and it intersects the basins $W(r_1)$, $W(r_3)$ and the separator $\text{Re}(x) = 1/2$. Therefore it is disjoint from the two basins $W(r_2)$ and $W(r_4)$. By definition, $Q_3(x, y, B)$ is the equation for the n -th inverse image of the x -axis. So, for a given B , the locus $Q_3(x, y, B) = 0$ is also disjoint from the two basins $W(r_2)$ and $W(r_4)$.

For every B , the critical value parabola C goes through the four roots r_1, r_2, r_3 , and r_4 , so it intersects all four basins of attraction. By definition, C is the zero locus $Q_1(x, y, B) = 0$. Therefore, if Q_1 divides Q_3 , there is a component of the zero locus $Q_3(x, y, B) = 0$

intersecting all four basins $W(r_1), W(r_2), W(r_3)$ and $W(r_4)$ for every B . This is impossible, so Q_1 cannot divide Q_3 .

□ Lemma B.0.7.

Because $R_n \cup T_n$ is finite $S_n = \Omega - (R_n \cup T_n)$ is an open-dense set.

□ Lemma B.0.5.

Since S_n is a dense open set in Ω for each n and $S = \bigcap_{n=0}^{\infty} S_n$, so it follows from Baire's Theorem that S is uncountable and dense in the parameter space Ω .

□ Theorem 5.1.1.

Appendix C

Blow-ups of complex surfaces at a point.

Blow-ups are explained in [24, pp. 182-189 and 473-478] and in the introduction of [30], where some nice examples are computed. In this dissertation, we will only need blow-ups of complex surfaces M at individual points.

C.1 Blowing up \mathbb{C}^2 at a point

The first situation in which one considers doing blow-ups is to make a rational mapping $R : \mathbb{C}^2 \rightarrow \mathbb{C}^2$ well defined at a point of indeterminacy. Suppose that R has $(0,0)$ as a point of indeterminacy. One can try to extend R to the blow up of \mathbb{C}^2 at $(0,0)$:

$$\tilde{\mathbb{C}}_{(0,0)}^2 = \{(z, l) \in \mathbb{C}^2 \times \mathbb{P}^1 : z \in l\} \quad (\text{C.1})$$

where we consider \mathbb{P}^1 to be the space of directions in \mathbb{C}^2 .

The same definition, but a slightly different perspective, is obtained by considering $\tilde{\mathbb{C}}_{(0,0)}^2 \subset \mathbb{C}^2 \times \mathbb{P}^1$ as the hypersurface defined by the equations

$$z_1 l_2 = z_2 l_1 \quad z_2 l_1 = z_1 l_2$$

where $z = (z_1, z_2)$ are Euclidean coordinates in \mathbb{C}^2 and $l = [l_1, l_2]$ are the corresponding homogeneous coordinates on \mathbb{P}^1 .

There is a natural projection $\rho : \tilde{\mathbb{C}}_{(0,0)}^2 \rightarrow \mathbb{C}^2$ given by $\rho(z, l) = z$. The set $E_{(0,0)} = \rho^{-1}((0,0))$ is referred to as the *exceptional divisor*.

A standard check shows that the blow-up is independent of the choose of coordinates, so the blow-up of a complex surface M at a point z is well-defined.

A rational map $R : \mathbb{C}^2 \rightarrow \mathbb{C}^2$ can be lifted to a new rational mapping $\tilde{R} : \tilde{\mathbb{C}}_{(0,0)}^2 - E_{(0,0)} \rightarrow \mathbb{C}^2$ be defining $R(x, l) = R(x)$ for $x \neq 0$. The exceptional divisor $E_{(0,0)}$ is a closed subset of $\tilde{\mathbb{C}}_{(0,0)}^2$ of real-codimension 2, so one can try to extend \tilde{R} by continuity. If the indeterminacy in R at $(0,0)$ was reasonably tame, \tilde{R} extends to all of $E_{(0,0)}$ by continuity. This happens, when the definition of R at $(0,0)$ depends only on the direction of approached to $(0,0)$. Otherwise, there will be points of indeterminacy of \tilde{R} on $E_{(0,0)}$ at which \tilde{R} cannot be extended, and one can try further blow-ups at these points to resolve these new points of indeterminacy. The extension of \tilde{R} to $E_{(0,0)}$ is analytic except at any new points of indeterminacy because $E_{(0,0)}$ is a space of complex co-dimension 1.

C.2 Examples:

The quickest way to understand blow-ups is to do a few. In this section we work through some of these easiest cases.

Example 1. $R(x, y) = \left(1, \frac{x}{y}\right)$.

The second coordinate of R is indeterminate at $(0, 0)$, so we blow up there. It is often easiest to do computations in local coordinates. Suppose (x, y) are the standard coordinates on \mathbb{C}^2 . There are two coordinate charts on $\tilde{\mathbb{C}}^2_{(0,0)}$ given by $(x, m) \rightarrow (x, xm, m)$ and given by $(m, y) \rightarrow (my, y, \frac{1}{m})$.

In the first chart, we have $\tilde{R}(x, m) = R(x, xm) = \left(1, \frac{x}{xm}\right)$ for $x \neq 0$. Clearly, we can extend to $x = 0$ by continuity, defining $\tilde{R}(0, m) = \left(1, \frac{1}{m}\right)$. In the second chart, we have $\tilde{R}(m, y) = R(my, y) = \left(1, \frac{ym}{y}\right)$ for $y \neq 0$. Clearly, we can extend to $y = 0$ by continuity, defining $\tilde{R}(m, 0) = (1, m)$.

Therefore, the extension $\tilde{R} : \tilde{\mathbb{C}}^2_{(0,0)} \rightarrow \mathbb{C}^2$ maps $E_{(0,0)}$ isomorphically to the line $x = 1$.

Example 2. $R(x, y) = \left(1 + \frac{y}{x}, \frac{x}{y}\right)$.

This time, both coordinates of R are indeterminate at $(0, 0)$. Computing \tilde{R} in both local coordinates, we find:

- $\tilde{R}(x, m) = R(x, xm) = \left(1 + \frac{xm}{x}, \frac{x}{xm}\right)$ for $x \neq 0$, which extends by continuity to $\tilde{R}(0, m) = \left(1 + m, \frac{1}{m}\right)$.
- $\tilde{R}(m, y) = R(my, y) = \left(1 + \frac{y}{my}, \frac{my}{y}\right)$ for $x \neq 0$, which extends by continuity to $\tilde{R}(m, 0) = \left(1 + \frac{1}{m}, m\right)$.

So, this time $\tilde{R} : \tilde{\mathbb{C}}^2_{(0,0)} \rightarrow \mathbb{C}^2$ maps $E_{(0,0)}$ to the curve $x = 1 + \frac{1}{y}$ by isomorphism.

Example 3. $R(x, y) = (2x + y^2 + 1, 2y + 1)$.

This mapping R has no points of indeterminacy in \mathbb{C} , but we can still do a blow-up at $(0, 0)$ to see what happens.

- $\tilde{R}(x, m) = R(x, xm) = (2x + (xm)^2 + 1, 2xm + 1)$ for $x \neq 0$, which extends by continuity to $\tilde{R}(0, m) = (1, 1)$.
- $\tilde{R}(m, y) = R(my, y) = (2my + y^2 + 1, 2y + 1)$ for $y \neq 0$, which extends by continuity to $\tilde{R}(m, 0) = (1, 1)$.

Because R does not have a point of indeterminacy $(0, 0)$ \tilde{R} collapses $E_{(0,0)}$ to the point $R((0, 0)) = (1, 1)$.

Example 4.

Suppose that we have already blown-up \mathbb{C}^2 at $(1, 1)$ obtaining $\tilde{\mathbb{C}}^2_{(1,1)}$ and the extension $R_1 : \tilde{\mathbb{C}}^2_{(1,1)} \rightarrow \mathbb{C}^2$ of $R(x, y) = (2x + y^2 + 1, 2y + 1)$.

We can also instead think of R_1 as a map from $\tilde{\mathbb{C}}^2_{(1,1)}$ to $\tilde{\mathbb{C}}^2_{(1,1)}$, but each of the points mapped by R to $(1, 1)$ becomes a point of indeterminacy. In this case the only inverse image is $(0, 0)$. To resolve the indeterminacy at $(0, 0)$ we can blow up again obtaining a map $R_2 : \tilde{\mathbb{C}}^2_{(1,1),(0,0)} \rightarrow \tilde{\mathbb{C}}^2_{(1,1)}$ in the following way:

In a neighborhood of $(0, 0)$ we can use the original coordinates (x, y) from \mathbb{C}^2 as if they are now coordinates on $\tilde{\mathbb{C}}^2_{(1,1)}$.

- $R_2(x, m) = R_1(x, xm) = \left(2x + (xm)^2 + 1, 2xm + 1, \frac{2x + (xm)^2}{2xm}\right)$ for $x \neq 0$, which extends by continuity to $R_2(0, m) = \left(1, 1, \frac{1}{m}\right)$.
- $R_2(m, y) = R_1(my, y) = \left(2my + y^2 + 1, 2y + 1, \frac{2my + y^2}{2y}\right)$ for $y \neq 0$, which extends by continuity to $R_2(m, 0) = (1, 1, m)$.

where the third coordinate is expressed in both extensions in the same chart on $E_{(1,1)} = \mathbb{P}^1$. Hence, because we had already blown up at $(1, 1)$ we now have that \tilde{R} maps $E_{(0,0)}$ to $E_{(1,1)}$ by an isomorphism.

Example 5.

For this final example, suppose that $R(x, y) = (x^2 + 1, y^2 + x^2 + 1)$ and suppose again that we have already blown-up at $(1, 1)$ obtaining $R_1 : \tilde{\mathbb{C}}^2_{(1,1)} \rightarrow \mathbb{C}^2$ extending $R(x, y) = (x^2 + 1, x^2 + y^2 + 1)$. If we then decide to blow-up at $(0, 0)$ we can obtain a map $R_2 : \tilde{\mathbb{C}}^2_{(1,1),(0,0)} \rightarrow \tilde{\mathbb{C}}^2_{(1,1)}$ in the following way:

In a neighborhood of $(0, 0)$ we can use the original coordinates (x, y) from \mathbb{C}^2 as if they are now coordinates on $\tilde{\mathbb{C}}^2_{(1,1)}$.

- $R_2(x, m) = R_1(x, xm) = \left(x^2 + 1, x^2 + (xm)^2 + 1, \frac{x^2}{x^2 + (xm)^2}\right)$ for $x \neq 0$, which extends by continuity to $R_2(0, m) = \left(1, 1, \frac{1}{1+m^2}\right)$.
- $R_2(m, y) = R_1(my, y) = \left((my)^2 + 1, (my)^2 + y^2 + 1, \frac{(my)^2}{(my)^2 + y^2}\right)$ for $y \neq 0$, which extends by continuity to $R_2(m, 0) = \left(1, 1, \frac{m^2}{1+m^2}\right)$.

where the third coordinate is expressed in both extensions in the same chart on $E_{(1,1)} = \mathbb{P}^1$. Hence, because we had already blown up at $(1, 1)$ we now have that R_2 maps $E_{(0,0)}$ to $E_{(1,1)}$ the degree 2 rational map: $m \mapsto \frac{1}{1+m^2}$.

C.3 Effect of blow-ups on homology

When we did a blow-up at $0 \in \mathbb{C}^2$, we obtained $\tilde{\mathbb{C}}_{(0,0)}^2 = \{(x, l) \in \mathbb{C}^2 \times \mathbb{P}^1 \mid x \in l\}$ which may be familiar to the reader, it is the “canonical line bundle” over \mathbb{P}^1 . In any case, it is easy to check that $\tilde{\mathbb{C}}_{(0,0)}^2$ has the homotopy type of the exceptional divisor \mathbb{P}^1 . Hence, $H_2(\tilde{\mathbb{C}}_{(0,0)}^2) = \mathbb{Z}^{\{[E_{(0,0)}]\}}$, while the other homology groups of $\tilde{\mathbb{C}}_{(0,0)}^2$ are trivial, the same as those of \mathbb{C}^2 . (Here, and elsewhere $\mathbb{Z}^{\{[N]\}}$ will mean *the module \mathbb{Z} that is generated by the fundamental class $[N]$* .)

This follows from the general fact:

Proposition C.3.1. *If M is a complex surface and x is any point in M , then the blow-up \tilde{M}_x has the following homology:*

- $H_2(\tilde{M}_x) \cong H_2(M) \oplus \mathbb{Z}^{\{[E_x]\}}$
- $H_i(\tilde{M}_x) \cong H_i(M)$ for $i \neq 2$

Proof: This is simply a matter of doing a Mayer-Vietoris computation and using a knowledge of the homology of $\tilde{\mathbb{C}}_{(0,0)}^2$.

Let $\phi : \mathbb{C}^2 \rightarrow M$ be some chart with $\phi(0) = x$. If B_ε is the open unit ball of radius ε in \mathbb{C}^2 centered at 0, let $U = \phi(B_{2\varepsilon})$ and let $V = M - \phi(B_\varepsilon)$. Then, $U \cup V = M$, and $U \cap V$ has the homotopy type of \mathbb{S}^3 .

If we blow up U at $\phi(0)$, obtaining \tilde{U} , we have that $\tilde{U} \cup V = \tilde{M}_x$ and $\tilde{U} \cap V$ still has the homotopy type of \mathbb{S}^3 . Using that \tilde{U} has trivial homology, except in dimensions 0 and 2, the Mayer-Vietoris exact sequence gives:

$$\begin{aligned} 0 \rightarrow H_4(V) \rightarrow H_4(\tilde{M}_x) \rightarrow \mathbb{Z} \rightarrow H_3(V) \rightarrow H_3(\tilde{M}_x) \rightarrow 0 \rightarrow \mathbb{Z}^{\{[E_x]\}} \oplus H_2(V) \rightarrow H_2(\tilde{M}_x) \rightarrow \\ 0 \rightarrow H_1(V) \rightarrow H_1(\tilde{M}_x) \rightarrow \mathbb{Z} \rightarrow \mathbb{Z} \oplus H_0(V) \rightarrow H_0(\tilde{M}_x) \rightarrow 0 \end{aligned}$$

We easily obtain that $H_2(\tilde{M}_x) \cong H_2(V) \oplus \mathbb{Z}^{\{[E_x]\}} \cong H_2(M) \oplus \mathbb{Z}^{\{[E_x]\}}$, using that $H_2(V) \cong H_2(M)$ since V has the homotopy type of M with a single point removed. Checking that $\partial : H_4(\tilde{M}_x) \rightarrow H_3(\tilde{U} \cap V) \cong \mathbb{Z}$ is surjective, we see that $H_i(\tilde{M}_x) \cong H_i(M)$ for $i \neq 2$. \square

Although we will not prove it here, it is a general fact that the fundamental class $[E_z]$ has self-intersection number -1 . If further blow-ups are made, each time a point on E_z is blown up, the self intersection number $[E_z] \cdot [E_z]$ decreases by 1. (See [24], for proof.)

C.4 Repeated blow-ups

The following propositions help to clarify the sequence of blow-ups from Section 5.1. One might think of this sequence of blow-ups as a very difficult process but the blow-ups at inverse images of the points of indeterminacy p and q are relatively easy to compute. The blow up at one of these inverse images will depend on whether DN is non-singular, singular but non-zero, or zero. (The case where $DN = 0$ never occurs in the sequence of blow-ups, but it does occur when we blow-up one at one of the roots r_i .)

Proposition C.4.1. *Suppose M is a complex surface that has already been blown up at z and suppose $R : \tilde{M}_z \rightarrow M$ is a rational map. If $R(w) = z$ and $DR(w)$ is non-singular, then R extends to a rational map $\tilde{R} : \tilde{M}_{z,w} \rightarrow M_z$ mapping E_w to E_z via an isomorphism.*

As in the last two examples, we consider $R : \tilde{M}_z \rightarrow \tilde{M}_z$ and every inverse image of z becomes a point of indeterminacy of R . (In particular w is a point of indeterminacy of R .)

Proof: Suppose that $z = (z_1, z_2)$ and let (x_1, x_2) be a system of coordinates centered at w . Since $R(w) = z$ and $DR(w)$ is non-singular, R has a Taylor series expansion centered at w :

$$R \begin{pmatrix} x_1 \\ x_2 \end{pmatrix} = \begin{pmatrix} z_1 \\ z_2 \end{pmatrix} + \begin{bmatrix} \partial_{x_1} R_1 & \partial_{x_2} R_1 \\ \partial_{x_1} R_2 & \partial_{x_2} R_2 \end{bmatrix} \begin{pmatrix} x_1 \\ x_2 \end{pmatrix} + \begin{pmatrix} S_1(x_1, x_2) \\ S_2(x_1, x_2) \end{pmatrix}$$

where $S_1(x_1, x_2)$ and $S_2(x_1, x_2)$ are of degree 2 and higher in x_1 and x_2 .

We compute the extension of R to $\tilde{M}_{z,w}$ in the chart $(x_1, m) \rightarrow (x_1, mx_1, m)$:

$$\tilde{R} \begin{pmatrix} x_1 \\ m \end{pmatrix} = \begin{pmatrix} z_1 + \partial_{x_1} R_1 x_1 + \partial_{x_2} R_1 mx_1 + S_1(x_1, mx_1) \\ z_2 + \partial_{x_1} R_2 x_1 + \partial_{x_2} R_2 mx_1 + S_2(x_1, mx_1) \\ \frac{\partial_{x_1} R_1 x_1 + \partial_{x_2} R_1 mx_1 + S_1(x_1, mx_1)}{\partial_{x_1} R_2 x_1 + \partial_{x_2} R_2 mx_1 + S_2(x_1, mx_1)} \end{pmatrix}$$

for $x_1 \neq 0$. If DR is non-singular, we can factor out x_1 from the numerator and denominator of the third component. Then, the mapping from E_w to E_z is given by the third coordinate, with $x_1 = 0$:

$$m \mapsto \frac{\partial_{x_1} R_1 + \partial_{x_2} R_1 m}{\partial_{x_1} R_2 + \partial_{x_2} R_2 m}$$

which is a non-degenerate linear-fractional transformation, since DR is non-singular. Hence it is an isomorphism from E_w to E_z . (To be entirely precise, one must also check the extension in the other chart $(m, x_2) \rightarrow (mx_2, x_2, m)$ to be sure that the map extends to E_w at the one point not covered in this chart. We leave this for the reader.)

□

Proposition C.4.2. *Suppose M is a complex surface, $R : \tilde{M}_z \rightarrow M$ is a rational map, $R(w) = z$ and that $DR(w)$ is singular but non-zero. Let m_k be the slope in E_w corresponding to the kernel of $DR(w)$.*

Then:

- *R extends to a rational map $\tilde{R} : \tilde{M}_{z,w} \rightarrow M_z$ mapping all of $E_w - m_k$ to a single point on E_z . The point m_k becomes a point of indeterminacy of \tilde{R} .*
- *If the second derivative $D_2 R$ is non-singular, a further blow-up at m_k allows for an extension of \tilde{R} to E_{m_k} mapping E_{m_k} isomorphically to E_z .*

Proof: Suppose that $z = (z_1, z_2)$ and let (x_1, x_2) be a system of coordinates centered at w . We will compute the blow-up in the charts $(x_1, m) \mapsto (x_1, mx_1, m)$ as we did in the proof of Proposition C.4.1. (We assume that $\partial_{x_1} R_2$ or $\partial_{x_2} R_2$ is non-zero, otherwise a similar computation would have to be done in the other chart $(m, x_2) \rightarrow (mx_2, x_2, m)$.)

We can then factor x_1 from the numerator and denominator and then, the mapping from E_w to E_z is given by the third coordinate, with $x_1 = 0$, that is:

$$m \mapsto \frac{\partial_{x_1} R_1 + \partial_{x_2} R_1 m}{\partial_{x_1} R_2 + \partial_{x_2} R_2 m}$$

Since DR is singular, the numerator is a multiple, λ , of the denominator, hence \tilde{R} maps every $m \in E_w$ to $\hat{\lambda} \in E_z$ except for m_k , the point in E_w corresponding to the kernel of $DN(w)$, which is a point of indeterminacy.

Blowing up at m_k we compute the extension of \tilde{R} in a neighborhood of E_{m_k} . For this proof, we assume that m_k is in the image of the coordinate chart $(x_1, m) \rightarrow (x_1, mx_1, m)$ that we used to compute the extension to E_w . (Otherwise, another chart will do.) We use the chart $(x_1, n) \rightarrow (x_1, nx_1 + m_k, n) \rightarrow (x_1, x_1(nx_1 + m_k), nx_1 + mc, n) = (x_1, nx_1^2 + x_1 m_k, nx_1 + m_k, n)$ in a neighborhood of E_{m_k} . In this extension, we find

$$\frac{\partial_{x_1} R_1 x_1 + \partial_{x_2} R_1 (nx_1^2 + x_1 m_k) + S_1(x_1, nx_1^2 + x_1 m_k)}{\partial_{x_1} R_2 x_1 + \partial_{x_2} R_2 (nx_1^2 + x_1 m_k) + S_2(x_1, nx_1^2 + x_1 m_k)}$$

The extension to E_{m_k} is given by in the limit as $x_1 \rightarrow 0$. We find:

$$\lim_{x_1 \rightarrow 0} \frac{\partial_{x_2} R_1 nx_1^2 + x_1^2 S_1(1, m_k)}{\partial_{x_2} R_2 nx_1^2 + x_1^2 S_2(1, m_k)} = \frac{\partial_{x_2} R_1 n + S_1(1, m_k)}{\partial_{x_2} R_2 n + S_2(1, m_k)}$$

which is non-constant so long as either $S_1(1, m_k) \neq 0$ or $S_2(1, m_k) \neq 0$. Therefore it provides an isomorphism from $E_{m_k} \rightarrow E_z$. \square

Proposition C.4.3. *Suppose M is a complex surface and suppose $R: \tilde{M}_z \rightarrow M$ is a rational map. If $R(w) = z$, $DR(w) = 0$, and D^2R is non-singular, then R extends to a rational map $\tilde{R}: \tilde{M}_{z,w} \rightarrow M_z$ mapping E_w to E_z via rational map of degree 2.*

Proof:

Suppose that $z = (z_1, z_2)$ and let (x_1, x_2) be a system of coordinates centered at w . R has a Taylor series expansion of the form

$$R \begin{pmatrix} x_1 \\ x_2 \end{pmatrix} = \begin{pmatrix} z_1 \\ z_2 \end{pmatrix} + \begin{pmatrix} S_1(x_1, x_2) \\ S_2(x_1, x_2) \end{pmatrix} + \begin{pmatrix} T_1(x_1, x_2) \\ T_2(x_1, x_2) \end{pmatrix}$$

where $S_1(x_1, x_2)$ and $S_2(x_1, x_2)$ are of degree 2 in x_1 and x_2 and $T_1(x_1, x_2)$ and $T_2(x_1, x_2)$ are of degree 3 and higher in x_1 and x_2 .

We compute the extension of R to $\tilde{M}_{z,w}$ in the chart $(x_1, m) \rightarrow (x_1, mx_1, m)$:

$$\tilde{R} \begin{pmatrix} x_1 \\ m \end{pmatrix} = \begin{pmatrix} z_1 + S_1(x_1, mx_1) + T(x_1, mx_1) \\ z_2 + S_2(x_1, mx_1) + T_2(x_1, mx_1) \\ \frac{S_1(x_1, mx_1) + T_1(x_1, mx_1)}{S_2(x_1, mx_1) + T_2(x_1, mx_1)} \end{pmatrix}$$

for $x_1 \neq 0$. To understand the extension to E_w , we must extend to $x_1 = 0$. As usual, the only difficulty is in the third coordinate:

$$\frac{S_1(x_1, mx_1) + T_1(x_1, mx_1)}{S_2(x_1, mx_1) + T_2(x_1, mx_1)}$$

To extend this to $x_1 = 0$ we factor out x_1^2 from the numerator and denominator, obtaining:

$$\frac{S_1(1, m) + T_1(x_1, mx_1)/x_1^2}{S_2(1, m) + T_2(x_1, mx_1)/x_1^2}$$

this extends to $m \mapsto \frac{S_1(1, m)}{S_2(1, m)}$, which is a non-degenerate rational map of degree 2, since S is non-degenerate. \square

BIBLIOGRAPHY

- [1] Eric Bedford, Mikhail Lyubich, and John Smillie. Polynomial diffeomorphisms of \mathbb{C}^2 . IV. The measure of maximal entropy and laminar currents. *Invent. Math.*, 112(1):77–125, 1993.
- [2] Eric Bedford and John Smillie. Polynomial diffeomorphisms of \mathbb{C}^2 : currents, equilibrium measure and hyperbolicity. *Invent. Math.*, 103(1):69–99, 1991.
- [3] Eric Bedford and John Smillie. Polynomial diffeomorphisms of \mathbb{C}^2 . II. Stable manifolds and recurrence. *J. Amer. Math. Soc.*, 4(4):657–679, 1991.
- [4] Eric Bedford and John Smillie. Polynomial diffeomorphisms of \mathbb{C}^2 . III. Ergodicity, exponents and entropy of the equilibrium measure. *Math. Ann.*, 294(3):395–420, 1992.
- [5] Eric Bedford and John Smillie. Polynomial diffeomorphisms of \mathbb{C}^2 . V. Critical points and Lyapunov exponents. *J. Geom. Anal.*, 8(3):349–383, 1998.
- [6] Eric Bedford and John Smillie. Polynomial diffeomorphisms of \mathbb{C}^2 . VI. Connectivity of *J. Ann. of Math. (2)*, 148(2):695–735, 1998.
- [7] Eric Bedford and John Smillie. External rays in the dynamics of polynomial automorphisms of \mathbb{C}^2 . In *Complex geometric analysis in Pohang (1997)*, volume 222 of *Contemp. Math.*, pages 41–79. Amer. Math. Soc., Providence, RI, 1999.
- [8] Eric Bedford and John Smillie. Polynomial diffeomorphisms of \mathbb{C}^2 . VII. Hyperbolicity and external rays. *Ann. Sci. École Norm. Sup. (4)*, 32(4):455–497, 1999.
- [9] Glen E. Bredon. *Topology and geometry*, volume 139 of *Graduate Texts in Mathematics*. Springer-Verlag, New York, 1993.
- [10] Jean-Yves Briend. *Exposants de Liapounof et points périodiques d'endomorphismes holomorphes de $\mathbb{C}\mathbb{P}^k$* . PhD thesis, Toulouse, 1997.
- [11] Jean-Yves Briend and Julien Duval. Deux caractérisations de la mesure d'équilibre d'un endomorphisme de $\mathbb{P}^k(\mathbb{C})$. *Publ. Math. Inst. Hautes Études Sci.*, (93):145–159, 2001.
- [12] Hans Brolin. Invariant sets under iteration of rational functions. *Ark. Mat.*, 6:103–144 (1965), 1965.
- [13] Maple computer algebra system. www.maplesoft.com.
- [14] R. Devaney and Z. Nitecki. Shift automorphisms in the Hénon mapping. *Comm. Math. Phys.*, 67(2):137–146, 1979.
- [15] Jeffrey Diller. Dynamics of birational maps of \mathbb{P}^2 . *Indiana Univ. Math. J.*, 45(3):721–772, 1996.

- [16] Tien-Cuong Dinh and Nessim Sibony. Dynamique des applications d'allure polynomiale. *J. Math. Pures Appl. (9)*, 82(4):367–423, 2003.
- [17] Tien-Cuong Dinh and Nessim Sibony. Dynamics of regular birational maps in \mathbb{P}^k . *J. Funct. Anal.*, 222(1):202–216, 2005.
- [18] Romain Dujardin. Hénon-like mappings in \mathbb{C}^2 . *Amer. J. Math.*, 126(2):439–472, 2004.
- [19] C. Favre and M. Jonsson. Brodin's theorem for curves in two complex dimensions. *Ann. Inst. Fourier (Grenoble)*, 53(5):1461–1501, 2003.
- [20] John Erik Fornæss. *Dynamics in several complex variables*, volume 87 of *CBMS Regional Conference Series in Mathematics*. Published for the Conference Board of the Mathematical Sciences, Washington, DC, 1996.
- [21] John Erik Fornæss and Nessim Sibony. Complex dynamics in higher dimension. I. *Astérisque*, (222):5, 201–231, 1994. Complex analytic methods in dynamical systems (Rio de Janeiro, 1992).
- [22] John Erik Fornæss and Nessim Sibony. Complex dynamics in higher dimensions. In *Complex potential theory (Montreal, PQ, 1993)*, volume 439 of *NATO Adv. Sci. Inst. Ser. C Math. Phys. Sci.*, pages 131–186. Kluwer Acad. Publ., Dordrecht, 1994. Notes partially written by Estela A. Gavosto.
- [23] John Erik Fornæss and Nessim Sibony. Complex dynamics in higher dimension. II. In *Modern methods in complex analysis (Princeton, NJ, 1992)*, volume 137 of *Ann. of Math. Stud.*, pages 135–182. Princeton Univ. Press, Princeton, NJ, 1995.
- [24] Phillip Griffiths and Joseph Harris. *Principles of algebraic geometry*. Wiley-Interscience [John Wiley & Sons], New York, 1978. Pure and Applied Mathematics.
- [25] Vincent Guedj. Dynamics of quadratic polynomial mappings of \mathbb{C}^2 . *Michigan Math. J.*, 52(3):627–648, 2004.
- [26] Vincent Guedj. Ergodic properties of rational mappings with large topological degree. *Annals of Mathematics*, 161:1589–1607, 2005.
- [27] Mako E. Haruta. Newton's method on the complex exponential function. *Trans. Amer. Math. Soc.*, 351(6):2499–2513, 1999.
- [28] Allen Hatcher. *Algebraic topology*. Cambridge University Press, Cambridge, 2002.
- [29] Lars Hörmander. *An introduction to complex analysis in several variables*, volume 7 of *North-Holland Mathematical Library*. North-Holland Publishing Co., Amsterdam, third edition, 1990.
- [30] John Hubbard, Peter Papadopol, and Vladimir Veselov. A compactification of Hénon mappings in \mathbb{C}^2 as dynamical systems. *Acta Math.*, 184(2):203–270, 2000.

- [31] John Hubbard, Dierk Schleicher, and Scott Sutherland. How to find all roots of complex polynomials by Newton's method. *Invent. Math.*, 146(1):1–33, 2001.
- [32] John H. Hubbard and Ralph W. Oberste-Vorth. Hénon mappings in the complex domain. I. The global topology of dynamical space. *Inst. Hautes Études Sci. Publ. Math.*, (79):5–46, 1994.
- [33] John H. Hubbard and Ralph W. Oberste-Vorth. Hénon mappings in the complex domain. II. Projective and inductive limits of polynomials. In *Real and complex dynamical systems (Hillerød, 1993)*, volume 464 of *NATO Adv. Sci. Inst. Ser. C Math. Phys. Sci.*, pages 89–132. Kluwer Acad. Publ., Dordrecht, 1995.
- [34] John H. Hubbard and Ralph W. Oberste-Vorth. Linked solenoid mappings and the non-transversality locus invariant. *Indiana Univ. Math. J.*, 50(1):553–566, 2001.
- [35] John H. Hubbard and Peter Papadopol. Newton's method applied to two quadratic equations in \mathbb{C}^2 viewed as a global dynamical system. To appear in the Memoires of the AMS.
- [36] John H. Hubbard and Peter Papadopol. Superattractive fixed points in \mathbb{C}^n . *Indiana Univ. Math. J.*, 43(1):321–365, 1994.
- [37] John Hamal Hubbard and Barbara Burke Hubbard. *Vector calculus, linear algebra, and differential forms*. Prentice Hall Inc., Upper Saddle River, NJ, 1999. A unified approach.
- [38] Mattias Jonsson. Dynamics of polynomial skew products on \mathbb{C}^2 . *Math. Ann.*, 314(3):403–447, 1999.
- [39] L. V. Kantorovič. On Newton's method. *Trudy Mat. Inst. Steklov.*, 28:104–144, 1949.
- [40] R. Mañé, P. Sad, and D. Sullivan. On the dynamics of rational maps. *Ann. Sci. École Norm. Sup. (4)*, 16(2):193–217, 1983.
- [41] Curt McMullen. Families of rational maps and iterative root-finding algorithms. *Ann. of Math. (2)*, 125(3):467–493, 1987.
- [42] Curt McMullen. Braiding of the attractor and the failure of iterative algorithms. *Invent. Math.*, 91(2):259–272, 1988.
- [43] John Milnor. *Dynamics in one complex variable*. Friedr. Vieweg & Sohn, Braunschweig, 1999. Introductory lectures.
- [44] Karl Papadantonakis. Fractalasm. A fast, generalized fractal exploration program. <http://www.math.cornell.edu/~dynamics/FA/index.html>.
- [45] Alexander Russakovskii and Bernard Shiffman. Value distribution for sequences of rational mappings and complex dynamics. *Indiana Univ. Math. J.*, 46(3):897–932, 1997.

- [46] Dierk Schleicher. On the number of iterations of Newton's method for complex polynomials. *Ergodic Theory Dynam. Systems*, 22(3):935–945, 2002.
- [47] Nessim Sibony. Dynamique des applications rationnelles de \mathbf{P}^k . In *Dynamique et géométrie complexes (Lyon, 1997)*, volume 8 of *Panor. Synthèses*, pages ix–x, xi–xii, 97–185. Soc. Math. France, Paris, 1999.
- [48] John Smillie. Complex dynamics in several variables. In *Flavors of geometry*, volume 31 of *Math. Sci. Res. Inst. Publ.*, pages 117–150. Cambridge Univ. Press, Cambridge, 1997. With notes by Gregory T. Buzzard.
- [49] Tetsuo Ueda. Fatou sets in complex dynamics on projective spaces. *J. Math. Soc. Japan*, 46(3):545–555, 1994.